

TWIST1 SILENCES FOXA1 EXPRESSION TO PROMOTE BREAST CANCER
PROGRESSION

A Dissertation

by

YIXIANG XU

Submitted to the Office of Graduate and Professional Studies of
Texas A&M University
in partial fulfillment of the requirements for the degree of

DOCTOR OF PHILOSOPHY

Chair of Committee,	Fen Wang
Co-Chair of Committee,	Jianming Xu
Committee Members,	Wallace L. McKeehan
	Peter J.A. Davies
	Yi Li
Head of Program,	Warren Zimmer

December 2016

Major Subject: Medical Sciences

Copyright 2016 Yixiang Xu

ABSTRACT

Twist1 is a basic helix-loop-helix transcription factor family that serves as one of the master regulators promoting epithelial-mesenchymal transition (EMT). Twist1 has been shown in many studies to promote EMT, stemness, invasiveness and metastasis in multiple cancers, including breast cancer. However, the genetic role of Twist1 in spontaneous breast cancer has not been investigated, and it is also unknown whether Twist1 is required for cell invasion and metastasis of spontaneously developed cancer. In this study, using a new TVA/RCIP mouse model, we disrupted Twist1 in certain mammary luminal epithelial cells and specifically induced tumors from these cells. We found that tumor cell-specific knockout of *Twist1* diminished lung metastasis without affecting primary tumor initiation or growth. The diminished lung metastasis is accompanied with the decreased EMT, angiogenesis and circulating tumor cells caused by *Twist1* knockout. Twist1 expression was positively associated with late-stage tumors and negatively associated with ER α and Foxa1 expression in mouse tumors. We then identified Foxa1 as a novel direct target of Twist1 in human breast cancer. We further found that Twist1 inhibits *Foxa1* expression through direct binding to its proximal promoter region and recruiting Mi2/nucleosome remodeling and deacetylase (Mi2/NuRD) transcriptional repressor complex in human breast cancer cells. Moreover, Twist1 also diminished transcriptional activator AP1 binding to *Foxa1* promoter. Twist1 mediated *Foxa1* down-regulation is essential for promoting breast cancer migration, invasion and metastasis. Restored Foxa1 expression significantly inhibits Twist1

dependent cell migration and invasion capability of MCF7 cells through inhibiting integrin α_5 , β_1 and MMP9 expression. Importantly, Twist1^{high} Foxa1^{low} correlates with the poorest prognosis in breast cancer patients. These findings highlight Twist1 as a key player in promoting breast cancer progression to a more malignant phenotype and a potential therapeutic target.

DEDICATION

I would like to dedicate this dissertation to my father Minqiang Xu, my mother Xiaomei Lan, my wife Jingwei Zhu and my son Jeremy Xu.

ACKNOWLEDGEMENTS

I would like to thank my mentor, Dr. Jianming Xu, and my committee members, Dr. Fen Wang, Dr. Jianming Xu, Dr. Wallace L. McKeehan, Dr. Peter J.A. Davies, and Dr. Yi Li, for their guidance and support throughout the course of this research. Dr. Xu has given me valuable suggestions guiding my thesis study in the lab. He is open-minded and gives me a lot of freedom in the research. More importantly, he trained me to become an independent and inspired researcher in biomedical science. I also want to thank the other committee members for sharing their precious time and inspiring suggestions in the meetings.

My gratitude also goes to the colleagues in Xu lab. I would like to thank the former visiting student Zhen Feng for initiating the RCAS-TVA system in the lab. I would like to thank Dr. Yan Xu for collaboration and contribution to the mouse model study in the project. I would like to thank Dr. Li Qin for her tremendous help in the discussion of data and techniques. I would like to thank Dr. Tong Sun, Dr. Hongmei Wu, Dr. Zhihui Yang for their valuable input in the project. I would like to thank Dr. Dongkee Lee for his help with improving immunostaining technique. I would like to thank Lan Liao and Suoling Zhou for their help in providing SCID mice and maintaining the stock of reagents and materials in the lab. Finally, I want to thank other members in the lab including Dr. Xiaobin Yu, Dr. Jean Ching Yi Tien, Yonghong Liu and Jarrod Martinez for their suggestions to the study.

Thanks also go to the department faculty and staff for making my time at Texas A&M University Institute of Bioscience and Technology a great experience, especially the program coordinator Cindy Lewis, who is always patient to students even when we make stupid mistakes or ask dumb questions. Of course, I would also thank my friends in IBT, Xi Lin, Wenjiao Li, Yuan Dai, Yanqing Huang, Ji Jing *et al.* It is their company that makes the life full of fun and happiness.

Finally, thanks to my family for their encouragement and especially to my wife for her patience and love.

CONTRIBUTORS AND FUNDING SOURCES

Contributors

This work was supervised by a thesis committee consisting of Professor Fen Wang [Chair] and Professor Jianming Xu [co-Chair], Professors Wallace L. McKeehan, Peter J.A. Davies of Institute of Bioscience and Technology and Professor Yi Li of Baylor College of Medicine.

The data in Figure 3.1 were provided by Dr. Zhen Feng in Dr. Jianming Xu's lab in Baylor College of Medicine. The fluorescent staining data in Figure 3.7 were done in collaboration with Dr. Dongkee Lee in Dr. Jianming Xu's lab in Baylor College of Medicine. All other work conducted for the thesis was completed by the student independently.

Funding Sources

This work was made possible in part by NIH grants CA112403 and CA193455 and Cancer Prevention and Research Institute of Texas grants RP120732-P5 and RP150197.

TABLE OF CONTENTS

	Page
ABSTRACT	ii
DEDICATION	iv
ACKNOWLEDGEMENTS	v
CONTRIBUTORS AND FUNDING SOURCES.....	vii
TABLE OF CONTENTS	viii
LIST OF FIGURES.....	x
LIST OF TABLES	xii
1. INTRODUCTION.....	1
1.1 Breast cancer	1
1.2 EMT	4
1.3 Twist1.....	16
1.4 Foxa1	22
2. MATERIAL AND METHODS	26
2.1 The TVA/RCIP system for induction of mouse mammary gland tumorigenesis with tumor cell-specific <i>Twist1</i> knockout.....	26
2.2 Western blot	27
2.3 X-gal staining.....	28
2.4 Cell culture	29
2.5 Circulating Tumor Cell (CTC) culture.....	29
2.6 H&E staining, immunohistochemistry (IHC) and immunohistofluorescence (IHF).....	30
2.7 Quantitative RT-PCR (qPCR).....	31
2.8 Genomic DNA extraction from paraffin embedded samples.....	31
2.9 Micro-vascular density calculation	32
2.10 Plasmids and cell transfection	32
2.11 ChIP assay	34
2.12 Cell migration and invasion assays	35
2.13 <i>In vivo</i> metastasis assay	35

2.14	Statistical analyses.....	36
3.	RESULTS.....	38
3.1	A new mouse model system for simultaneous deletion of the floxed alleles and expression of an oncogene in a subset of the mouse mammary epithelial cells.....	38
3.2	Tumor specific knock-out of <i>Twist1</i> using TVA/RCIP system in <i>Twist1</i> -floxed mice.....	41
3.3	Specific ablation of <i>Twist1</i> in the PyMT-induced mammary tumor cells does not affect primary tumor development in mice.....	44
3.4	Specific ablation of <i>Twist1</i> in the PyMT-induced mammary tumor cells inhibits lung metastasis.....	45
3.5	Specific ablation of <i>Twist1</i> in the PyMT-induced mammary tumor cells inhibits EMT and invasiveness.....	49
3.6	<i>Twist1</i> expression is turned off in lung metastasis foci.....	52
3.7	<i>Twist1</i> is expressed at late tumor stage and is associated with reduced ER and <i>Foxa1</i> expression in mouse tumors.....	53
3.8	<i>Twist1</i> expression inversely associates with <i>Foxa1</i> expression in human breast cancer.....	57
3.9	<i>Twist1</i> directly silences <i>Foxa1</i> mRNA transcription by recruiting NuRD complex.....	60
3.10	<i>Twist1</i> silences <i>Foxa1</i> expression through inhibiting AP-1-promoted activation of the <i>Foxa1</i> promoter.....	67
3.11	<i>Twist1</i> -silenced <i>Foxa1</i> expression is not responsible for <i>Twist1</i> -induced cell morphological change but it mediates the expression of some <i>Twist1</i> -regulated genes.....	70
3.12	Silencing <i>Foxa1</i> expression is required for <i>Twist1</i> to promote migration, invasion and metastasis in breast cancer cells.....	72
3.13	Breast tumor patients with high <i>Twist1</i> and low <i>Foxa1</i> expression exhibit poor distant metastasis-free survival.....	76
4.	SUMMARY AND DISCUSSION.....	79
	REFERENCES.....	89

LIST OF FIGURES

	Page
Figure 1.1. Overview of cancer metastasis steps.....	2
Figure 1.2. Overview of the molecular networks that regulate EMT.	7
Figure 1.3 Consequences of EMT in breast cancer cells.	16
Figure 1.4. Possible regulatory network of Twist1 in cancer progression.....	20
Figure 1.5. Twist1 recruits Mi-2/NuRD complex to repress E-cadherin transcription in cancer progression.	22
Figure 3.1. The mammary tumorigenesis mouse model induced by the novel MMTV- TVA/RCIP system.	40
Figure 3.2. Mammary tumor cell-specific knockout of <i>Twist1</i> in mice.....	43
Figure 3.3. Tumor cell-specific knockout (TKO) of <i>Twist1</i> does not influence tumor initiation or growth in mice.	45
Figure 3.4. IHC staining of primary tumors	46
Figure 3.5. Tumor cell-specific knockout (TKO) of <i>Twist1</i> inhibits lung metastasis in mice.....	47
Figure 3.6. Ki67 staining and genomic DNA PCR of metastasis tumors	49
Figure 3.7. Vimentin and E-cadherin expression in Twist1 positive and negative tumor cells	51
Figure 3.8. TKO of <i>Twist1</i> in the PyMT-induced mammary tumor cells inhibits angiogenesis and invasion in to blood circulation.....	52
Figure 3.9. Twist1, Vimentin and E-cadherin expression in lung metastasis tumor foci of WT/RCIP and <i>Twist1</i> ^{TKO} /RCIP groups	54
Figure 3.10. Twist1, ER α and Foxa1 IHC in mouse tumors and IRS score	55
Figure 3.11. Downregulated genes by Twist1 overexpression in T47D human breast cancer cells.....	57

Figure 3.12. <i>Twist1</i> expression is negatively associated with <i>Foxa1</i> expression in human breast cancers.....	59
Figure 3.13. <i>Twist1</i> silences <i>Foxa1</i> expression in breast cancer cells.....	61
Figure 3.14. <i>Twist1</i> directly bind to E-box element of <i>Foxa1</i> promoter	63
Figure 3.15. Mutation of <i>Twist1</i> -binding sites or knockdown of <i>Twist1</i> mRNA increases <i>Foxa1</i> promoter-luciferase (Luc) reporter activity in SUM1315 cells.....	64
Figure 3.16. Overexpressed <i>Twist1</i> in MCF7 cells recruits NuRD complex to <i>Foxa1</i> promoter to repress its expression	66
Figure 3.17. Knockdown of <i>Twist1</i> mRNA reduced MTA2 and HDAC2 recruitments but increased H3K9-Ace and RNA polymerase II (RNA-Pol II) recruitment to the <i>Foxa1</i> promoter in SUM1315 cells	67
Figure 3.18. <i>Twist1</i> inhibits AP1-mediated activation of the <i>Foxa1</i> promoter by inhibiting AP1 recruitment	69
Figure 3.19. <i>Twist1</i> inhibits AP1-activated <i>Foxa1</i> promoter activity in SUM1315 cells.....	70
Figure 3.20. The effects of silenced <i>Foxa1</i> expression on <i>Twist1</i> -induced EMT cell morphogenesis and gene expression.....	72
Figure 3.21. Restored <i>Foxa1</i> expression inhibited <i>Twist1</i> -promoted migration, invasion and metastasis of breast cancer cells.....	74
Figure 3.22. Restored <i>Foxa1</i> expression increased the expression of most <i>Twist1</i> -suppressed luminal marker genes and decreased the expression of most <i>Twist1</i> -promoted basal marker genes in the xenograft tumors in mice.....	75
Figure 3.23. The association of <i>Twist1</i> and <i>Foxa1</i> expression levels with the clinical outcomes of the breast cancer patients	78
Figure 4.1. Summary of <i>Twist1</i> - <i>Foxa1</i> regulatory axis in breast cancer cells.....	86

LIST OF TABLES

	Page
Table 1.1. Markers of EMT.....	14
Table 2.1. Oligonucleotide primers and probes for PCR	37
Table 3.1. Clinical information for Twist1-positive breast tumors.....	60

1. INTRODUCTION

1.1 Breast cancer

1.1.1 Basic characteristics of cancer

The origin of the word “CANCER” is credited to the Greek physician Hippocrates, who is considered the “Father of Western Medicine.” Hippocrates used the terms *carcinosis* and *carcinoma* to describe non-ulcer forming and ulcer-forming tumors. Cancer begins when cells in a part of the body start to grow out of control. There are many kinds of cancer, but they all start because of out-of-control growth of abnormal cells which acquire genetic or epigenetic alterations. In the 2 review papers by D. Hanahan and R. Weinberg^{1,2}, they proposed that these alterations occur in most if not all cancer cells which contribute to the 10 hall marks of cancer including: deregulating cellular energetics, evading apoptosis, self-sufficiency in growth signals, insensitivity to anti-growth signals, avoiding immune destruction, limitless replicative potential, tumor-promoting inflammation, tissue invasion and metastasis, sustained angiogenesis, genome instability and mutation. For most of the solid tumors, the tumor related mortality is due to the metastasis to distant organs, which results from the acquired capability of tumor cells to invade and metastasize. Tumor metastasis is a multi-step process defined as the ability of tumor cells to migrate from its original site to colonize in distant organs³. Each

of these steps can be rate limiting, as blocking any of these steps could stop the entire process (Fig 1.1).

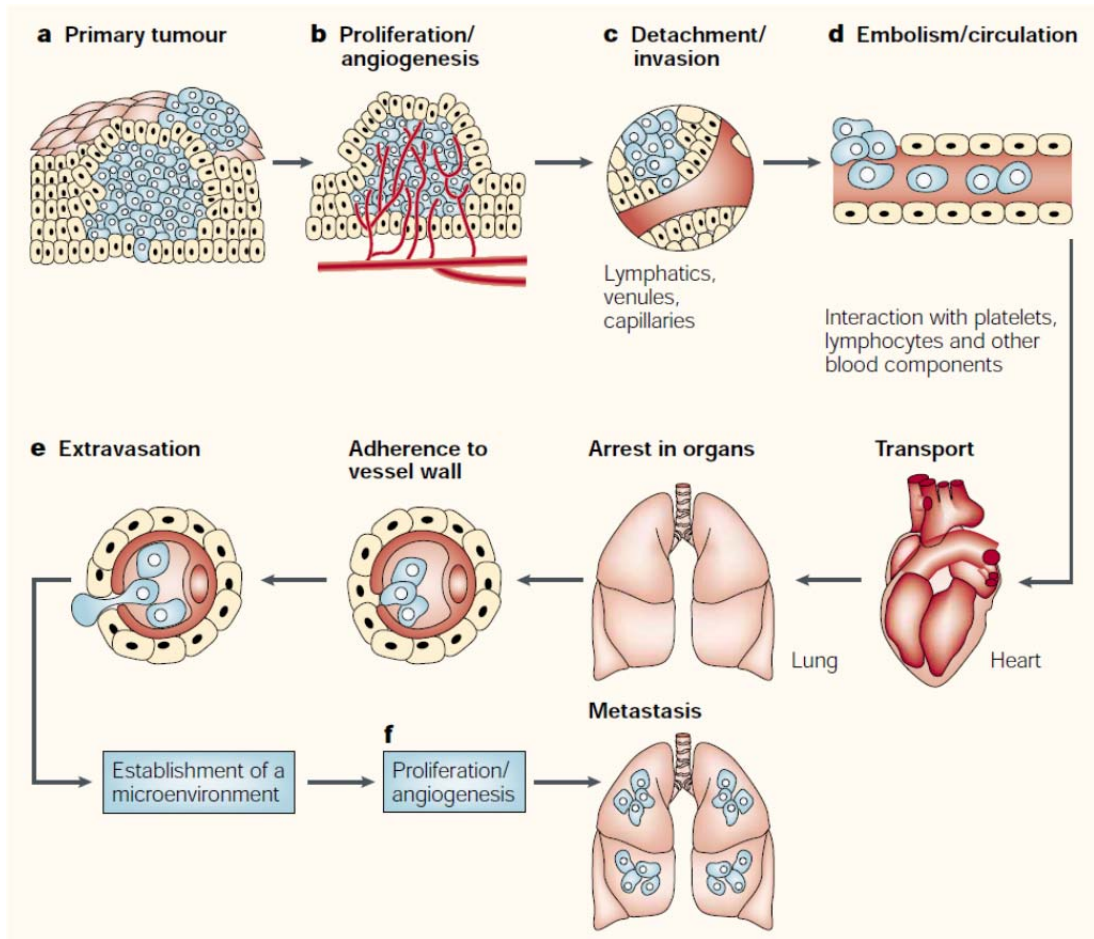


Figure 1.1. Overview of cancer metastasis steps. (From Isaiah J. Fidler, Nature Review: Cancer, 2003³)

1.1.2 Breast cancer and classification

Breast cancer is a heterogeneous disease with different clinical and pathological features.

Classification of breast cancer may help to predict prognosis and direct personalized treatment. Comprehensive molecular profiling of breast cancer using microarray-based technology^{4,6} demonstrated that the morphological heterogeneity of breast cancer was reflected at the transcriptional level^{7,8}. Their data show systematic variations of the expression profiles of breast cancer. These profiles could classify breast cancers into five subtypes: luminal A, luminal B, normal breast-like, ERBB2+ and basal-like breast carcinomas^{4,6,8,9}. The basal-like subtype was characterized by high expression of keratins 5 and 17, laminin, and FABP7, whereas the ERBB2+ subtype was characterized by high expression of several genes in the ERBB2 amplicon at 17q22.24 including ERBB2 and GRB7. Normal breast-like group showed the highest expression of many genes known expressed in adipose tissue and other non-epithelial cell types. On the other hand, luminal type of tumors can be further grouped into two subgroups: luminal subtype A, with the highest expression of the ER α gene, GATA3, XBP1, TFF3, Foxa1, and LIV-1; and luminal subtype B with low to moderate expression of the luminal-specific genes including the ER α cluster⁴.

More importantly, the molecular profile of tumor will not stay fixed as the progression of cancer. Several studies have shown that mouse mammary gland tumors progress from ER α positive/luminal A subtype to luminal B or ER α negative subtypes^{10,11}. Similarly, loss of ER α expression is also broadly observed in human breast cancers, concomitant with hormone resistance, invasiveness and poor prognosis¹².

Different gene expression profiles reflect variation in the cellular biology of the tumor subtypes and are associated with patients' clinical outcome^{8, 9}. Luminal A tumors have the most favorable prognosis, normal like tumors have an intermediate prognosis^{4, 5, 9, 13}. On the other hand, luminal B, ERBB2-positive and basal-like tumors are associated with poor relapse-free and overall survival. Basal-like breast cancer (BLBC) is a major clinical challenge due to its aggressive nature and the lack of expression of the available drug targets including steroid hormone receptors (ER and PR) and ERBB2. BLBCs do not response to currently available targeted therapies such as tamoxifen (ER inhibitor) or trastuzumab (HER2 inhibitor) therapy. The absence of effective targeted therapies and poor response to standard chemotherapy may be associated with poor prognosis of BLBC patients. BLBC also has stem-cell-like properties and activated EMT (epithelial-mesenchymal transition) program, suggesting that EMT regulators may play critical roles in BLBC progression.

1.2 EMT

1.2.1 Basics of EMT

Epithelial and mesenchymal cells differ in various functional and phenotypic characteristics. Epithelial cells form a single layer or multilayers that are closely adjoined through specialized intercellular junctions such as tight junctions, adheren junctions, desmosomes and gap junctions¹⁴. Epithelial cells also have apical-basolateral

polarization, as the epithelial cells are all polarized in the same manner. Every epithelial cell membrane can be divided into an apical domain and a basolateral domain, with the apical surface facing either the exterior environment or the luminal space and the basolateral domain can be further divided to basal subdomain mediating cell-extracellular matrix adhesion and lateral subdomain involved in cell-cell contact. Cells or cell aggregates lacking the above criteria are defined as mesenchymal cells. Mesenchymal cells contact neighboring mesenchymal cells only focally and do not associate with a basal lamina. In 2D cell culture, mesenchymal cells are characterized by spindle shaped, fibroblast-like morphology, whereas epithelial cells grow as clusters that maintain cell-cell adhesion. Cultured mesenchymal cells tend to be highly motile. Epithelial cells are also motile and can move away from their nearest neighbors, while remaining within the epithelial layer. However, cells do not detach and move away from the epithelial layer under normal conditions¹⁵.

While epithelial and mesenchymal cell types have long been recognized in early embryos, the conversion of epithelial cells into mesenchymal cell, which is known as epithelial-mesenchymal transition (EMT), was not defined until 1980s. Greenburg and Hay showed that when epithelial cells were cultured in 3D collagen gels, these cells elongated, detached from the explants, and migrated as individual cells, which are all belong to mesenchymal phenotypes¹⁶⁻¹⁸. The transition from epithelial- to mesenchymal-cell characteristics involves a spectrum of inter- and intracellular changes. Subsequent molecular studies loosely defined EMT by three major changes in cellular phenotype¹⁹.

²⁰. The first is morphological changes from monolayer of epithelial cells with an apical-basal polarity to dispersed, spindle-shaped phenotype. The second is differentiation marker changes from cell-cell junction proteins and cytokeratin intermediate filaments to vimentin filaments and fibronectin. The third is the functional changes associated with the conversion of relative stationary cells to motile cells that can invade through ECM. As not all three changes are always observed during EMT, acquisition of the ability to migrate and invade ECM as a single cell is then considered a functional hallmark of the EMT program.

Several *in vitro* and *in vivo* studies aimed to define the molecular regulation of EMT showed that EMT can be triggered by a crosstalk of extracellular signals including extracellular matrix (ECM) as well as soluble growth factors such as members of the TGF β and fibroblast growth factor (FGF) families, epidermal growth factor (EGF) and SF/HGF (Fig 1.2). These growth factors serve as ligands for their cell surface receptors, which are activated in response to these ligands and trigger the activation of intracellular effector molecules, such as members of the small GTPase family — Ras, Rho and Rac and members of the Src tyrosine-kinase family. These effectors are responsible for the disassembly of junctional complexes and the changes in cytoskeletal organization during EMT. On the other hand, several transcriptional regulators such as zinc-finger transcription factors snail²¹, slug²², ZEB1²³ and ZEB2(SIP1)²⁴ and bHLH transcription factors E47²⁵ and Twist1²⁶ were reported to regulate the changes in gene-expression patterns that underlie EMT.

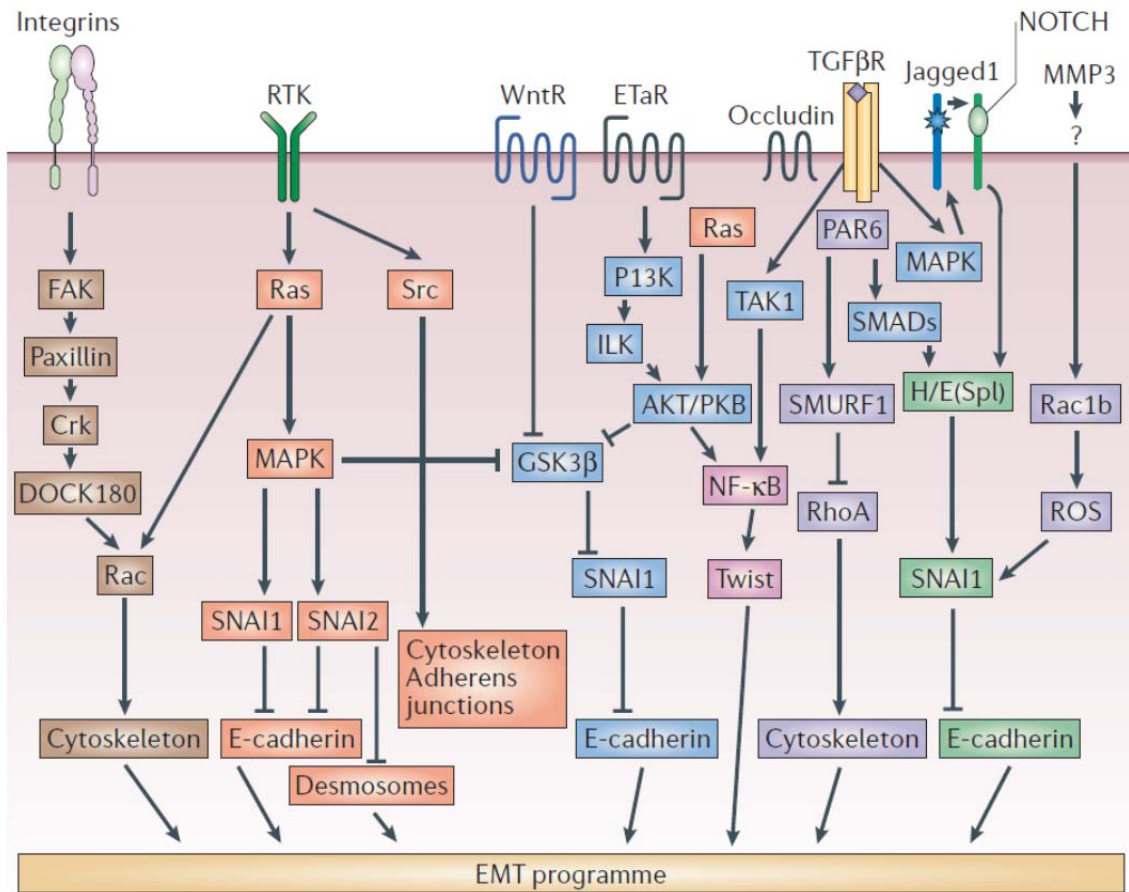


Figure 1.2. Overview of the molecular networks that regulate EMT. Signaling pathways that are activated by EMT regulators and a limited representation of their crosstalk are shown. RTKs (receptor tyrosine kinases); TGFβ (transforming growth factor-β); MMPs (Matrix metalloproteinases); ETaR (endothelin-A receptor); FAK (focal adhesion kinase); GSK3β (glycogen-synthase kinase-3 β); H/E(Spl) (hairy/enhancer of split); ILK (integrin-linked kinase); MAPK (mitogen-activated protein kinase); NF-κB (nuclear factor-κB); PAR6 (partitioning-defective protein-6); PI3K (phosphatidylinositol3-kinase); PKB (protein kinase-B); ROS (reactive oxygen species); TAK1 (TGFβ-activated kinase-1); TGFβR (TGFβ receptor); WntR (Wnt receptor). (From Jean Paul Thiery and Jonathan P. Sleeman, *Nature Reviews: Molecular Cell Biology*, 2006¹⁵)

1.2.2 EMT in development

During embryonic development, epithelial sheets can remodel through distinct processes and can also convert reversibly or irreversibly into mesenchymal cells through EMT. The process has been observed during a variety of tissue remodeling events, including mesoderm formation, neural crest development, heart valve development and secondary palate formation. Mesoderm formation and neural crest development occur during early embryonic development, epithelial cells undergo EMT, resulting in mesenchymal and neural crest cells that maintain the potential to further differentiate into various cell types. On the other hand, during heart valve development and secondary palate formation, EMT occurs in relatively well-differentiated epithelial cells that are destined to become defined mesenchymal cell types.

The earliest example of an EMT program participating in embryogenesis that been reported is the formation of mesoderm from the primitive ectoderm, mainly from model organisms including *Drosophila* and amphibian and avian embryos²⁷. Later studies indicate that the same basic principles also happen in mammalian embryos²⁸ as epithelial cells lose their tight cell-cell adhesions and remain attached to neighboring cells only by sparsely distributed focal contacts. Subsequently, these cells undergo mesenchymal differentiation and migrate along the narrow extracellular space underneath the ectoderm, indicating the EMT program during gastrulation. Another example of EMT in embryogenesis is the generation of the neural crest, a defining tissue of vertebrates,

which is composed of a population of precursor cells with the ability to migrate over long distances in the embryo. The emergence of neural crest cells begins with the presence of a distinct population of cells with rounded and pleiomorphic shapes at the boundary between the neural plate and the epidermal ectoderm, the presumptive neural crest cells, which proceed to lose N-cadherin-mediated cell-cell adhesion while becoming excluded from the neural epithelium²⁹. Detailed studies in avian and mouse embryos using immune-labeling and electron microscopic revealed that disruption of the basal lamina occurs immediately before or at the onset of neural crest cell migration in the cranial regions^{30, 31}. These observations demonstrate that neural crest cells actively invade through the basal lamina, which is, however, not present at the neural fold in the trunk region before the onset of neural crest migration³². These findings suggest that distinct types of subcellular machineries were employed to initiate EMT, invade the ECM, and migrate.

Heart valve in vertebrate embryos, which is derived from a precursor structure known as endocardial cushion, begins to form soon after the primitive linear heart tube begins to loop. Initially, the myocardial cells secrete a large amount of ECM and create endocardial cushions, and then the mesenchymal cells fill the cushion space³³. These mesenchymal cells were then found to derive from the endocardial cell layer by undergoing an EMT³⁴. Upon EMT-inducing stimuli, AV endocardial cells decrease N-CAM, lose cell-cell adhesion, and invade the newly deposited endocardial cushion, thereby establishing the presumptive cardiac septa and valves³⁵. Another well-studied

EMT is the formation of the secondary oral palate when researchers can trace the entire program of palate remodeling with electron microscopy and immunohistochemistry by dissecting the palatal tissue and introducing it into organ cultures. As fusion of the palatal shelves at the midline is required for development of the secondary palate, when the shelves approach one another from opposite sides of the developing oral cavity, epithelial cells covering the tip of each shelf intercalate and form the medial epithelial seam. Then these medial epithelial cells undergo EMT and are integrated into the mesenchymal compartment of the palate to finish the program of palatogenesis³⁶.

1.2.3 EMT in diseases

Under physiological condition, such as embryogenesis, EMT program plays an important role. However, as well as many other programs, similar cell changes could be recapitulated during pathological processes, such as fibrosis and cancer. Many studies have shown a remarkable similarity between the regulatory signaling pathways of EMT in physiological and pathological conditions.

Fibrosis is characterized by increased numbers of myofibroblasts that deposit interstitial ECM, and the origin for majority of these fibroblasts is thought to be tubular epithelial cells that undergo through EMT³⁷. In animal models of kidney disease, EMT occurs in tubular epithelial cells³⁸. Moreover, similar observations have been made in studies of human renal fibrosis³⁹. One of the mechanisms could be inflammatory processes in

response to injury of tissue lead to increased levels of factors such as TGF β , EGF and FGF2, which have been demonstrated to be EMT stimulators of tubular epithelial cells⁴⁰. Indeed, one study showed that in the peritoneal cavity, renal dialysis causes injury to the mesothelial lining and results in EMT of mesothelial cells and finally fibrosis through inducing TGF β expression⁴¹, which then has been confirmed in animal models⁴².

Beside fibrosis, numerous observations showed that EMT plays an important role in the progression of multiple cancers, especially in tumor metastasis. Majority of solid tumors are carcinomas that originate from epithelial cells. When the carcinoma cells metastasize, they must lose cell-cell adhesion and acquire motility, which shares many similarities with the extensive cell migration and tissue rearrangements that occur during the various developmental events mentioned above. Indeed, this highly conserved EMT program has been implicated in giving rise to the dissemination of single carcinoma cells from primary epithelial tumors⁴³. Many reports that study the function of EMT regulators and transcriptional factors in cancer revealed the central role of these factors in facilitating tumor cell migration, invasion and metastasis.

Thus, based on the functional consequences and biological context, EMT is classified into 3 distinct types, which are developmental (Type I), fibrosis and wound healing (Type II), and cancer (Type III)⁴⁴. As mentioned above, these 3 types of EMT occur at different micro-environmental context and show different characteristics. On the other hand, these 3 types of EMT share some common mechanisms. Biomarkers specific to

each subtype of EMT and also common to all subtypes have been defined, as summarized in a recent review paper of EMT⁴⁵ (Table 1.1).

Tumor cells metastasize to distant organs is the major reason of mortality in breast cancer patients. However, the mechanism by which epithelial tumor cells escape from the primary tumor and colonize a distant site is not entirely understood. Numerous studies in breast cancer and other cancers have postulated EMT as an important mechanism for tumor metastasis. Except for several rare subtypes such as diffuse lobular carcinoma, in most breast cancer, similar to other epithelial carcinomas, EMT rarely occurs homogenously across the whole tumor. However, the direct evidence of EMT existence is not easy to find as once the epithelial tumor cells undergo EMT, they may be phenotypically indistinguishable from fibroblasts. In addition, since most metastatic lesions exhibit an epithelial phenotype, whether EMT indeed occurs in breast tumor progression is still debatable until a transgenic mice study provides direct evidence of EMT in the local invasion of tumor cells in breast cancer⁴⁶. Furthermore, microarray analysis of breast tumors showed that certain types of breast cancer cells are primed to undergo EMT and spread, such as the basal or triple negative breast cancer subtype which exhibits an aggressive phenotype and correlates with the poorest clinical outcomes⁴⁷. Similar results were observed in breast cancer cells lines as basal B subtype breast cancer cell lines also display a mesenchymal phenotype⁴⁸. These work revealed the existence of EMT in primary breast cancer, which is supported by more and more evidence to be a reversible and transient process. This could explain why metastatic cells

at a secondary site are likely undergo a reversion EMT or MET, permitting colonization of the distant site⁴⁹.

1.2.4 EMT in breast cancer

It was hypothesized that developmental programs are reactivated during tumorigenesis and contribute to tumor progression. The fact that numerous EMT regulators in development are also inappropriately expressed in human cancer and correlate with features of EMT is a strong evidence to support the hypothesis^{22, 23, 26}. E-cadherin, an important caretaker of the epithelial phenotype, is down-regulated by these EMT transcriptional regulators. In both cell culture and tumor mouse models, ectopically expression of E-cadherin in certain invasive carcinoma cells can inhibit their capability to invade and metastasize. Conversely, downregulation of E-cadherin (or mutations that occur in cancer) has several important consequences that are of direct relevance to EMT and subsequent cell motility and metastasis. Decrease of E-cadherin level in carcinoma cells results in the loss of E-cadherin-dependent intercellular epithelial junctional complexes, and abolished sequestering of β -catenin in the cytoplasm, subsequently release the carcinoma cells from the neighbor cells.

Acquired markers		Attenuated markers	
Name	EMT type	Name	EMT type
Cell-surface proteins			
N-cadherin	1,2	E-cadherin	1,2,3
OB-cadherin	3	ZO-1	1,2,3
$\alpha 5\beta 1$ integrin	1,3		
$\alpha V\beta 6$ integrin	1,3		
Syndecan-1	1,3		
Cytoskeleton markers			
FSP1	1,2,3	Cytokeratin	1,2,3
α -SMA	2,3		
Vimentin	1,2		
β -catenin	1,2,3		
ECM proteins			
$\alpha 1$ (I) collagen	1,3	$\alpha 1$ (IV) collagen	1,2,3
$\alpha 1$ (III) collagen	1,3	Laminin 1	1,2,3
Fibronectin	1,2		
Laminin 5	1,2		
Transcription factors			
Snail1	1,2,3		
Snail2	1,2,3		
ZEB1	1,2,3		
CBF-A/KAP-1 complex	2,3		
Twist1	1,2,3		
LEF-1	1,2,3		
Ets-1	1,2,3		
FOXC2	1,2		
Goosecoid	1,2		
MicroRNAs			
miR10b	2	Mir-200 family	2
miR-21	2,3		

Table 1.1. Markers of EMT (From Michael Zeisberg and Eric G. Neilson, *J.Clin. Invest.*, 2009⁴⁵)

Besides promoting tumor cell invasion and metastasis, EMT is reported to be involved in multiple aspects of tumor progression including cell survival, chemo-resistance, stemness and cancer cell transition into endothelial cells⁵⁰ (Fig 1.3). For example, Robert A. Weinberg's group reported that the induction of EMT in immortalized human mammary epithelial cells (HMLEs) results in the acquisition of mesenchymal traits and in the expression of stem cell markers. Moreover, stem-like cells isolated from HMLEs, mouse or human mammary glands and mammary carcinomas undergo EMT⁵¹. They then update their study recently showing that distinct EMT programs control normal mammary stem cells and tumor-initiating cells⁵². Another study showed that Six1 expands the mouse mammary epithelial stem/progenitor cell pool, which is correlated with EMT⁵³. The acquisition of a cancer stem cell-like phenotype enables a subset of tumor cells to self-renew and likely to ultimately metastasize to distant organs.

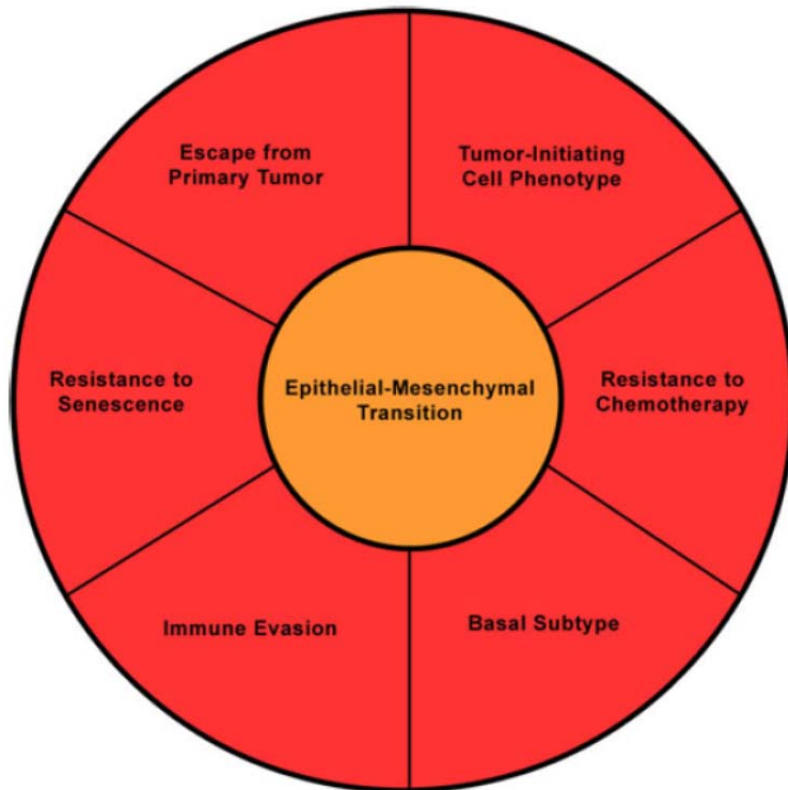


Figure 1.3 Consequences of EMT in breast cancer cells. In addition to the well-characterized role for EMT in local spread of tumor cells, induction of EMT also correlates with numerous other properties including a tumor-initiating cell phenotype, resistance to chemotherapy and senescence, evasion of the immune system and induction of a basal gene expression profile. (From Douglas S. Micalizzi, Susan M. Farabaugh, Heide L. Ford, J Mammary Gland Biol Neoplasia, 2010⁵⁰)

1.3 Twist1

1.3.1 Twist1 in development and human disease

A mutant *Drosophila* embryos failed to gastrulate normally, produced no mesoderm and died at the end of embryogenesis with a ‘twisted’ appearance⁵⁴, thus the gene that is responsible for the phenotype is named “*twist*”. The human and mouse homolog of *twist*

gene are found and named *Twist1*. The *twist* gene encodes a transcription factor containing a basic helix-loop-helix (bHLH) domain⁵⁵ involved in the regulation of organogenesis^{56, 57}. The critical roles of Twist1 protein in mesoderm associated organogenesis, especially in the morphogenesis of the cranial neural tube⁵⁸, have been well illustrated by genetic studies. In *Drosophila*, *twist* transcription is activated by Dorsal in the presumptive mesoderm and the expressed twist protein forms a steep gradient across the presumptive mesoderm-neuroectoderm border in the early embryo^{59, 60}. During later stage, *twist* expression decreases to relatively low levels in the mesodermal layer cells. The similar effect of Twist1 is found in mouse mesoderm development. After birth, Twist1 can be seen in adult mesenchymal cells such as muscle stem cells, referred to as adult muscle precursors in *Drosophila*, while in mouse, *Twist1* is expressed in the adult stem cells of the mesenchyme^{61, 62}. Previous study in our lab revealed that Twist1 is expressed in a few tissues, including fibroblasts of the mammary glands and dermal papilla cells of the hair follicles in young and adult mice. Conditional *Twist1* knockout in 6-week-old males and female mice did not influence body weight gain, heart rate, or total lean and fat components. The knockout also did not alter blood pressure in males, although it slightly reduced blood pressure in females. These results indicate that Twist1 is not essential for maintaining an overall healthy condition in young and adult mice⁶³. In summary, *Twist1* is highly expressed in the mesoderm-derived mesenchyme during embryonic development and is primarily expressed in relatively quiescent adult stem cells located in mesoderm-derived mesenchymal tissues postnatally⁶⁴.

In humans, *Twist1* gene mutations are responsible for an autosomal dominant inheritance disease named Saethre-Chotzen syndrome (SCS), which is characterized by a broad spectrum of malformations including short stature, craniosynostoses, high forehead, ptosis, small ears with prominent crus, and maxillary hypoplasia with a narrow and high palate^{65, 66}. Non-sense mutations and mis-sense mutations at conserved residue across species within bHLH domain were found in human SCS patients. Since majority of mutations are heterozygous, leading to loss of function of Twist1 protein, it suggests that protein level is essential for the function of Twist1 in cells, which is supported by the gradient expression of Twist1 protein at the development stage in *Drosophila*. Gene ablation experiments of mouse models demonstrated that the heterozygous *Twist1* null mice⁵⁸ manifest craniofacial and limb abnormalities resembling those in SCS patients. Since the last decade, numerous studies have shown that Twist1 also plays important roles in cancer progression, especially in cancer metastasis^{26, 67, 68}.

1.3.2 Twist1 promotes EMT in cancer

Yang *et al.*²⁶ reported that increased *Twist1* expression correlates with breast cancer cell invasion and metastasis, and suppression of *Twist1* expression inhibits the cells' capability to metastasize from the xenograft tumor cells in mammary gland to the lung. They also observed that expression of Twist1 protein in the epithelial cell lines results in partial EMT and induction of cell motility. Subsequent studies revealed that Twist1 promotes cancer cell survival, drug resistance, cancer stem-like cell number,

invadopodia formation for extracellular matrix degradation, and cancer cell transition into endothelial cells, respectively^{12, 69-72}. Previous studies revealed several regulators of *Twist1* and Twist1 target genes in breast cancer. Ling and Arlinghaus⁷³ observed that knockdown of STAT3 eliminated *Twist1* expression, which does not affect cells proliferation but impair cell invasiveness. These observations suggest that STAT3 enhances *Twist1* expression in its promotion of breast cancer progression. Another study⁷⁴ showed that activation of STAT3 increased *Twist1* expression while inhibition of STAT3 significantly reduced *Twist1* expression in the aggressive human breast cancer cell lines. This study also showed that STAT3 binds directly to the second proximal STAT3-binding site on the human *Twist1* promoter and activates *Twist1* transcription. Together with another observation that Twist1 transcriptionally induces AKT2 to promote oncogenic functions⁷⁵. Cheng et al.⁷⁰ proposed that STAT3, Twist1 and AKT2 form a functional signaling axis to enhance tumor invasion, which suggests an attractive target for cancer therapy. Interestingly, a recent study demonstrates that AKT1 inhibits EMT in breast cancer through Twist1 degradation⁷⁶. Our group found that the steroid receptor coactivator-1 (SRC-1) specifically promotes breast cancer metastasis without affecting primary tumor growth⁷⁷ in a PyMT mouse breast cancer model. Subsequent investigation revealed that SRC-1 serves as a coactivator for the transcription factor PEA3 to enhance *Twist1* expression, suggesting a molecular mechanism by which SRC-1 promotes breast cancer invasiveness and metastasis⁷⁸. A recent study showed an inverse relationship between TRIM29 and Twist1 and more importantly, TRIM29 and Twist1 inhibit each other in breast cancer cells⁷⁹. Twist1 also plays a critical role in

transducing the mechanical signal through G3BP2, which explains how matrix stiffness drives EMT and tumor metastasis⁸⁰.

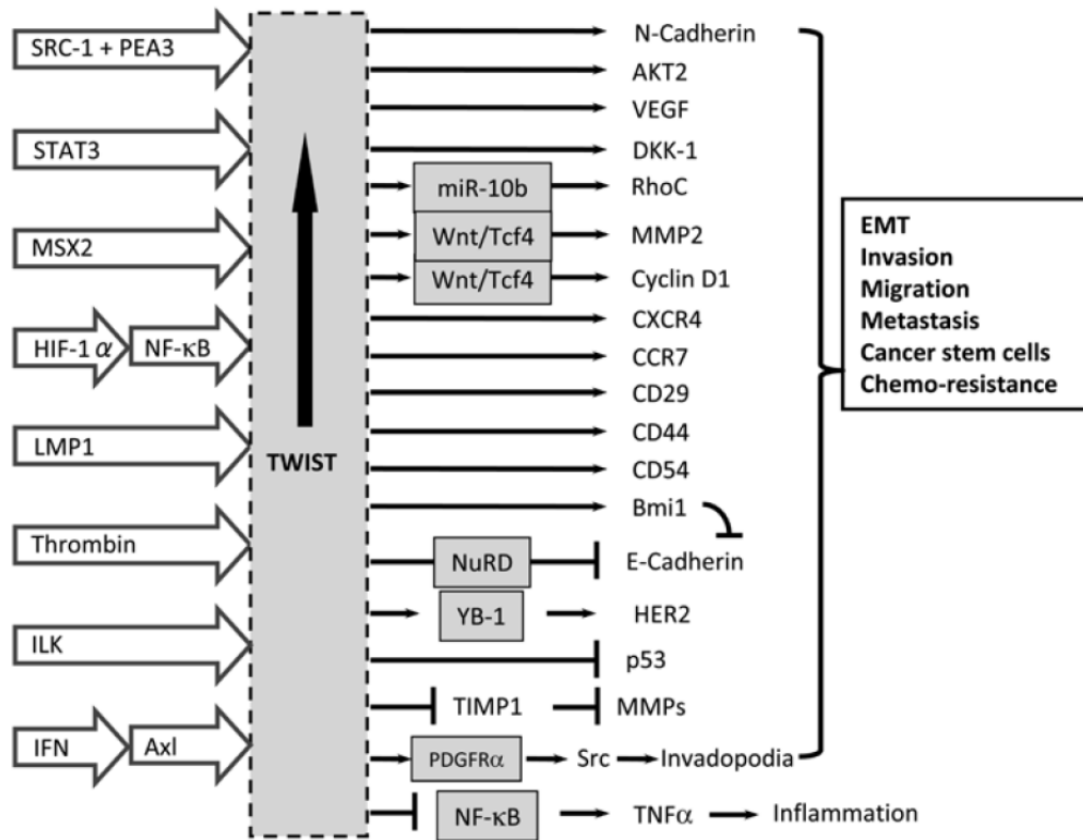


Figure 1.4. Possible regulatory network of Twist1 in cancer progression. Twist1 is activated at transcriptional and post-transcriptional levels and promotes EMT, invasion, migration, metastasis, cancer stemness and chemo-resistance through multiple signaling pathways. (From Qian Qin, Young Xu, Tao He, Chunlin Qin, Jianming Xu, Cell Research, 2011⁶⁴)

As a transcription factor, Twist1 could either activate or repress its target genes. SET8 is a member of methyltransferase family that specifically targets H4K20 for

monomethylation^{81, 82} and is implicated in regulating either activation⁸³ or repression⁸² of gene transcription. Feng Yang⁸⁴ and colleagues reported that SET8 physically associates with Twist1 to act as a dual epigenetic modifier of Twist1 target genes: repressing E-cadherin and activating N-cadherin. A recent study by Jian Shi⁸⁵ and colleagues demonstrated that Twist1 binds to BRD4 thereby constructing an activated Twist1/BRD4/P-TEFb/RNA-Pol II complex at the WNT5A promoter and enhancer to promote invasion, cancer stem cell (CSC)-like properties, and tumorigenicity of BLBC cells. Fu et al. reported that Twist1 interacts with several components of the Mi2/nucleosome remodeling and deacetylase (Mi2/NuRD) protein complex, including metastasis-associated protein 2 (MTA2), Rb-associated protein 46 (RbAp46), Mi2 and histone deacetylase 2 (HDAC2)⁶⁸. Twist1 recruits this gene repression protein complex to the E-cadherin promoter, resulting in repression of the E-cadherin promoter activity and E-cadherin expression. Another study showed that Twist1 recruited DNA methyltransferase 3B (DNMT3B) to the ER α promoter, leading to a significantly higher degree of ER α promoter methylation. Furthermore, they demonstrated that Twist1 interacted with histone deacetylase 1 (HDAC1) at the ER α promoter, causing histone deacetylation and chromatin condensation, further reducing ER α transcript levels¹².

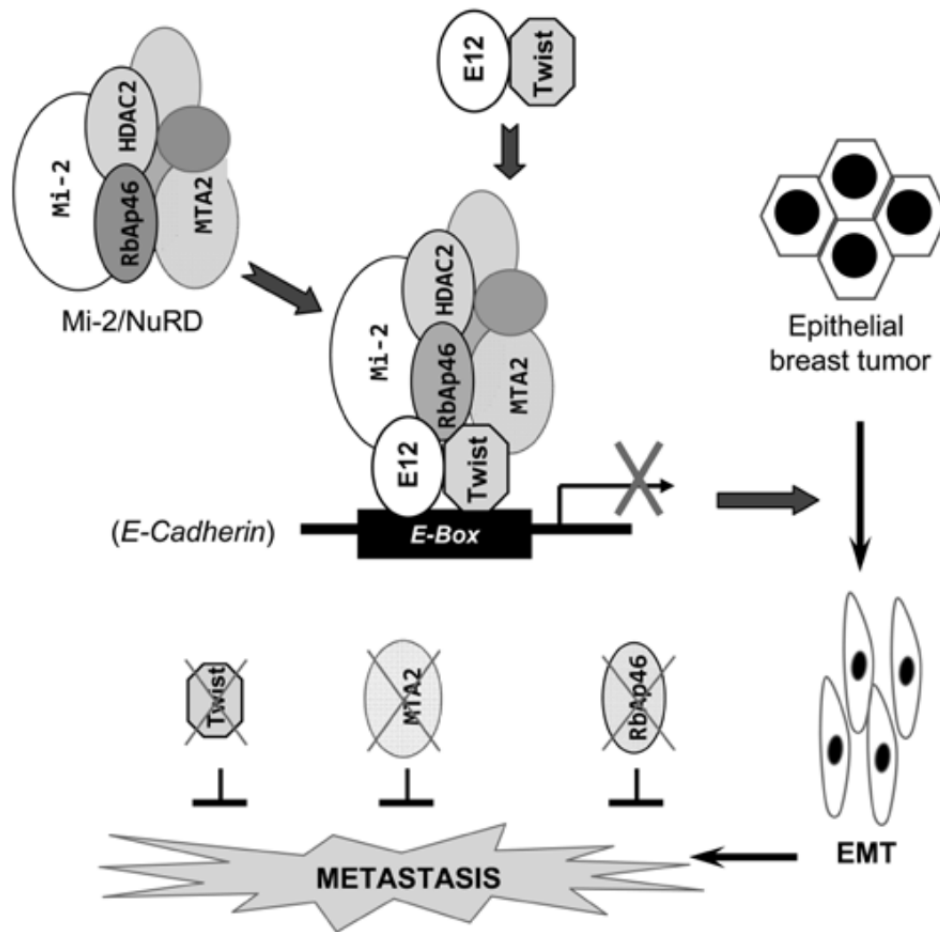


Figure 1.5. Twist1 recruits Mi-2/NuRD complex to repress E-cadherin transcription in cancer progression. Twist1 forms heterodimer with E12, and physically interact with MTA2 (metastasis-associated protein 2), RbAp46 (Rb-associated protein 46) and Mi-2 in the Mi-2/NuRD transcription repressor complex. (From Qian Qin, Young Xu, Tao He, Chunlin Qin, Jianming Xu, Cell Research, 2011⁶⁴)

1.4 Foxa1

1.4.1 Foxa1 in development

Hepatocyte Nuclear Factor (HNF) was initially cloned and purified from mammalian liver, and then found also expressed in other organs. Later on, the HNF superfamily was

identified as sharing a highly conserved central motif with that of the *Drosophila melanogaster* forkhead protein (fkh), known to bind DNA and regulate processes necessary for early fly development. The HNF transcriptional regulators represent a unique subclass of DNA binding proteins that play a critical role in tissue-specific differentiation and organogenesis⁸⁶⁻⁸⁸. The subsequent genome-wide analysis in multiple systems uncovered hundreds of forkhead transcription factors, over 40 of which were known to be expressed in mammalian systems that could be classified into more than 19 subclasses⁸⁹. To better clarify the nomenclature, the vertebrate HNF family was renamed “FOX” for Forkhead Box, with a letter showing the subclass, such as FOXA, FOXB⁹⁰. The FOXA family which contains 3 members (Foxa1, FOXA2 and FOXA3) plays pivotal roles in mammalian embryonic development and organogenesis.

Foxa1 is expressed in the liver, pancreas, bladder, prostate, colon, lung as well as mammary gland in mice. Early studies showed that Foxa1 and another family member Foxa2 display overlapping roles in development and differentiation of the pancreas, liver and neurological system. On the other hand, Foxa1 alone appears to be the master regulator in tissues that dependent on sex hormone signaling, such as the breast and prostate glands. In the developing mammary gland, Foxa1 and ER α are co-expressed within luminal epithelial cells, with strong expression observed in the terminal end buds. *Foxa1* deletion results in phenotype similar to ER α null phenotype in ductal morphogenesis but not in alveologensis. Foxa1 may also play a role in sustaining the luminal epithelium in an undifferentiated state.⁹¹

1.4.2 Foxa1 in human cancers

Foxa1 and FOXA2 were reported to play various roles in multiple human cancers, including pancreatic cancer, thyroid cancer, prostate cancer and breast cancer⁹². The relationship between Foxa1 and nuclear receptors has gained a lot of attention ever since the identification of this co-factor. Mapping of ER α specific binding sites on chromosomes 21 and 22 showed that ER α predominantly occupies enhancer-like regions near oestrogen responsive genes. And remarkably, they found forkhead motifs enriched in 56% of ER α -bound chromatin at nearby region. Further analyses revealed that Foxa1 occupies these regions even before ER α was recruited and serves as a pioneer transcription factor that facilitates an open chromatin structure in the absence of estrogen.⁹³⁻⁹⁶

Several studies have shown that Foxa1 is required for optimum expression of around 50% of ER α regulated genes and estrogen-induced proliferation.^{93, 94, 97} Sunil Badve *et al* did immunohistochemistry for Foxa1 protein in breast carcinoma tissues of 438 patients and correlated Foxa1 expression with various established disease markers and with breast cancer-specific survival. They conclude that Foxa1 expression is associated with ER α positivity, the luminal subtype A, and better breast cancer specific survival.⁹⁸ Concomitant studies showed similar result and also indicated Foxa1 is a critical determinant of ER α activity and endocrine response in breast cancer.^{99, 100}

Foxa1 is not only playing a role as ER α co-factor in breast cancer, but also has its own contribution to breast cancer progression such as repressing basal phenotype¹⁰¹, and cross-talk to ERBB2 signaling pathway¹⁰². Transient Foxa1 silencing results in a molecular profile transition toward basal phenotype and increases the in vitro aggressiveness of luminal breast cancer cells. Indeed, loss of Foxa1 may lead to growth arrest of a subpopulation of differentiated tumor cells, while the remaining cells may have greater chance to de-differentiate towards the basal phenotype. Foxa1 silencing may enrich this population, resulting in the observed shift toward the basal subtype.¹⁰¹ This notion is supported by several studies based on MMTV-PyMT model: Elaine Y. Lin et al reported that MMTV-PyMT transgenic breast cancer model developed at late stage are characterized by decreased or loss of ER α and PR expression¹⁰; and Kasi McCune et al further discovered tumor transition from luminal A subtype to luminal B subtype concomitant with decreased ER α and Foxa1 expression¹¹. However, the underlying mechanisms of Foxa1 silencing are still unknown.

In this study, we examined the endogenous Twist1's function in breast cancer progression using a novel RCIP-TVA system-mediated tumor cell specific knockout of *Twist1*. We found that specific knock out of *Twist1* in mammary gland tumor cells does not influence tumor initiation or growth but significantly decreased tumor EMT and metastasis. We also identified *Foxa1* as a direct target of Twist1 in breast cancer. Twist1 inhibits *Foxa1* expression at transcriptional level and promotes breast cancer cell basal-like phenotype, invasiveness and metastasis.

2. MATERIAL AND METHODS

2.1 The TVA/RCIP system for induction of mouse mammary gland tumorigenesis with tumor cell-specific *Twist1* knockout

The Cre DNA fragment with a Not I and an Asc I sites was amplified by PCR, and a small IRES DNA fragment^{103, 104} with an Asc I and a Pac I sites was chemically synthesized. These two fragments were cloned to the upstream of the PyMT-HA coding sequence through a Not I and a Pac I sites in the RCAS-PyMT avian-viral vector¹⁰⁵. The constructed RCAS-Cre-IRES-PyMT-HA (RCIP) vector was transfected into DF1 cells to produce RCIP avian virus as described previously^{105, 106}. The MMTV-TVA transgenic mouse line was described previously¹⁰⁵. MMTV-TVA mice were crossbred with the ROSA26R Cre reporter mice^{107, 108} to generate MMTV-TVA;ROSA26R bi-genic mice. MMTV-TVA mice were also crossbred with *Twist1*^{F/F} mice obtained from Mutant Mouse Regional Resource Centers (016842-UNC)^{63, 109} to generate MMTV-TVA control (MMTV-TVA;*Twist1*^{+/+}) and MMTV-TVA;*Twist1*^{F/F} mice. All mice used in experiments were backcrossed at least for two generations in FVB strain background. PCR-based genotype analyses were carried out as described previously for the WT, floxed and deleted *Twist1* alleles¹⁰⁹, the ROSA26R Cre reporter allele^{107, 108} as well as the MMTV-TVA transgene¹⁰⁵. PCR primers were listed in Supplemental Table S1. For inducing mammary tumorigenesis, RCIP virus was intraductally introduced into the 4th mammary gland(s) of mice as described previously^{105, 106}. The injected mice were closely examined for mammary tumor initiation by palpation, tumor growth by

estimating tumor volume, and distant metastasis by eye and microscopic examinations as described previously^{68, 110}. Mice with mammary tumors were sacrificed 12 or 18 weeks after viral injection. Mice were euthanized according to the NIH guidelines. The animal protocols were approved by the IACUC of Baylor College of Medicine.

2.2 Western blot

Western blot was carried out as described previously^{63, 111}. Briefly, 20 µg of protein in cell lysate was separated in SDS-PAGE gel and blotted onto a nitrocellulose membrane. After being blocked with phosphate-buffered saline containing 5% bovine serum albumin (BSA), the membrane was incubated with a primary antibody overnight at 4°C. These primary antibodies included antibodies against Twist1 (ab50887), Foxa1 (ab23738), c-FOS (ab53036, Abcam, Cambridge, MA), E-cadherin (610182, BD Bioscience, San Jose, CA), VIMENTIN (5741), c-JUN (9165), HA (3724, Cell Signaling, Danvers, MA) and β-actin (Sigma, St Louis, MO). Then, the membrane was washed 3 times in phosphate-buffered saline with Tween-20 (PBST) and incubated with horseradish peroxidase (HRP) conjugated secondary antibody (Bio-rad, Hercules, CA) for 1 hour. In certain assays, the TrueBlot Western Blot Kit (eBioscience, San Diego, CA) with the secondary antibody was used to eliminate IgG bands according to the manufacture's instruction. Finally, the membrane was incubated with the SuperSignal West Pico Chemiluminescent Substrate (30479; Thermo Scientific, Rockford, IL) and imaged by exposing to X-ray films.

Western blot was carried out as described previously^{63, 111}. Briefly, 20 µg of protein in cell lysate was separated in SDS-PAGE gel and blotted onto a nitrocellulose membrane. After being blocked with phosphate-buffered saline containing 5% bovine serum albumin (BSA), the membrane was incubated with a primary antibody overnight at 4°C. These primary antibodies included antibodies against Twist1 (ab50887), Foxa1 (ab23738), c-FOS (ab53036, Abcam, Cambridge, MA), E-cadherin (610182, BD Bioscience, San Jose, CA), VIMENTIN (5741), c-JUN (9165), HA (3724, Cell Signaling, Danvers, MA) and β-actin (Sigma, St Louis, MO). Then, the membrane was washed 3 times in phosphate-buffered saline with Tween-20 (PBST) and incubated with horseradish peroxidase (HRP) conjugated secondary antibody (Bio-rad, Hercules, CA) for 1 hour. In certain assays, the TrueBlot Western Blot Kit (eBioscience, San Diego, CA) with the secondary antibody was used to eliminate IgG bands according to the manufacture's instruction. Finally, the membrane was incubated with the SuperSignal West Pico Chemiluminescent Substrate (30479; Thermo Scientific, Rockford, IL) and imaged by exposing to X-ray films.

2.3 X-gal staining

The RCIP virus-infected inuinal mammary glands of MMTV-TVA;ROSA26R mice were collected on day 3, 21 or 48 after the virus was introduced. The mammary glands were slightly fixed and stained by X-gal as described previously¹¹². The X-gal-stained mammary glands were further fixed in 4% paraformaldehyde (PFA), washed in

phosphate-buffered saline (PBS), dehydrated in ethanol and embedded in paraffin blocks as described ¹¹². Five- μm thick tissue sections were prepared and used for H&E staining.

2.4 Cell culture

DF1 chicken fibroblast cells, HEK293T human embryonic kidney cells and MCF7 human breast cancer cells were cultured in MDEM medium containing 10% of fetal bovine serum (FBS). BT549 cells were cultured in RPMI-1640 medium with 10% of FBS. SUM1315 cells were cultured in Hyclone Nutrient Mixture with 5% of FBS, 5 $\mu\text{g/ml}$ of insulin and 10 ng/ml of epidermal growth factor. All cells were cultured at 37°C in a tissue culture incubator supplied with 5% CO_2 .

2.5 Circulating Tumor Cell (CTC) culture

About one milliliter of blood sample was collected from each mouse with mammary gland tumors. CTCs were enriched by removing red blood cells using RBC lysis buffer (420301, Biolegend, San Diego, CA) according to the manufacture's instruction. CTCs were cultured in MDEM medium containing 10% of fetal bovine serum (FBS) at 37°C in a tissue culture incubator supplied with 5% CO_2 for 2 weeks. CTCs that form colonies which contain more than 10 cells were counted and colony numbers from two groups of mice were analyzed with student T-test.

2.6 H&E staining, immunohistochemistry (IHC) and immunohistofluorescence

(IHF)

Mammary tumors and/or lungs were dissected from euthanized MMTV-TVA;*Twist1*^{F/F} and MMTV-TVA mice as well as SCID mice injected with MCF7^{Ctrl}, MCF7^{Twist1} and MCF7^{Twist1+Foxa1} cells. Isolated tissues were fixed overnight at 4°C in 4% PFA, washed in PBS, dehydrated in ethanol and embedded in paraffin blocks. Five-µm thick tissue sections were prepared and used for H&E staining, IHC and IHF as described previously^{63, 113}. Lung sections used for estimating metastasis extent were prepared as we described previously^{77, 114}. For antibodies with a mouse origin, the M.O.M Mouse-on-Mouse Immunodetection kit (Vector Laboratories, Burlingame, CA) was used to block the immunostaining background from the endogenous mouse IgG. This study used the primary antibodies against Twist1 (ab50887), Foxa1 (ab23738, Abcam, Cambridge, MA), E-cadherin (610182, BD Bioscience, San Jose, CA), VIMENTIN (5741) and HA (3724, Cell Signaling, Danvers, MA). The secondary antibodies for IHC were biotinylated anti-Rabbit IgG and biotinylated anti-mouse IgG (Vector Laboratories, Burlingame, CA), which were used at a 1:400 dilution. The immunostaining signal was enhanced by using the VECTASTAIN ABC system (PK-6100, Vector Laboratories, Burlingame, CA), and then visualized by using the DAB kit (SK-4103, Vector Laboratories, Burlingame, CA). The tissue slides were counterstained with Harris Modified Hematoxylin and mounted with Permount. Double IHF was performed using the Tyramide Signal Amplification kit (Life technologies, Grand Island, NY) according

to the manufacturer's instructions. Stained tissue slides were examined and imaged under appropriate microscopes. Tumor and lung areas in the lung images were measured by using the NIH ImageJ software as described previously^{77, 114}.

2.7 Quantitative RT-PCR (qPCR)

Total RNA was isolated from WT/RCIP and *Twist1*^{TKO}/RCIP mammary tumors and BT549, Sum1315, MCF7, MCF7^{Ctrl}, MCF7^{Twist1} and MCF7^{Twist1+Foxa1} cells using the TRIZOL reagent (Life technologies, Grand Island, NY). Reverse transcription was performed with 1 µg of RNA by using the Reverse Transcriptase Core kit (Eurogentec; Fremont, CA). qPCR was performed by using the matched Universal Taqman probes (Roche, Nutley, NJ) and gene-specific primer pairs (Table 2.1). The measurement of 18 S or β-actin mRNA was used as an endogenous normalizer.

2.8 Genomic DNA extraction from paraffin embedded samples

Genomic DNA was isolated from lung paraffin sections of both groups of mice using QIAamp DNA FFPE Tissue Kit (56404, Qiagen, Hilden, Germany). The genomic DNA was used for PCR analysis of the *Twist1* gene knockout allele.

2.9 Micro-vascular density calculation

Microvascular density was determined as described previously¹¹⁵. In brief, blood vessels were visualized by CD31 immunohistochemistry in the tissue sections prepared from mouse tumors. Tumor areas which contain greatest vessel density were defined as hot spots regions. Images of hot spots regions were taken under a microscope at 200× magnification. Any stained endothelial cells were counted to represent a single vessel if it was clearly separated from adjacent microvessels and other connective tissue elements.

2.10 Plasmids and cell transfection

For constructing the Foxa1-Luc promoter-reporter plasmid, the 1.5 kb 5' regulatory sequence of the human *Foxa1* gene was amplified by PCR using specific primers (Supplemental Table S1) from the genomic DNA of MCF7 cells and subcloned into the Kpn I and Nco I sites of the pGL3-basic-luciferase plasmid. The human E-cadherin-Luc and CSF1-Luc plasmids were described previously^{68, 106}. The pCDNA-Twist1-2×flag expression plasmid was constructed by subcloning human *Twist1* cDNA into the pCDNA-2×flag plasmid. The pCDH-Foxa1 plasmid was a gift from Dr. Bin He at Baylor College of Medicine.

For assaying the activity of a promoter-reporter construct, MCF7 cells were transfected

with the expression vectors and promoter-luciferase reporter plasmid as indicated in the Results section using the polyethylenimine reagent (23966-2, Polyscience, Niles, IL) ¹¹⁶. The transfected cells were harvested 24 hours and lysed with the Reporter Lysis buffer (Promega, Madison, WI) for luciferase assay as described ¹⁰⁶. The relative luciferase activity was normalized to the total amount of protein assayed.

To generate MCF7^{Twist1} cell lines, MCF7 cells were transfected with pCDNA-2×flag and pCDNA-Twist1-2×flag plasmids using the Polyethylenimine reagent. Transfected cells were cultured in DMEM medium containing 2 µg/ml of Hygromycin for 2 weeks. To generate MCF7^{Twist1+Foxa1} cell lines, two MCF7^{Twist1} cell lines were transfected with pCDH-Foxa1 plasmid and growth-selected for 14 days in DMEM medium containing 4 µg/ml of Puromycin. The surviving colonies in each experiment were individually isolated, expanded in growth medium and analyzed by Western blot.

In siRNA-based knocking down experiments, non-targeting control siRNAs and siRNAs targeting human *Twist1* and *c-Fos* mRNAs were purchased from Dharmacon (Lafayette, CO). BT549, Sum1315 and MCF7 cells were transfected with siRNAs using the HiPerFect Transfection Reagent (301705, QIAGEN, Valencia, CA).

Knockdown of Twist1 mRNA by stable expression of shRNAs: pGIPZ-shCtrl lentiviral vector coding for a non-targeting shRNA (5'-CTTACTCTCGCCCAAGCGAGAG) and 2 pGIPZ-shTwist1 lentiviral vectors coding for two different Twist1 mRNA-targeting

sequences (TGAATGCATTTAGACACCG and AGAGGAAGTCGATGTACCT) were obtained from the Cell-Based Assay Screening Service Core at Baylor College of Medicine. Lentivirus was packaged in 293T cells transfected with pMD2.G, psPAX2, and pGIPZ shRNA vectors in the ratio of 1:3:4. The culture medium was refreshed 6 hours after transfection. 24 hours after transfection, the medium containing viral particles was collected and polybrene was added to a concentration of 4 μ g/ml for infecting cells. SUM1315 and MDA-MB-436 cells were infected with the prepared viral particles and selected in the culture medium containing 1 μ g/ml of puromycin for 10 days. Survived cells were expanded and used for experimental analysis.

2.11 ChIP assay

The DNA-bound proteins in BT549, Sum1315, MCF7^{Ctrl} and MCF7^{Twist1} cells were cross-linked using 1% formaldehyde for 10 minutes. ChIP assays were performed as described previously^{68, 106}. Antibodies used in these ChIP assays were for Twist1 (ab50887), c-JUN (ab31419, Abcam, Cambridge, MA), MTA2 (28791), HDAC2 (7899x, Santa Cruz, Dallas, TX), c-FOS (2250, Cell Signaling, Danvers, MA), Histone H3K9ac (39585, Active motif, Carlsbad, CA), RNA pol II (PLA0127, Sigma-Aldrich, St. Louis, MO) and M2 Flag antibody beads (A2220, Sigma-Aldrich, St. Louis, MO). ChIP-grade mouse IgG and rabbit IgG (Abcam, Cambridge, MA) were used as negative controls. The sequences of PCR primers used for amplifying the precipitated DNA samples are listed in Table 2.1.

2.12 Cell migration and invasion assays

Cell migration and invasion capabilities were measured as described previously⁷⁸. Briefly, individual cell migration was directly traced in a 96-well plate for 18 hours using the Cell Motility HCS Reagent kit (K08-000-11, Thermo Scientific, Rockford, IL). The track areas on the electronic images were quantitatively measured using the Image J software. Cell invasion was assayed by using BioCoat Matrigel Invasion Chambers (BD Biosciences, San Jose, CA). A total of 25,000 cells were seeded in each upper chamber with serum-free DMEM medium and the lower chamber was filled with DMEM containing 5% FBS. After cultured for 24 hours, non-migrating cells on the upper chambers were removed by a cotton swab, and cells invaded through the Matrigel layer to the underside of the membrane were stained with crystal violet and counted.

2.13 *In vivo* metastasis assay

MCF7^{Ctrl}, MCF7^{Twist1} or MCF7^{Twist1+Foxa1} cells (1×10^6) were injected into 8-week-old female SCID mice through the tail vein. These mice were sacrificed in 4 weeks after the injection. Their lung tissues were collected, photographed and processed for paraffin section. Metastasis was evaluated by counting the visible metastatic foci on the lung surface and measuring metastasis tumor area versus the lung area on H&E-stained lung sections as described previously^{77,114}.

2.14 Statistical analyses

All data were collected from several independent experiments. Each assay was performed in triplicate whenever applicable. All data were expressed as Mean \pm SEM. Prism 4 Software (GraphPad, La Jolla, CA) was used to perform Student's t test to analyze the data sets of mRNA level, tumor volume, luciferase activity, cell migration and invasion, metastatic tumor number and index. Log-rank test was used to analyze the data sets of mouse tumor-free survival and human breast cancer patient DMFS. Fisher's exact test was used to analyze the data sets of Foxa1 IHC scores. Person's Correlation test was used to analyze the *Twist1* and *Foxa1* expression data sets. In all statistical analyses, $p < 0.05$ was considered significant.

Oligo Names	Sequences	TaqMan Probe #
Twist1 genotyping 112	agcggatcatagaaaacagcc	N/A
Twist1 genotyping 114	ccggatctatttgcattttaccatgggtca tc	N/A
Twist1 genotyping 115	cctctacctgaccgttagatggactcgg	N/A
TVA genotyping F	ctgctgcccggtaacgtgaccgg	N/A
TVA genotyping R	gccttggggaaggtcctgccc	N/A
Mouse Twist1 F	agctacgccttctccgtct	58
Mouse Twist1 R	tccttctctggaacaatgaca	58
Mouse Foxa1 F	gaacagctactacgcggaca	82
Mouse Foxa1 R	cggagttcatgttgctgaca	82
Mouse 18S F	ctcaacacgggaacctcac	77
Mouse 18S R	cgctccaccaactaagaacg	77
Mouse ACTB F	ctaaggccaaccgtgaaaag	64
Mouse ACTB R	accagaggcatacagggaca	64
Human Twist1 F	gggccggagacctagatg	50
Human Twist1 R	ttccaagaaaatctttggcata	50
Human Foxa1 F	cccccttctctctctacc	81
Human Foxa1 R	ctgcaaagcaagaagcagagt	81
Human c-Fos F	actaccactcaccgcagac	67
Human c-Fos R	ccaggtccgtgcagaagt	67
Human MMP9 F	tcttccctggagacctgaga	27
Human MMP9 R	gagtgtaacatagcgggtacagg	27
Human ITGA5 F	ccgtgtggttttaggtggac	68
Human ITGA5 R	ttgatcaggctactcggggtaa	68
Human ITGA v F	catgtcctcttatacaattttactgg	46
Human ITGA v R	gcagctacagaaaatccgaaa	46
Human ITGB1 F	caagttgcagtttggtgatca	66
Human ITGB1 R	agtgaaacccggcatctg	66
Human ITGB3 F	gcaagatcacgggcaagta	2
Human ITGB3 R	ggagtcacacaggcagtc	2
Human ACTB F	attggcaatgagcgggtc	11
Human ACTB R	cgtggatgccacaggact	11
Human 18S F	gaggccgtaggcttattgtg	11
Human 18S R	gagtagctcatatgtcttccctacct	11
Human CSF1 ChIP F	cttctggcactccgagaat	N/A
Human CSF1 ChIP R	tccaggctgattcagtgcta	N/A
Human CDH1 ChIP F	ccaagtgtaaaagccctttctg	N/A
Human CDH1 ChIP R	ttgctagggtctaggtgggta	N/A
Human Foxa1 ChIP 5k F	agtaggggaaaagacaaaaccagt	N/A
Human Foxa1 ChIP 5k R	gcttgtgtctgtgtctttgtgt	N/A
Human Foxa1 ChIP 4k F	cctgctaataatggaaggacctgt	N/A
Human Foxa1 ChIP 4k R	gatattcaccaggcaggtagaagc	N/A
Human Foxa1 ChIP 3k F	catcacgctatgaaaagtggattt	N/A
Human Foxa1 ChIP 3k R	caaatgttcttttagcccactcc	N/A
Human Foxa1 ChIP 2k F	gcagtacaacaaacacatggtcac	N/A
Human Foxa1 ChIP 2k R	gttggtgatagattgggagatggt	N/A
Human Foxa1 ChIP 1k F	gtgctgtgactcacctgctcttag	N/A
Human Foxa1 ChIP 1k R	ccacttttctctctcactagaaa	N/A
Human Foxa1-Luc F	tgggtaccgtccaggaccgattaggaacc	N/A
Human Foxa1-Luc R	gcccattggatacaacctccagccctgtg	N/A

Table 2.1. Oligonucleotide primers and probes for PCR

3. RESULTS*

3.1 A new mouse model system for simultaneous deletion of the floxed alleles and expression of an oncogene in a subset of the mouse mammary epithelial cells

Du et al. has previously generated MMTV-TVA mouse line, in which the transgene for the *tva* avian virus subgroup A receptor is driven by MMTV (mouse mammary tumor virus) promoter and specifically expressed in the mammary gland luminal epithelial cells¹⁰⁵. Intraductal instillation of the avian leukosis virus RCAS (replication-competent avian sarcoma-leukosis virus LTR splice acceptor) carrying PyMT caused the infection of a small subset of the TVA-expressing mammary epithelial cells in MMTV-TVA mice, resulting in rapid mammary tumorigenesis¹⁰⁵. In order to inactivate a floxed gene of interest in the mammary tumor cells induced by the MMTV-TVA/RCAS-PyMT system, we constructed the RCAS-Cre-IRES-PyMT (RCIP) vector (Fig. 3.1A) and generated RCIP avian virus with this vector. Western blot analysis revealed that both Cre and PyMT proteins were expressed in the RCIP virus-infected DF1 cells but not in the RCAS control virus-infected DF1 cells (Fig. 3.1B). These results demonstrate that the RCAS promoter is strong enough to drive both Cre and PyMT protein expression after the viral DNA is integrated into the cell genome.

* Part of the data reported in this section is reprinted from “Twist1 Promotes Breast Cancer Invasion and Metastasis by Silencing Foxa1 Expression” by Yixiang Xu *et al*, 2016. Oncogene, Epub ahead of print. Yixiang Xu retains the copyright of the article as stated on the publisher’s website.

Next, we generated MMTV-TVA;ROSA26R bi-genic mice by crossbreeding MMTV-TVA and ROSA26R mice and injected RCIP avian virus into the mammary gland ducts of these mice. The ROSA26R locus contains a floxed transcriptional STOP sequence that silences the β -galactosidase (β -gal) expression and thus, serves as a reporter for Cre activity^{107, 108}. The mammary glands were isolated on the 3rd, 21st and 48th days post viral injection and analyzed by X-gal staining and histopathological examination (Fig. 3.1C). In the virus-injected mammary glands of MMTV-TVA;ROSA26R female mice, individually scattered β -gal-positive mammary gland epithelial cells were detected by day 3. One to multiple epithelial hyperplasia lesions consisting of only the β -gal-positive cells were developed by day 21 and invasive mammary gland tumors with β -gal-positive cells were formed by day 48 (Fig. 3.1D). Double immunofluorescent staining revealed that both PyMT and β -gal proteins were co-expressed in these tumor cells, indicating these tumor cells were derived from RCIP virus-infected mammary epithelial cells and Cre expressed in these cells worked effectively (Fig. 3.1E). In contrast, no β -gal-positive or PyMT-positive mammary epithelial cells or tumor cells were observed in the MMTV-TVA;ROSA26R mouse mammary glands without viral injection or in the ROSA26R mouse mammary glands with injection of RCIP virus (data not shown). These results demonstrate that the MMTV-TVA/RCIP (hereafter designated as TVA/RCIP) system is fully capable to express both Cre and an oncogene in the same mammary epithelial cells for simultaneous and effective deletion of a floxed gene and induction of tumorigenesis.

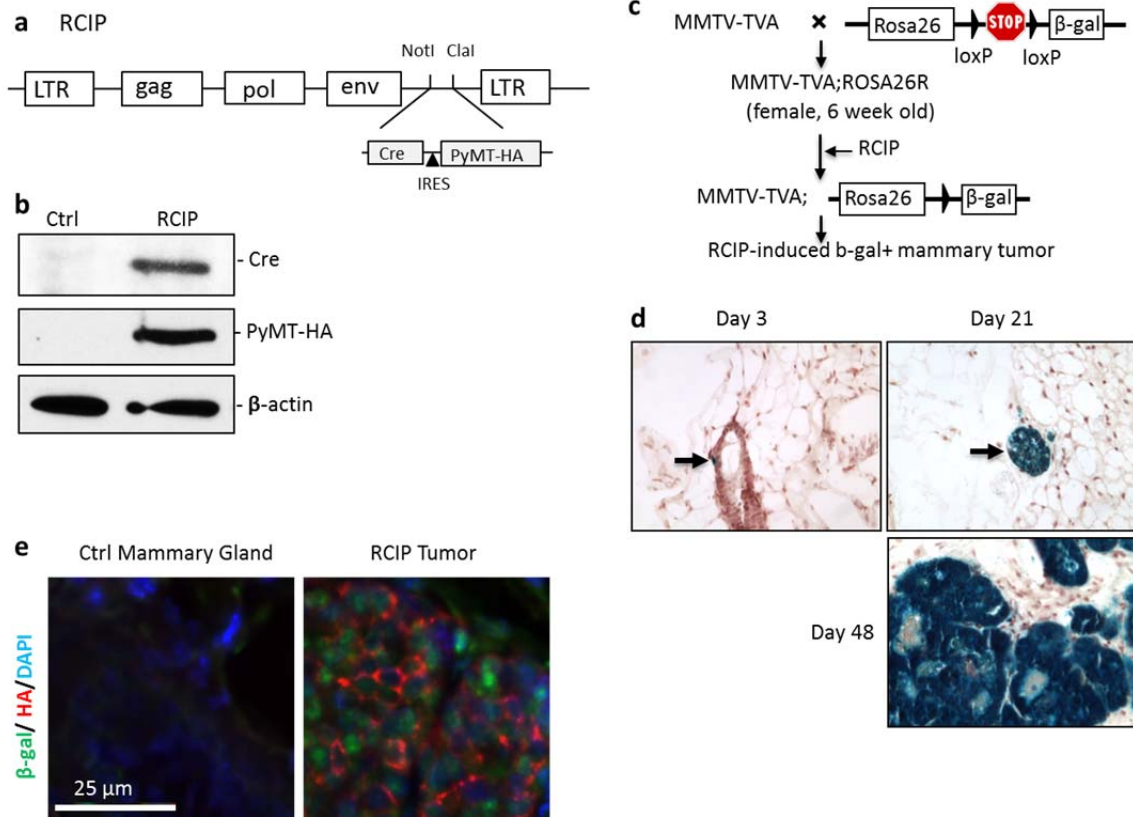


Figure 3.1. The mammary tumorigenesis mouse model induced by the novel MMTV-TVA/RCIP system. **A.** The RCAS-Cre-IRES-PyMT-HA (RCIP) vector of the avian virus. **B.** Detection of both Cre and PyMT-HA proteins in the RCIP vector-transfected DF1 cells by Western blotting, while these proteins were not present in the untransfected DF1 (Ctrl) cells. **C.** The strategies to induce β -gal-labeled mammary tumors in the female MMTV-TVA;ROSA26R mice by using the RCIP system. **D.** X-gal staining to show RCIP virus-infected and induced mammary tumor cells (blue color) in the mammary glands of MMTV-TVA;ROSA26R mice after intraductal injection of RCIP virus for 3, 21 and 48 days. **E.** Double immunofluorescence (IF) staining for PyMT-HA (red) and β -gal (green) in a RCIP-induced mammary tumor isolated from MMTV-TVA;ROSA26R mice. A section of a mammary gland isolated from a normal female mouse served as a negative control for HA and β -gal IF staining.

3.2 Tumor specific knock-out of *Twist1* using TVA/RCIP system in *Twist1*-floxed mice

To knockout *Twist1* in PyMT-induced mammary tumor cells by using TVA/RCIP system, we generated female MMTV-TVA and MMTV-TVA;*Twist1*^{F/F} mice with the same strain background by crossbreeding MMTV-TVA and the floxed *Twist1* (*Twist1*^{F/F}) mice^{63, 105, 109}. To get *Twist1*^{TKO}/RCIP tumors (RCIP-induced tumors with tumor cell-specific *Twist1* knockout), we injected RCIP virus into the ductal lumens of either one or two of their 4th mammary glands, when MMTV-TVA;*Twist1*^{F/F} mice were 8 weeks old. PyMT oncogene induces tumorigenesis only in the *Twist1* knockout mammary epithelial cells (Fig. 3.2A). MMTV-TVA mice were used as control group to get WT/RCIP tumors.

To evaluate *Twist1* knockout efficiency, we prepared genomic DNA, RNA and protein samples from RCIP virus-induced mammary tumors, and performed genotype, Q-PCR and Western blot analyses. As expected, genotype analysis only detected wild type *Twist1* allele in WT/RCIP tumors, but detected both the deleted and the floxed *Twist1* alleles in *Twist1*^{TKO} tumors due to the presence of both the tumor cells with *Twist1* deletion and the non-tumor cells with the floxed *Twist1* in the tumor tissues (Fig. 3.2B). Q-PCR analysis detected a 14-fold decrease in *Twist1* mRNA expression in *Twist1*^{TKO}/RCIP tumors compared with WT/RCIP tumors (Fig. 3.2C). Western blot analysis revealed a significant reduction of Twist1 protein in *Twist1*^{TKO}/RCIP tumors

versus WT/RCIP tumors (Fig. 3.2D). We further performed immunostaining and confirmed that variable levels of Twist1 protein was expressed in a sub-population (~6%) of tumor cells and certain stromal cells in WT/RCIP tumor tissues, but Twist1 protein was only detected in the stromal cells in *Twist1^{TKO}*/RCIP tumor tissues. Moreover, Twist1 and PyMT-HA double positive tumor cells were observed in WT/RCIP tumors, while only PyMT-HA single positive tumor cells were seen in *Twist1^{TKO}*/RCIP tumors (Fig. 3.2E). These results demonstrate that Twist1 is expressed in a subset of mammary tumor cells and certain stromal cells in WT/RCIP tumors, while in *Twist1^{TKO}*/RCIP tumors Twist1 was completely knocked out in the tumor cells but normally expressed in the infiltrating stromal cells.

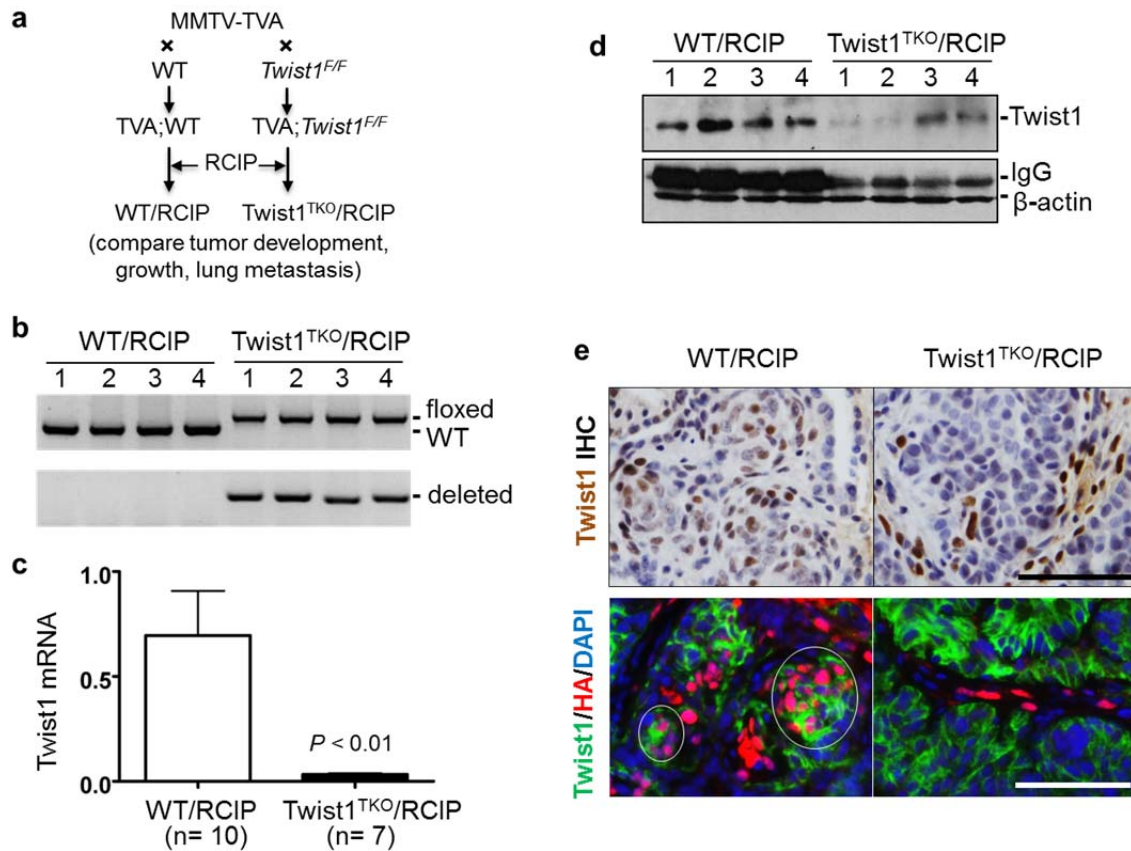


Figure 3.2. Mammary tumor cell-specific knockout of *Twist1* in mice. **A.** Experimental strategies to induce mammary tumors with and without TKO of *Twist1* using the MMTV-TVA/RCIP system. TVA, MMTV-TVA mice; WT, wild type mice. **B.** PCR-based analysis of the wild type (WT), floxed (*Twist1^F*) and Cre-deleted (*Twist1^{TKO}*) *Twist1* alleles in WT/RCIP and *Twist1^{TKO}/RCIP* mouse mammary tumors. **C.** Q-PCR-based analysis of *Twist1* mRNA in WT/RCIP and *Twist1^{TKO}/RCIP* mouse mammary tumors. Data are presented as Mean ± SEM. **D.** Western blot analysis of *Twist1* protein in WT/RCIP (n=4) and *Twist1^{TKO}/RCIP* (n=4) mammary tumors. The β -actin served as an endogenous loading control. The mouse IgG band was recognized by the secondary antibody. **E.** Detection of *Twist1* (brown) by IHC in both tumor and stromal cells in WT/RCIP tumors but only in stromal cells in *Twist1^{TKO}/RCIP* tumors (upper panels). In lower panels, double IF staining detected *Twist1* (arrowheads) in PyMT-HA-expressing tumor cells in WT/RCIP tumors, but no *Twist1* in PyMT-HA-expressing tumor cells in *Twist1^{TKO}/RCIP* tumors. Scale bars, 50 μ m.

3.3 Specific ablation of *Twist1* in the PyMT-induced mammary tumor cells does not affect primary tumor development in mice

Palpable mammary tumors were detected in both genotype groups of mice within 6-10 weeks after viral injection, showing no difference in the latency of tumor initiation between MMTV-TVA;*Twist1*^{F/F} and MMTV-TVA mice (Fig. 3.3 A). Thirty-five and 26 tumors were developed from 60 virus-infected mammary glands in MMTV-TVA;*Twist1*^{F/F} mice and 42 virus-infected mammary glands in MMTV-TVA mice, respectively. The tumorigenic rate was about 60% for both groups. These results indicate that specific inactivation of *Twist1* in the mammary epithelial cells does not affect PyMT-induced mammary tumor formation.

We measured tumor growth for 10 weeks after a palpable tumor was detected in the RCIP virus-infected mammary gland of MMTV-TVA;*Twist1*^{F/F} or MMTV-TVA mice. The tumor growth data was only collected from mice bearing a single tumor. We found that the average tumor growth rates in the two groups of mice were very similar (Fig. 3.3B). Cell proliferation rates assayed by Ki67 immunohistochemistry also showed no significant difference between *Twist1*^{TKO}/RCIP mammary tumors isolated from MMTV-TVA;*Twist1*^{F/F} mice and WT/RCIP mammary tumors (RCIP-induced tumors with wild type *Twist1*) isolated from MMTV-TVA mice (Fig. 3.4A). Analysis of cell apoptosis by cleaved-caspase 3 staining and macrophage recruitment by F4-80 staining also revealed no difference between these two groups (Fig. 3.4 B&C). These results indicate

that the autonomous cellular function of *Twist1* is not required for the growth of PyMT-induced mammary tumors in mice.

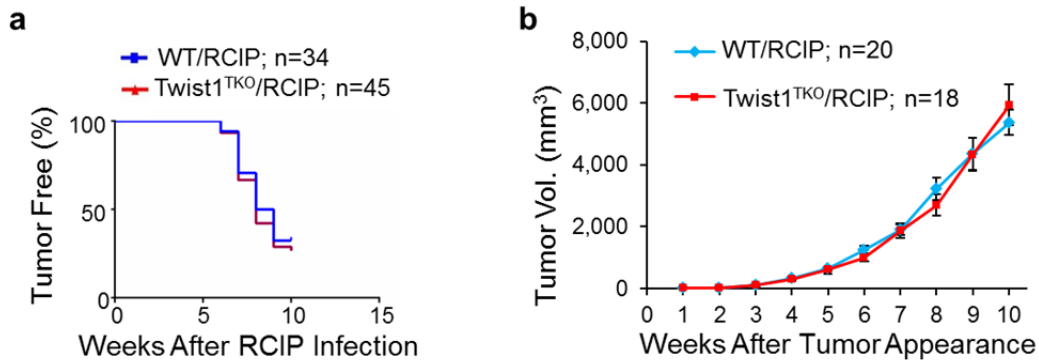


Figure 3.3. Tumor cell-specific knockout (TKO) of *Twist1* does not influence tumor initiation or growth in mice. **A.** Tumor-free survival curves for WT/RCIP (RCIP-infected MMTV-TVA mice) and *Twist1*^{TKO}/RCIP (RCIP-infected MMTV-TVA;*Twist1*^{F/F} mice) mice. Mammary tumor development was monitored by palpation. **B.** WT/RCIP and *Twist1*^{TKO}/RCIP mammary tumor growth curves generated by measuring tumor volumes (Vol.) once a week after palpable tumors were detected.

3.4 Specific ablation of *Twist1* in the PyMT-induced mammary tumor cells inhibits lung metastasis

Next, we examined lung metastasis in the RCIP virus-infected MMTV-TVA and MMTV-TVA;*Twist1*^{F/F} mice in which a palpable tumor had grown for 10 weeks. We observed lung metastases in 67% (12/18) of MMTV-TVA mice with 5.38 metastatic foci/lung in average number. However, we only observed lung metastases in 39% (7/18) of MMTV-TVA;*Twist1*^{F/F} mice with 0.38 metastatic foci/lung in average (Fig. 3.5A). On the lung tissue sections, the

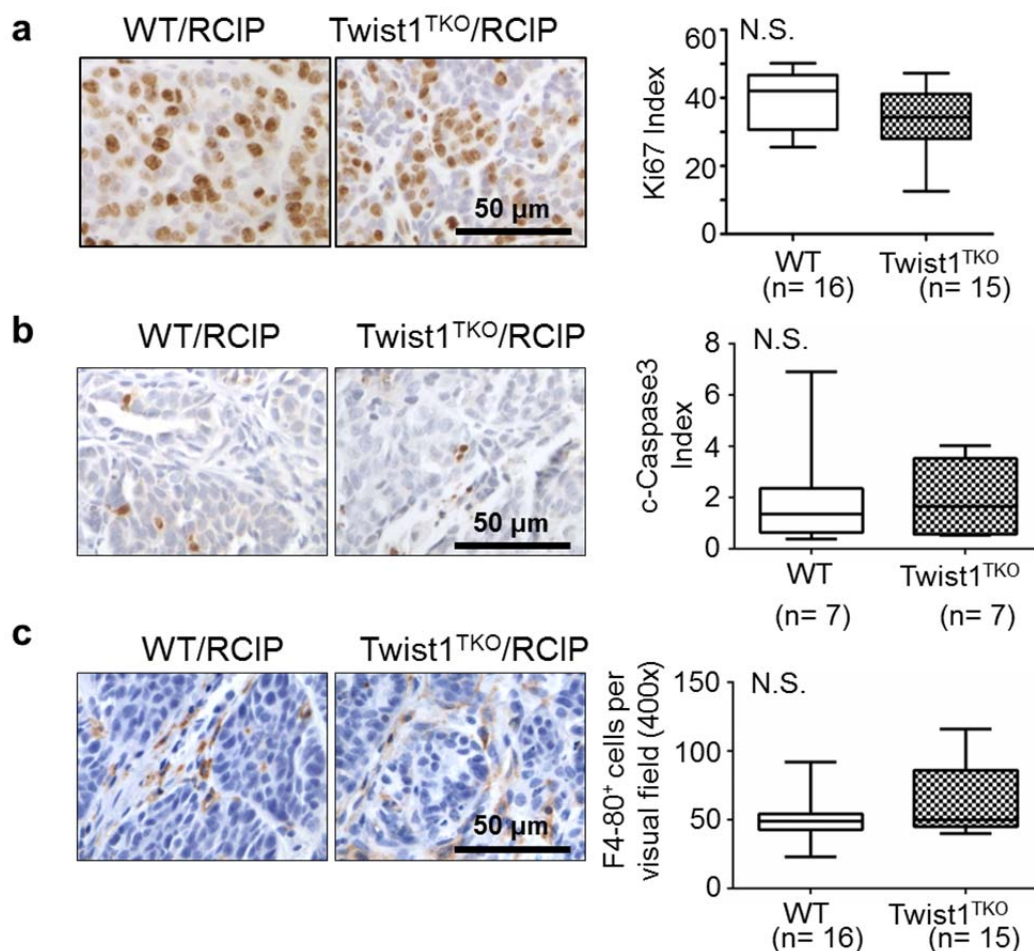


Figure 3.4 IHC staining of primary tumors. **A.** Representative images of Ki67 IHC on WT/RCIP and *Twist1*^{TKO}/RCIP primary tumor sections and the quantification of staining result. **B.** Representative images of c-Caspase3 (cleaved caspase3) IHC on WT/RCIP and *Twist1*^{TKO}/RCIP primary tumor sections and the quantification of staining result. **C.** Representative images of F4-80 IHC on WT/RCIP and *Twist1*^{TKO}/RCIP primary tumor sections and the quantification of staining result.

average percentage of metastasis area to total lung area, which is an index for metastasis extent, was also drastically reduced in MMTV-TVA;*Twist1*^{F/F} mice versus MMTV-TVA mice (Fig. 3.5B). These results demonstrate that *Twist1* null mammary tumor cells have a drastically decreased metastasis capability compared with *Twist1* WT mammary tumor cells.

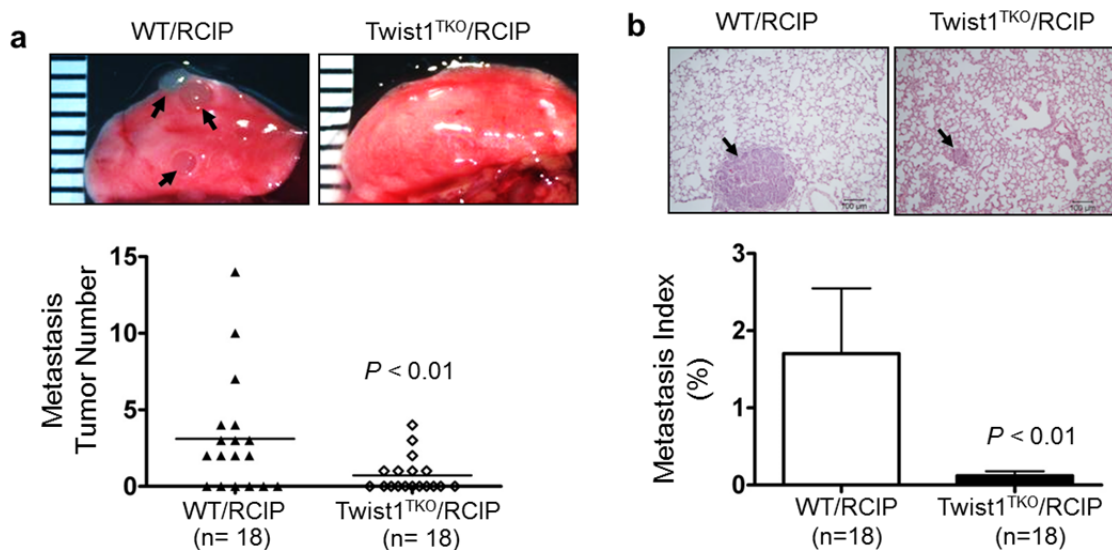


Figure 3.5. Tumor cell-specific knockout (TKO) of *Twist1* inhibits lung metastasis in mice. **A.** The images of lungs isolated from MMTV-TVA/RCIP and MMTV-TVA;*Twist1*^{F/F}/RCIP mice bearing palpable mammary tumors for 10 weeks (upper panels). Arrowheads indicate metastasis foci observed on the lung surface. The numbers of metastasis foci observed in the sections of individual lungs of both mouse groups are presented in the lower panel. **B.** H&E-stained lung sections of mice with WT/RCIP and *Twist1*^{TKO}/RCIP mammary tumors for 10 weeks. Arrowheads indicate metastasis foci (upper panels). Metastasis index was presented as the average percentage of metastasis tumor areas to total lung areas measured on the electronic images recorded from H&E-stained lung sections. Scale bars, 100 μ m.

We also performed Ki67 immunostaining and found higher proliferating ratio in MMTV-TVA;*Twist1*^{F/F} mice metastasis tumors than in MMTV-TVA mice metastasis tumors (Fig. 3.6A). This result suggests that the reduced metastasis of *Twist1* null tumor cells in MMTV-TVA;*Twist1*^{F/F} mice was not caused by any decrease in tumor cell proliferation in the lung. Instead, the lung metastasis may happen at a later stage in MMTV-TVA;*Twist1*^{F/F} mice versus MMTV-TVA mice.

We isolated genomic DNA from lung paraffin section with metastasis foci. Genotype analysis showed wild type *Twist1* allele is only detected in WT/RCIP groups and floxed allele is only detected in *Twist1*^{TKO} group (Fig. 3.6B). However, deleted *Twist1* alleles were detected in some *Twist1*^{TKO} lungs, suggesting that *Twist1* null tumor cells could also metastasize to lung but have a drastically decreased metastasis capability compared with *Twist1* WT mammary tumor cells.

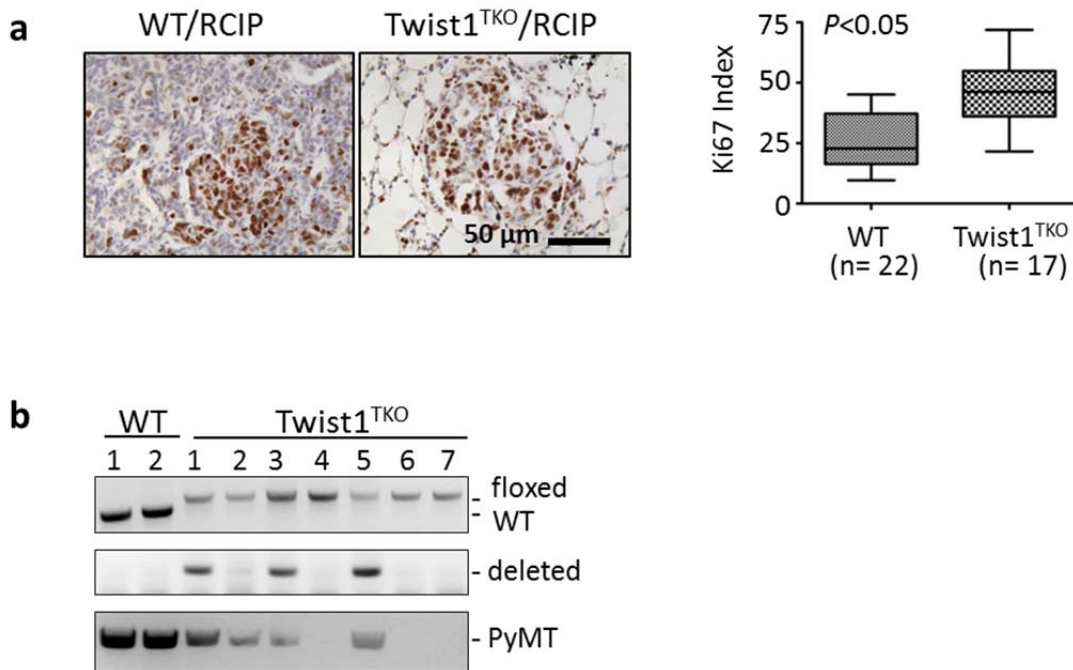


Figure 3.6. Ki67 staining and genomic DNA PCR of metastasis tumors. A. Representative images of Ki67 IHC on WT/RCIP and *Twist1*^{TKO}/RCIP lung metastasis sections and the quantification of staining result. **B.** PCR-based analysis of the wild type (WT), floxed (*Twist1*^F) and Cre-deleted (*Twist1*^{TKO}) *Twist1* alleles and tumor marker PyMT in WT/RCIP and *Twist1*^{TKO}/RCIP mouse lung sections with metastasis foci.

3.5 Specific ablation of Twist1 in the PyMT-induced mammary tumor cells inhibits

EMT and invasiveness

Cell line based studies showed that Twist1 promotes EMT, angiogenesis and local invasiveness. Thus, we examined EMT status of both *Twist1*^{TKO}/RCIP and WT/RCIP tumors by triple fluorescent IHC staining of Twist1/PyMT-HA/E-cadherin or Twist1/PyMT-HA/Vimentin. We found that Twist1 positive tumor cells (Twist1/PyMT-HA double positive) showed increased Vimentin expression and decreased E-cadherin

expression compared with Twist1 negative tumor cells in WT/RCIP tumor sections (Fig. 3.7A and B). On the other hand, we did not see any Twist1 positive tumor cells from the *Twist1*^{TKO}/RCIP tumor sections. However, we did see a few Twist1 negative tumor cells from both groups showed decreased E-cadherin or increased Vimentin (Fig. 3.7 A and B), suggesting that Twist1 is not the only regulator of EMT in the tumor cells. Quantification of the staining showed there are about 9.0 % Vimentin positive tumor cells and about 45% of which are Twist1 positive in WT group. In *Twist1*^{TKO}/RCIP tumors, about 2.6% of tumor cells are Vimentin positive. Vimentin and E-cadherin expression levels in Twist1 positive and negative tumor cells in WT/RCIP group were scored in a scale of 0-3 (0 means negative/non-detectable while 3 means strong expression). Twist1 positive tumor cells showed significant higher Vimentin score but lower E-cadherin score. These data suggest that Twist1 is a master inducer of EMT in the mouse mammary gland tumors.

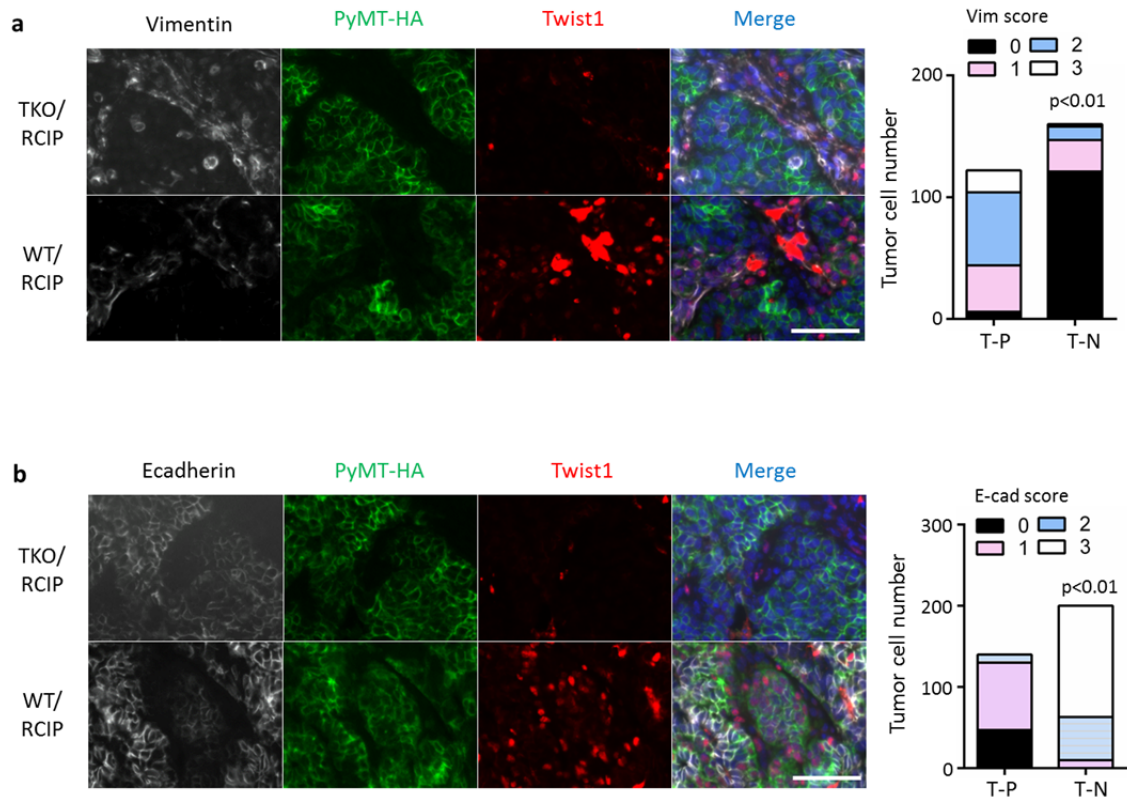


Figure 3.7. Vimentin and E-cadherin expression in Twist1 positive and negative tumor cells. **A.** IF staining of Vimentin, PyMT-HA and Twist1 in WT/RCIP and *Twist1^{TKO}*/RCIP mammary tumors. Vimentin expression level in Twist1 positive tumor cells and Twist1 negative tumor cells were scored and shown in right panel. **B.** IF staining of E-cadherin, PyMT-HA and Twist1 in WT/RCIP and *Twist1^{TKO}*/RCIP mammary tumors. E-cadherin expression level in Twist1 positive tumor cells and Twist1 negative tumor cells were scored and shown in right panel. Scale bar, 50 μ m.

Micro-vascular density is an important marker for invasiveness, thus we performed CD31 IHC on both *Twist1^{TKO}*/RCIP and WT/RCIP tumor sections. Knockout of *Twist1* in tumor cells significantly decreased Micro-vascular density by around 50% (Fig. 3.8A). Consistent with the active EMT and angiogenesis promoted by Twist1, we detected more circulating tumor cells (CTCs) from the blood of mice with WT/RCIP tumors compared with those mice with *Twist1^{TKO}*/RCIP tumors (Fig. 3.8B). Taken

together, Twist1 promotes EMT and angiogenesis to facilitate primary mammary gland tumor cell invasiveness and intravasation into the blood circulation.

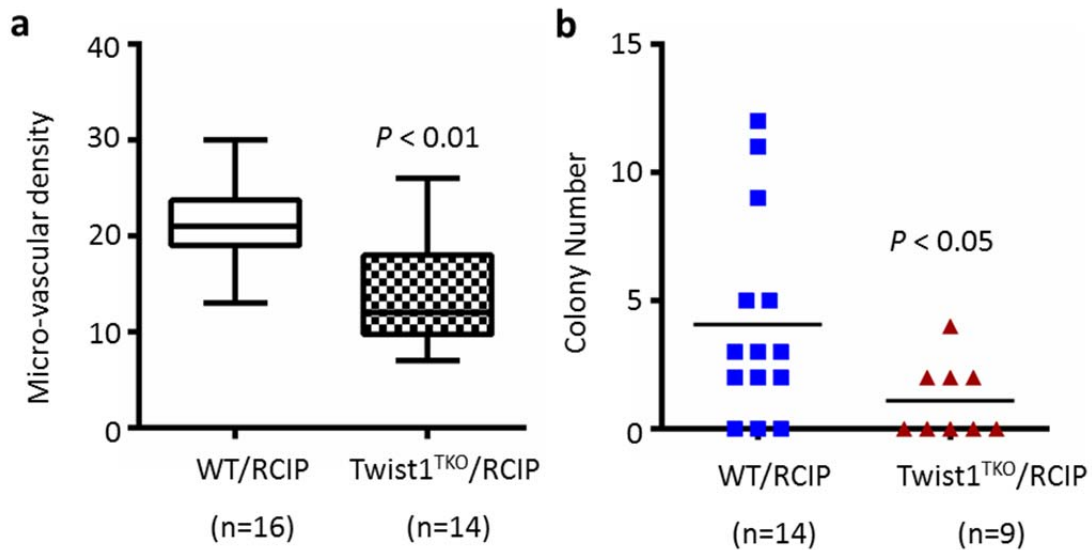


Figure 3.8. TKO of *Twist1* in the PyMT-induced mammary tumor cells inhibits angiogenesis and invasion in to blood circulation. A. Micro-vascular density of WT/RCIP and *Twist1*^{TKO}/RCIP mouse mammary tumors. **B.** Circulating tumor cells (CTCs) colony culture from mice with WT/RCIP or *Twist1*^{TKO}/RCIP mammary tumors.

3.6 Twist1 expression is turned off in lung metastasis foci

To figure out Twist1's role in metastasis tumors, we examined Twist1 expression in lung metastasis foci. Interestingly, double staining of Twist1 and tumor marker PyMT-HA showed that metastasis foci do not expression Twist1 protein in either WT/RCIP or *Twist1*^{TKO}/RCIP groups (Fig 3.9A). This phenotype is consistent with the previous report that Twist1 is turned off in metastasis tumors through MET⁴⁹. We then performed double staining of PyMT-HA with E-cadherin or Vimentin and found that all metastasis

tumor cells are E-cadherin positive but Vimentin negative. Double staining of E-cadherin and Vimentin also showed no overlapping, further supports the conclusion that Twist1 is turned off in the metastasis foci and metastasis tumor showed epithelial phenotype. (Fig. 3.9B, C and D).

3.7 Twist1 is expressed at late tumor stage and is associated with reduced ER and Foxa1 expression in mouse tumors

Above data showed that Twist1 was non-essential in early stage of tumor progression, however, it was unclear whether Twist1 is expressed but does not contribute to early stage tumor progression or it is not expressed at all. Thus we examined Twist1 protein expression by IHC in both groups of tumors at early stage (6weeks after tumor became palpable, volume $\approx 0.5 \text{ cm}^3$) and late stage (10 weeks after tumor became palpable, volume $\approx 1.0 \text{ cm}^3$). Interestingly, we found no Twist1 immunoreactivity was detected in the early stage tumor cells, while ER α protein was detected at high levels in both tumor cells and non-tumor mammary epithelial cells (Fig. 3.10A). In late stage tumors, about 6% of WT/RCIP tumor cells express Twist1, suggesting that Twist1 mainly functions at late stage.

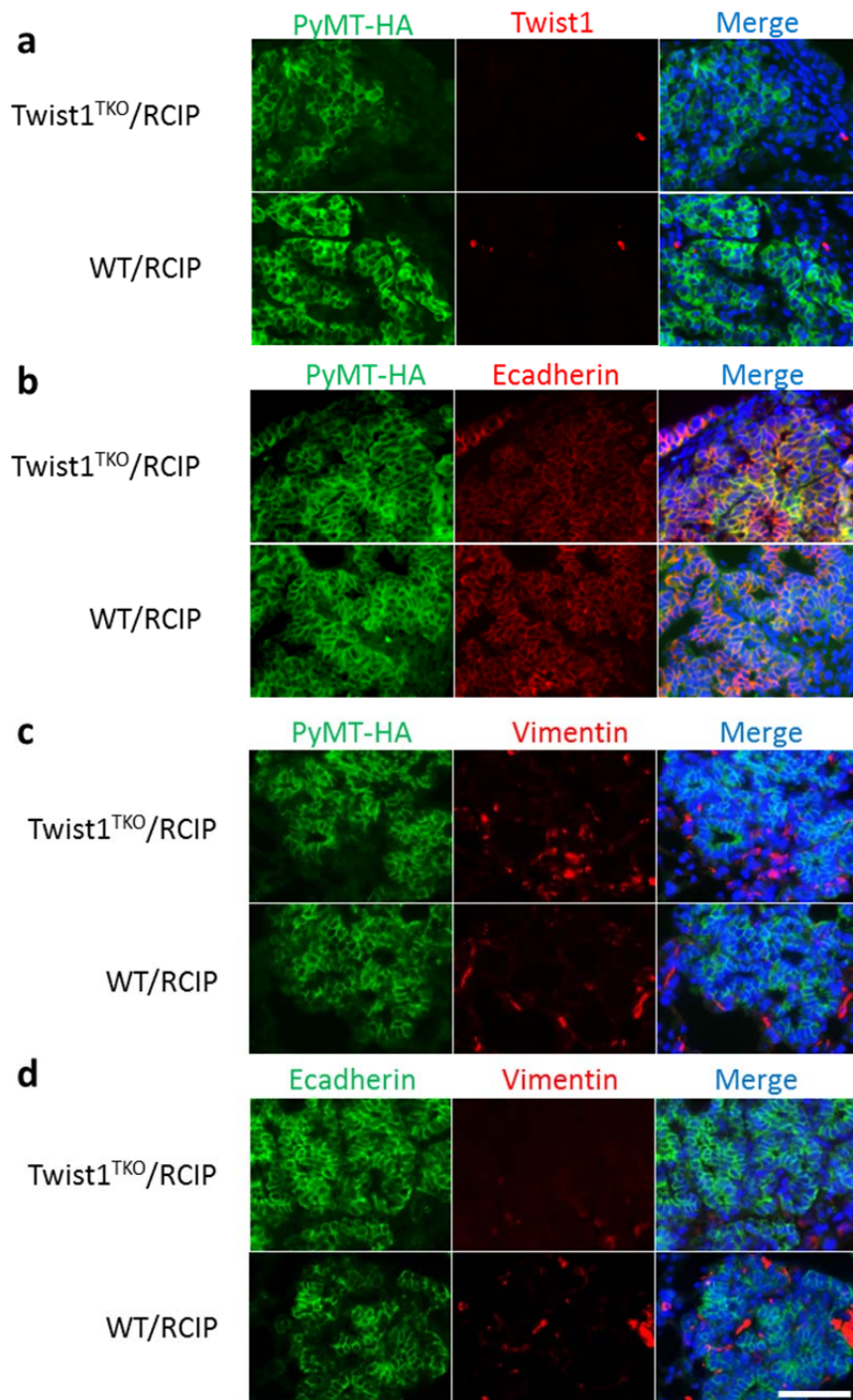


Figure 3.9. Twist1, Vimentin and E-cadherin expression in lung metastasis tumor foci of WT/RCIP and *Twist1*^{TKO}/RCIP groups. **A.** IF staining of Twist1 and PyMT-HA in lung metastasis foci of both groups. **B.** IF staining of E-cadherin and PyMT-HA in lung metastasis foci of both groups. **C.** IF staining of Vimentin and PyMT-HA in lung metastasis foci of both groups. **D.** IF staining of E-cadherin and Vimentin in lung metastasis foci of both groups.

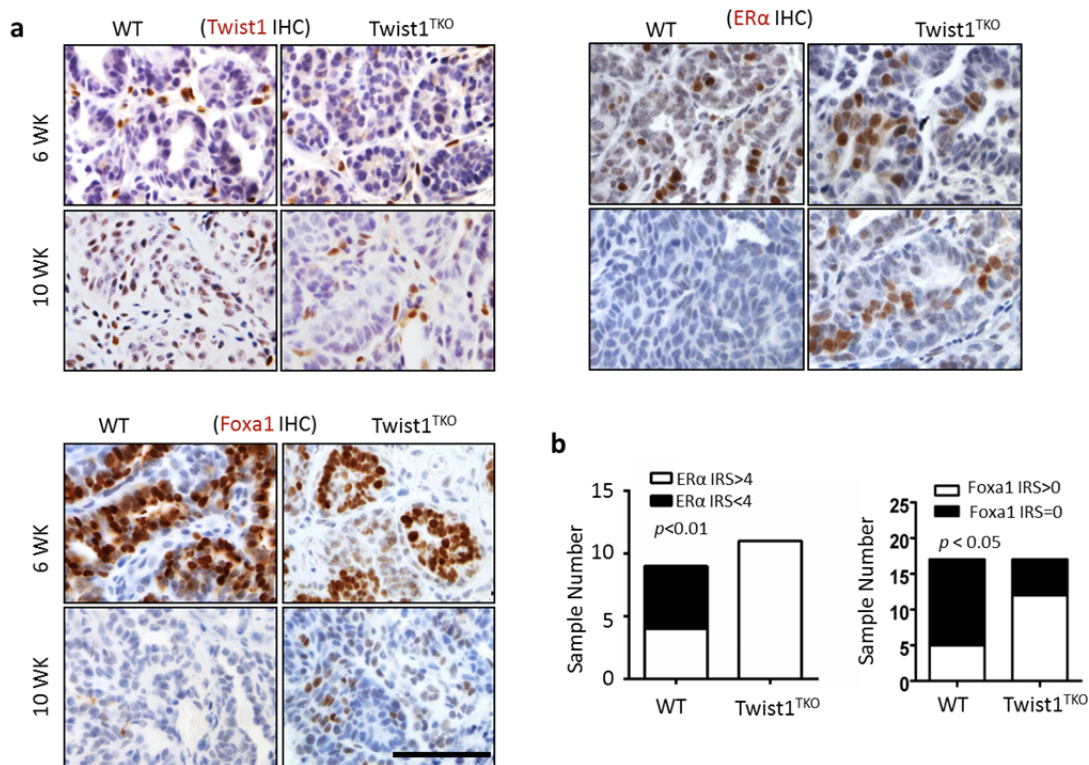


Figure 3.10. Twist1, ER α and Foxa1 IHC in mouse tumors and IRS score. A. IHC for Twist1 ER α and Foxa1 (brown) in WT/RCIP and *Twist1*^{TKO}/RCIP mammary tumors at 6 and 10 weeks after becoming palpable in mice. **B.** The sample distribution and Fisher's Exact test of ER α (strong positive (IRS>4) and weak positive or negative (IRS \leq 4)) and Foxa1 (negative (IRS=0) and positive (IRS>0)) in WT/RCIP and *Twist1*^{TKO}/RCIP mouse mammary tumors at 10 weeks after becoming palpable in mice.

As a semi-quantitative analysis, we evaluated the immunoreactivity scores (IRS) of ER α and Foxa1 in both groups of tumors using the Allred Scoring System¹¹⁷. In late stage tumors ER α immunoreactivity was drastically decreased compared with that detected in the early stage (20% vs 58% positivity). Interestingly, although ER α was also reduced in

most of the tumor cells of late stage *Twist1^{TKO}*/RCIP tumors compared with early stage, there were still 59% of tumor cells expressing detectable ER α and 14% of tumor cells expressing high level ER α . As an ER α co-activator and a determinant of ER α signaling in breast cancer, Foxa1 protein showed similar expression pattern as ER α . Foxa1 was detected at high levels in both tumor cells and non-tumor mammary epithelial cells at early stage (Fig. 3.10A). However, Foxa1 immunoreactivity was very weak (12%) or negative (71%) in WT/RCIP tumor cells, while there were still 71% of tumor cells with detectable Foxa1 and 8% of tumor cells with high level Foxa1 in large *Twist1^{TKO}*/RCIP tumor group. Using Allred Scoring System, we found that late stage tumors are still ER α positive (IRS > 2, as generally accepted for determining positivity of ER α in human breast cancer patients), thus we compared ER α strong positive (IRS>4) to ER α weak positive or negative (IRS \leq 4) ratios in the two groups of tumors and found that *Twist1^{TKO}*/RCIP tumors are all ER α strong positive while more than 50% of WT/RCIP tumors turn to ER α weak positive or negative (Fig. 3.10B left panel). On the other hand, Foxa1 expression level is low in both groups of tumors, thus we compared Foxa1 negative (IRS = 0) to Foxa1 weak or strong positive (IRS > 0) ratios between the two groups. As shown in the right panel of Fig. 3.10B, the ratio of Foxa1-positive tumors was significantly higher in *Twist1^{TKO}*/RCIP tumor group versus WT/RCIP tumor group. Together, these results demonstrate that the level of Twist1 expression negatively correlates with the level of ER α and Foxa1 expression in the PyMT-induced mouse mammary tumors. ER α has been shown to be a direct target of Twist1 in human breast cancer cells, thus we next investigated whether and how Foxa1 is regulated by Twist1.

3.8 Twist1 expression inversely associates with Foxa1 expression in human breast cancer

Based on the mouse tumor IHC result, we hypothesized that Twist1 inhibits *Foxa1* expression to promote breast cancer invasiveness. To identify whether this regulation is true in human breast cancer, we analyzed a dataset deposited in the NCBI GEO database (GSE53222)⁸⁵ and found that Twist1 expressed in the T47D ER-positive breast cancer cells decreased the expression of a group of luminal epithelial genes including *Foxa1*, *ESR1*, *PRLR*, *PGR*, *MUC1* and *CLDN3* (Fig. 3.11), further supporting the hypothesis that *Foxa1* is target of Twist1 in breast cancer.

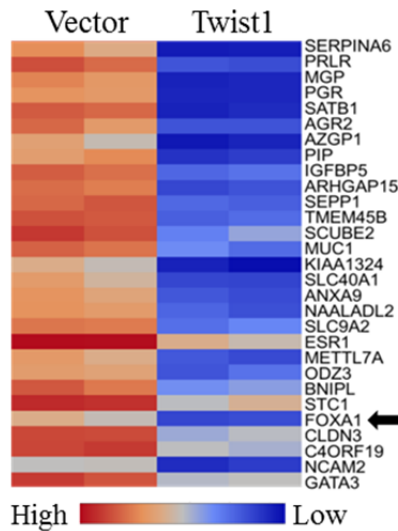


Figure 3.11. Downregulated genes by Twist1 overexpression in T47D human breast cancer cells. Several known luminal type breast cancer marker genes are downregulated by Twist1 overexpression, including *Foxa1*, *ESR1*, *GATA3*, *MUC1*. (Data source: Shi J *et al*, Cancer Cell, 2014⁸⁵)

We further analyzed the correlation between the expression levels of *Twist1* and *Foxa1*

mRNAs in human breast cancer using another dataset from 281 human breast tumors in NCBI GEO (GSE2034)¹¹⁸. This analysis also revealed a significant negative correlation between the levels of *Twist1* and *Foxa1* mRNA expression (Fig. 3.12A). We also analyzed the correlation between the expression levels of *Twist1* and *Foxa1* mRNAs in luminal and basal subtype human breast cancer cell lines by using GEO2R software and a dataset in the NCBI GEO database (GSE15361)¹¹⁹. Among 44 breast cancer cell lines with RNA-profiling data, the level of *Twist1* mRNA negatively correlated with the level of *Foxa1* mRNA (Fig. 3.12D). The average level of *Twist1* mRNA was significantly higher in basal-like breast cancer cell lines compared with luminal type of breast cancer cell lines (Fig. 3.12B). In contrast, the average level of *Foxa1* mRNA was significantly lower in basal-like breast cancer cell lines compared with luminal type of breast cancer cell lines (Fig. 3.12C). To validate these data at protein levels, we performed Western Blot for Twist1 and Foxa1 in a group of breast cancer cells lines. We found that Twist1 is highly expressed in basal-like breast cancer cell lines, while Foxa1 is exclusively expressed in luminal type breast cancer cell lines. We further analyzed a cohort of 276 human breast tumors by IHC staining of both Twist1 and Foxa1. Twist1 protein was detected in 13 out 276 (5%) tumors and Foxa1 is detected in 94% tumors (245 out of 261), indicating that this cohort mainly consists of luminal breast tumors. Interestingly, 179 out of 261 (68.6%) tumors showed very high (>6) Foxa1 immunoreactive scores (IRs). However, the 13 Twist1-positive tumors had IRs of 6 or lower. The immunoreactive scores of Twist1 and Foxa1 and the ER α , PR and HER2 expression profiles for these 13 Twist1 positive tumors are provided in Table 3.1. Among these 13

Twist1-positive tumors, 5 tumors showed significantly decreased Foxa1 protein compared with Twist1-negative tumors (Fig. 3.12F). Twist1 protein levels were also negatively correlated with Foxa1 protein levels among these 13 Twist1-positive tumors (Fig. 3.12G). These results demonstrate that the levels of Twist1 expression are negatively correlated with the levels of Foxa1 expression in human breast tumors. Thus we proposed that Twist1 could directly silence *Foxa1* expression to promote de-differentiation and metastasis of breast cancer cells.

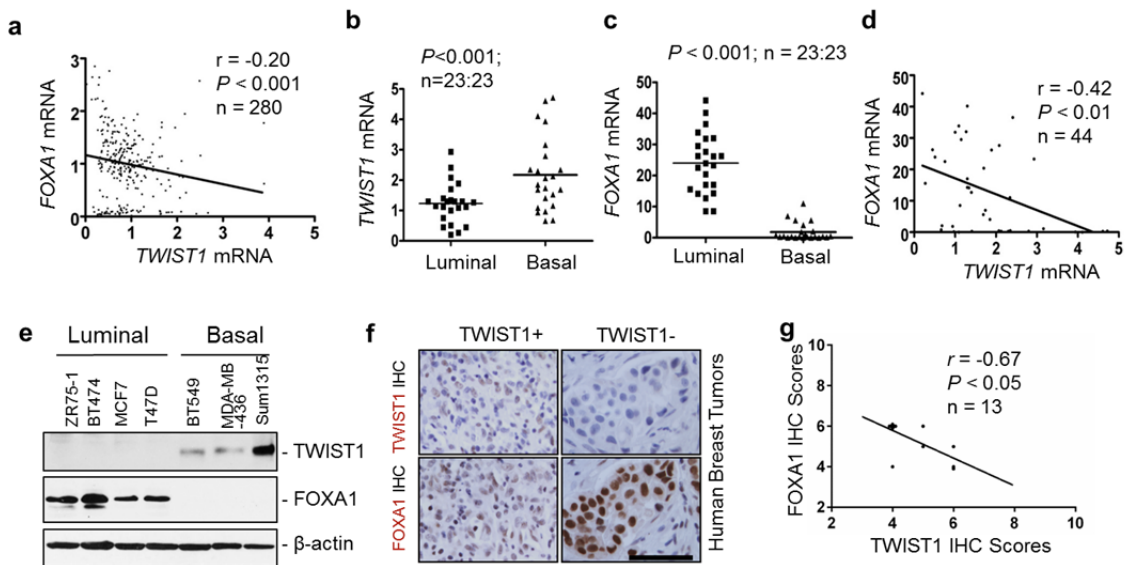


Figure 3.12. *Twist1* expression is negatively associated with *Foxa1* expression in human breast cancers. A. Pearson's Correlation test of *Twist1* and *Foxa1* mRNA expression levels in a published data set of human breast tumor cohort¹¹⁸. B and C. Expression levels of *Twist1* (Panel B) and *Foxa1* (Panel C) mRNAs in luminal and basal breast cancer cell lines. Data analysis was based on a published data set¹¹⁹. D. Pearson's Correlation analysis between *Twist1* and *Foxa1* mRNA expression in breast cancer cell lines shown in Panels B and C. E. Western blotting analysis of Twist1 and Foxa1 in human breast cancer cell lines. F and G. Representative images of IHC for Twist1 and Foxa1 in human breast tumors. Adjacent tumor sections were used for Twist1 and Foxa1 IHC (Panel F). Twist1 and Foxa1 protein levels are inversely correlated in Twist1-positive breast tumors. The r and p values were obtained by Pearson's correlation analysis (Panel G). The scale bar in Panel F, 50 μ m.

Tumor Sample #	ER	PR	HER2	Twist1 IRS	Foxa1 IRS
2011-07134C	N	N	N	4	6
2013-00701C	P	P	N	4	6
2013-00945C	P	P	N	4	6
2013-4269C	P	P	N	4	6
2013-4275C	P	P	N	4	6
2013-7639C	P	P	N	4	4
2013-11189C	P	P	P	4	6
2013-11208C	P	P	N	4	6
2011-3968C	P	P	N	5	5
2013-4773C	P	N	N	5	6
2012-2420C	N	P	N	6	4
2012-3647C	P	P	N	6	5
2013-7200C	P	P	P	6	4

Table 3.1 Clinical information for Twist1-positive breast tumors. ER, estrogen receptor; PR, progesterone receptor; HER2, human epithelial growth factor receptor 2; IRS, immunoreactivity score; N, negative; P, positive

3.9 Twist1 directly silences Foxa1 mRNA transcription by recruiting NuRD complex

The luminal type breast cancer cell line MCF7 expresses ER α and Foxa1, but not Twist1. To establish a cellular model for investigating the molecular mechanisms responsible for Twist1 to regulate *Foxa1* expression, we generated stable MCF7 cell lines with either the empty control vector (MCF7^{Ctrl}) or the Twist1-expressing vector (MCF7^{Twist1}). Twist1 expression in MCF7^{Twist1} cells drastically decreased Foxa1 mRNA and protein levels (Fig. 3.13A). Conversely, knockdown of *Twist1* mRNA in the basal-

like SUM1315 human breast cancer cells with high *Twist1* and low *Foxa1* expressions moderately increased the expression levels of *Foxa1* mRNA and protein (Fig. 3.13B). However, ectopic expression of *Foxa1* in either SUM1315 or BT549 breast cancer cells did not alter the expression levels of *Twist1* mRNA and protein (Fig. 3.13 C and D). These results indicate that *Twist1* suppresses *Foxa1* expression, while *Foxa1* does not regulate *Twist1* expression.

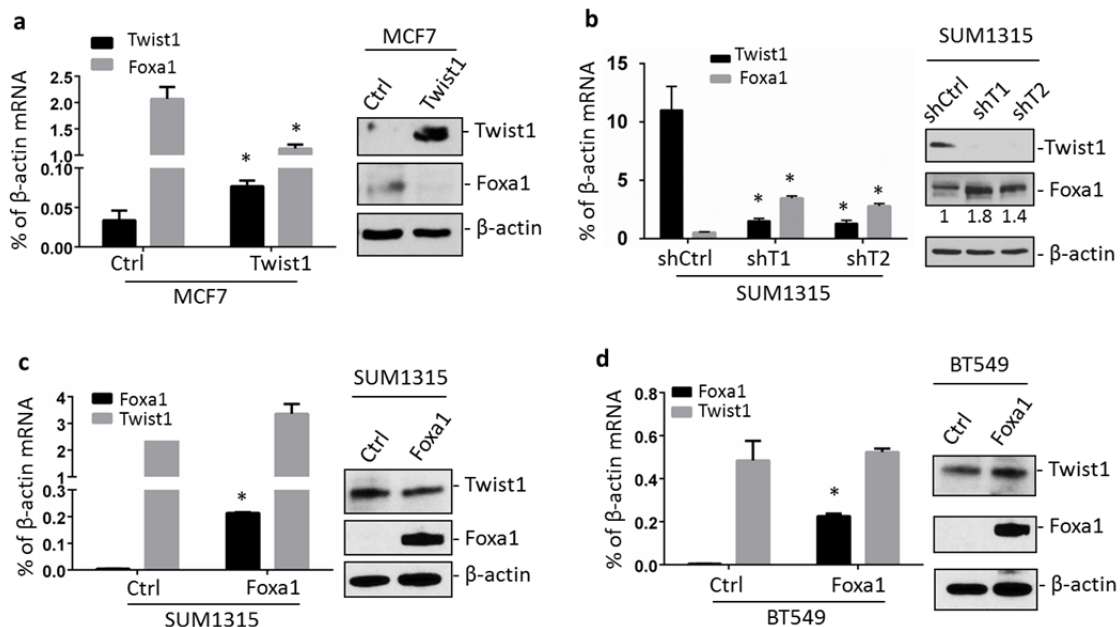


Figure 3.13. *Twist1* silences *Foxa1* expression in breast cancer cells. A. Expression of *Twist1* in MCF7 cells reduced *Foxa1* mRNA and protein as measured by Q-PCR and Western blotting. B. Knockdown of *Twist1* mRNA in SUM1315 cells by using *Twist1* siRNA (si*Twist1*) increased *Foxa1* mRNA and protein. C and D. Overexpression of *Foxa1* did not influence *Twist1* mRNA and protein in either BT549 or SUM1315 cells. All experiments were repeated 3 times and the representative data are presented. *, $P < 0.05$ by Student's t test.

To examine whether *Twist1* was recruited to the enhancer/promoter regions of the

Foxa1 gene, we performed chromatin immunoprecipitation (ChIP) assays by using a Twist1 antibody to pull down Twist1-associated genomic DNA in BT549 breast cancer cells and PCR to measure specific DNA regions of the *Foxa1* enhancer or promoter. We found that Twist1 was associated with the 5' regulatory region at -1 kb from the transcriptional starting site (TSS), but it was not associated with -2, -3, -4 and -5 kb regions (Fig. 3.14A). To examine the specific role of Twist1 in regulating the transcriptional activity of *Foxa1* promoter, we constructed a *Foxa1* promoter-luciferase (Foxa1-Luc) reporter containing 1.46-kb 5' regulatory sequence with the Twist1-binding region (Fig. 3.14B). Expression of Twist1 significantly decreased the activity of Foxa1-Luc reporter in MCF7 cells. As expected for positive and negative controls, Twist1 decreased the activity of CDH1-Luc reporter, but did not affect the activity of CSF1-Luc reporter (Fig. 3.14C) ^{68, 106}. These results indicate that Twist1 is recruited to the 5' regulatory region proximal to the *Foxa1* promoter.

In silico analysis of the proximal *Foxa1* promoter region revealed 11 E-boxes. Twist1 is more likely to bind two (EB3 and EB7) of these E-boxes as predicted by MatInspector Software (Genomatix) (Fig. 3.14B). Deletion of either EB3 site in Foxa1-Luc (EB3M-Luc) reporter or EB7 site in Foxa1-Luc (EB7M-Luc) reporter significantly relieved Twist1-repressed *Foxa1* promoter activity in MCF7 cells. Double deletions of both EB3 and EB7 sites in Foxa1-Luc (EB3/7M-Luc) reporter additively relieved Twist1-repressed *Foxa1* promoter activity (Fig. 3.14 B and D). Since the activity of EB3/7M-Luc reporter was still partially silenced by Twist1 in MCF7 cells, Twist1 might also bind to other E-

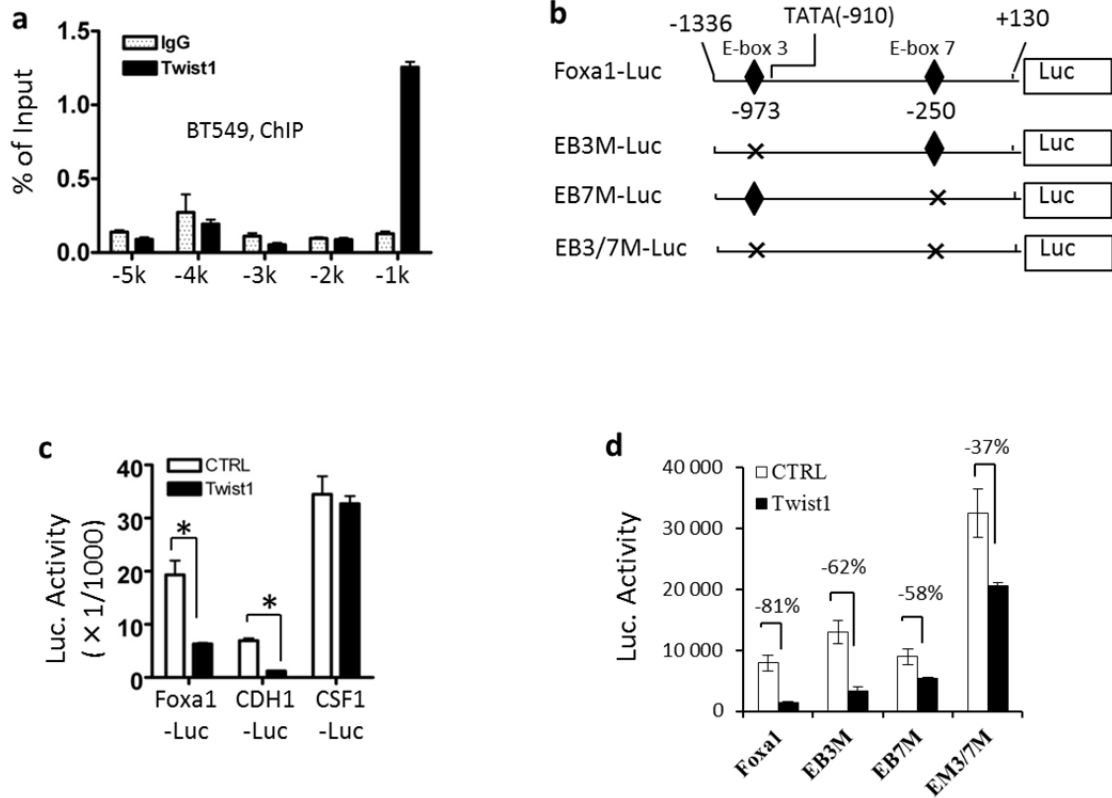


Figure 3.14. Twist1 directly bind to E-box element of *Foxa1* promoter. A. ChIP assays performed with BT549 breast cancer cells and Twist1 antibody. Non-immune IgG served as a negative control. Immunoprecipitated DNA was assayed by real time PCR with primers specific to the *Foxa1* 5' regulatory sequences at the indicated locations. B. The wild type and mutated constructs of the *Foxa1* promoter-luciferase reporter (*Foxa1*-Luc). EB3M-Luc, EB7M-Luc and EB3/7M-Luc had mutated E-box3, E-box7 or both of them, respectively. C & D. Cell transfection assays. Twist1 expression in MCF7 cells repressed the activities of Foxa1-Luc (the tester) and CDH1-Luc (a positive control), while it did not affect the activity of CSF1-Luc (a negative control) (Panel C). Twist1 showed much less repression on the activities of EB3M-Luc, EB7M-Luc and EB3/7M-Luc versus Foxa1-Luc in MCF7 cells (Panel D). Control cells were transfected with equal amount of the empty vector DNA. *, P < 0.05 by Student's t test.

boxes to repress the *Foxa1* promoter. On the other hand, in SUM1315 cells with endogenous *Twist1* expression, mutation of EB3 and/or EB7 increased *Foxa1*-Luc reporter activity, while knockdown of *Twist1* resulted in lesser fold increases in the mutant *Foxa1* promoter activities versus the wild type promoter (Fig. 3.15 A and B). These results demonstrate that *Twist1* can use both EB3 and EB7 sites to silence the transcriptional activity of the *Foxa1* promoter. We previously reported that *Twist1* recruits nucleosome remodeling deacetylase (NuRD) complex to repress *CDH1* and estrogen

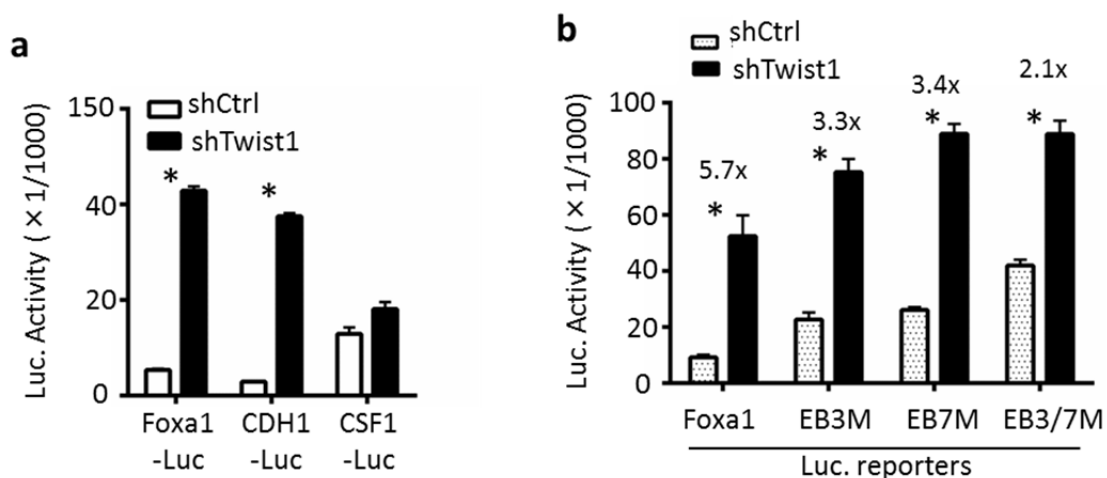


Figure 3.15. Mutation of *Twist1*-binding sites or knockdown of *Twist1* mRNA increases *Foxa1* promoter-luciferase (Luc) reporter activity in SUM1315 cells. A. Knockdown of *Twist1* mRNA in SUM1315 cells increased the activities of *Foxa1*-Luc (the tester) and *CDH1*-Luc (a positive control), but did not affect the activity of *CSF1*-Luc (a negative control). **B.** SUM1315 cells with normal *Twist1* (shCtrl) or with *Twist1* knockdown (shTwist1) were transfected with wild type *Foxa1* or mutant *Foxa1* promoter-Luc reporters as indicated. Mutation of either E-box 3 (EB3M-Luc), E-box 7 (EB7M-Luc) or both of them (EB3/7M-Luc) in the promoter sequence relieved *Twist1*-mediated suppression and thus, increased the basal activities of the mutant promoters in control cells. For the same reason, knockdown of *Twist1* expression showed less fold relieves of the three mutant *Foxa1* promoter-Luc reporters when compared with the wild type *Foxa1* promoter-Luc reporter. All experiments were repeated 3 times and the representative data with 3 technical replicates are presented as Mean \pm SEM. *, $P < 0.05$ by Student's *t* test.

receptor (ER α) promoters^{68, 120}. Here, our ChIP assays revealed that Twist1 was specifically recruited to the proximal promoter regions of both *CDH1* and *Foxa1* genes in MCF7^{Twist1} cells (Fig. 3.16A). The endogenous HDAC2 and MTA2 proteins, two of the NuRD complex components, were also recruited to the same chromatin regions of both *CDH1* and *Foxa1* genes in a Twist1 expression-dependent manner (Fig. 3.16 B and C). In agreement with the Twist1-recruited NuRD complex containing histone deacetylase activity, the levels of acetylated histone H3K9 (H3K9-ace) were markedly reduced in the same Twist1-binding regions of both *CDH1* and *Foxa1* genes in MCF7^{Twist1} cells versus MCF7^{Ctrl} cells (Fig. 3.16D). Accordingly, RNA polymerase II recruited to these gene promoters was significantly reduced in MCF7^{Twist1} cells versus MCF7^{Ctrl} cells (Fig. 3.16F). Furthermore, knockdown of Twist1 in SUM1315 cells decreased HDAC2 and MTA2 recruitments and increased H3K9-ace and RNA polymerase II recruitment on *Foxa1* promoter (Fig. 3.17). These results demonstrate that Twist1 largely silences the transcriptional activity of the *Foxa1* promoter by recruiting NuRD gene-repressing complex, the same mechanism as it represses *CDH1* transcription.

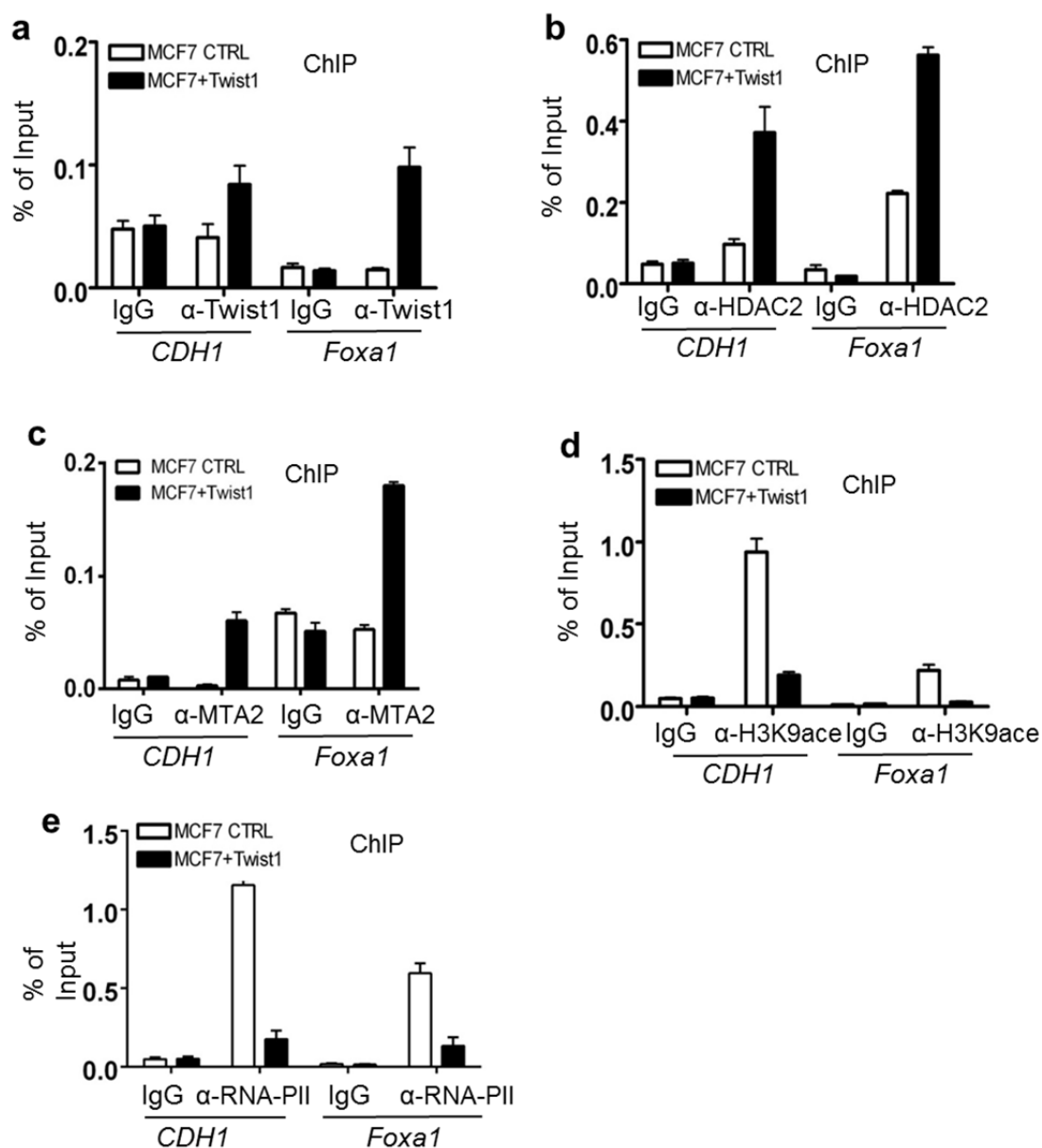


Figure 3.16. Overexpressed Twist1 in MCF7 cells recruits NuRD complex to *Foxa1* promoter to repress its expression. ChIP assays were performed in MCF7^{Ctrl} and MCF7^{Twist1} stable cell lines using antibodies against Twist1 (Panel A), HDAC2 (Panel B), MTA2 (Panel C), H3K9-ace (Panel D) and RNA-Pol II (Panel E). Non-immune IgG served as a negative control. Immunoprecipitated DNA was measured by real time PCR using primers for amplifying the Twist1-binding regions in the *CDH1* gene (a positive control) and the *Foxa1* gene (E-box3) as indicated. All experiments were repeated 3 times and the representative data are presented as Mean \pm SEM.

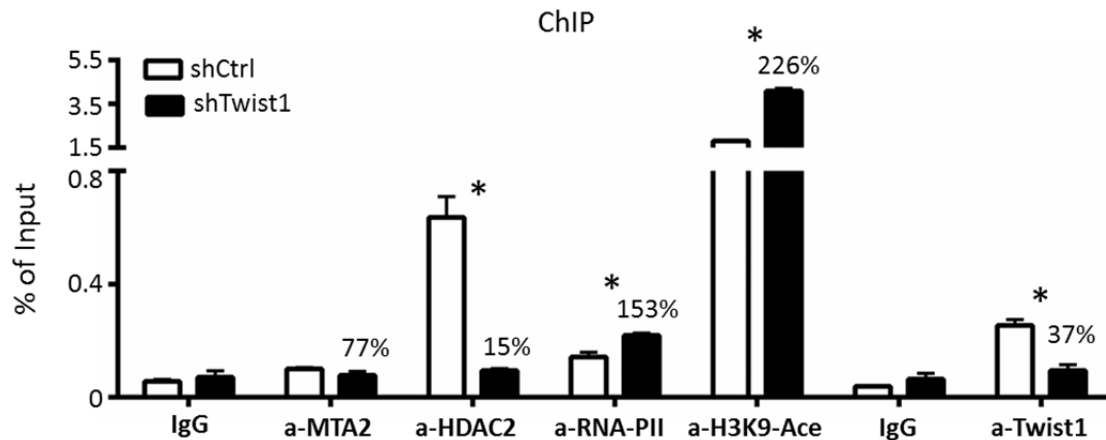


Figure 3.17. Knockdown of *Twist1* mRNA reduced MTA2 and HDAC2 recruitments but increased H3K9-Ace and RNA polymerase II (RNA-PII) recruitment to the *Foxa1* promoter in SUM1315 cells. ChIP assays were performed with SUM1315 cells with normal *Twist1* (shCtrl) or *Twist1* knockdown (shTwist1) and with non-immune IgG (negative control) or antibodies against *Twist1*, HDAC2, MTA2, H3K9-ace or RNA-PII as indicated. The input and precipitated DNA samples were analyzed by real-time PCR that amplifies the E-box 3 region of the *Foxa1* promoter. All experiments were repeated 3 times and the representative data with 3 technical replicates are presented as Mean \pm SEM. *, $P < 0.05$ by Student's t test.

3.10 *Twist1* silences *Foxa1* expression through inhibiting AP-1-promoted activation of the *Foxa1* promoter

Computational analysis of the *Foxa1* promoter region identified two AP-1 binding sites conserved in both human and mouse *Foxa1* genes (Fig. 3.18A). To define the role of AP-1 in regulating *Foxa1* promoter, we expressed c-Jun and c-Fos and assayed their effects on the *Foxa1*-Luc reporter in MCF7 cells. Expression of c-Jun and c-Fos significantly increased the activity of *Foxa1*-Luc reporter in a dose-dependent manner (Fig. 3.18B). In contrast, knockdown of *c-Fos* in MCF7 cells drastically reduced the

expression levels of *Foxa1* mRNA and protein (Fig. 3.18C). Furthermore, deletion of either AP-1 site at bp -895 or bp -798 or both diminished AP-1-promoted activities of the *Foxa1* AP1M1-Luc, AP1M2-Luc and AP1M1/2-Luc reporters (Fig. 3.18D). These results demonstrate that AP-1 is a transcriptional activator of the *Foxa1* promoter.

We further performed ChIP assays to examine whether Twist1 could inhibit c-Fos from being recruited to the AP-1 sites of the *Foxa1* proximal promoter region. Indeed, Twist1 expression in MCF7 cells abolished the recruitment of c-Fos to the *Foxa1* proximal promoter region (Fig. 3.18E). As a control, Twist1 did not inhibit c-Fos recruitment to the *CSF1* promoter region¹⁰⁶. These results suggest that Twist1 plays a crucial role to repress AP-1-mediated activation of the *Foxa1* promoter by preventing AP-1 recruitment to the *Foxa1* proximal promoter region. As expected, expression of Twist1 in MCF7 cells markedly repressed the transcriptional activity of the *Foxa1*-Luc reporter. However, Twist1 expression did not have an obvious effect on the activity of the *Foxa1* promoter with deleted AP-1 binding sites, including AP1M1-Luc, AP1M2-Luc and AP1M1/2-Luc reporters (Fig. 3.18F). Consistent results were also observed in SUM1315 cells with *Twist1* knockdown (Fig. 3.19 A and B). These results suggest that Twist1 plays a role in silencing AP-1-mediated activation of the *Foxa1* promoter.

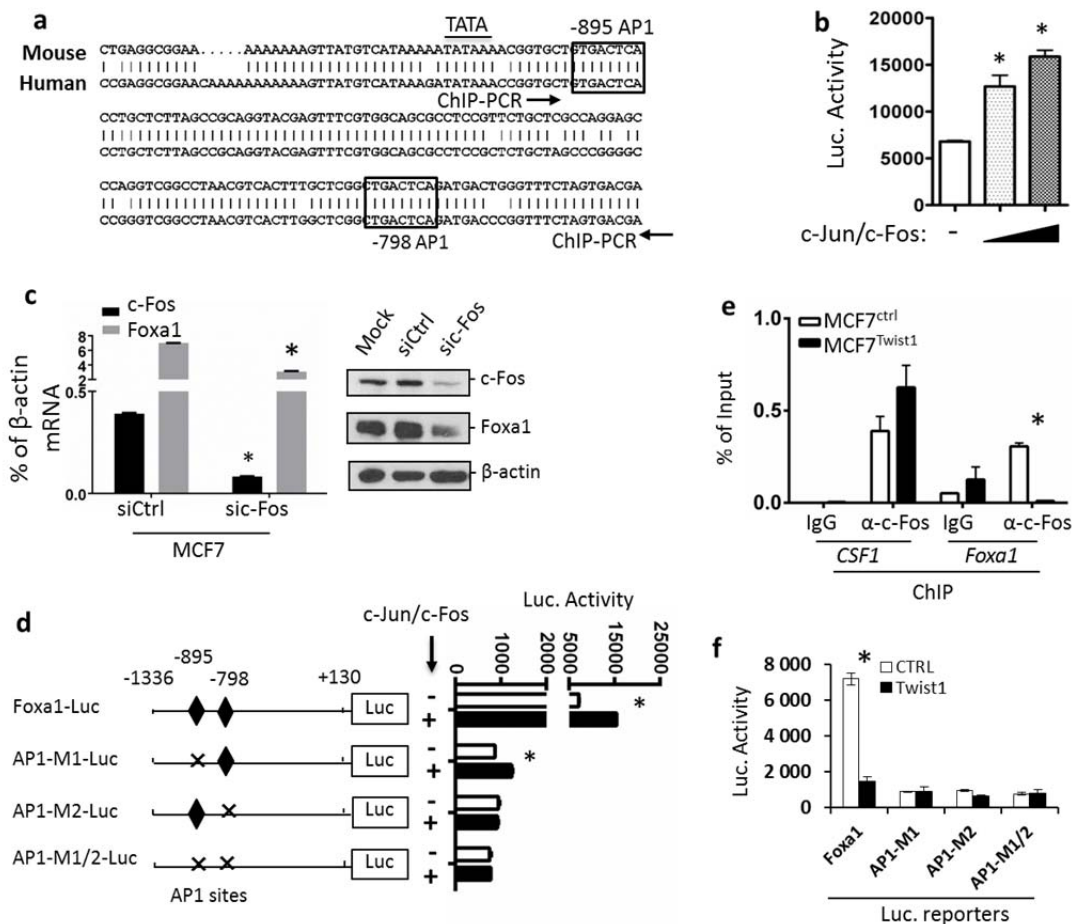


Figure 3.18. Twist1 inhibits AP1-mediated activation of the *Foxa1* promoter by inhibiting AP1 recruitment. A. The two conserved AP1 sites in both human and mouse *Foxa1* promoter regions. B. Luciferase activity of MCF7 cells transfected with Foxa1-Luc plasmid with the empty vector (-) or c-Jun and c-Fos expression vectors. C. Q-PCR and Western blot assays showing *Foxa1* mRNA and protein changes upon c-fos knockdown in MCF7 cells. D. Luciferase assay of MCF7 cells co-transfected with the indicated luciferase reporter and the empty vector (-) or c-Jun and c-Fos expression vectors. E. ChIP assays performed with MCF7^{ctrl} and MCF7^{Twist1} cells and non-immune IgG (negative control) or c-Fos antibody as indicated. The DNA fragment between the two arrowheads in Panel A was amplified by PCR from the immunoprecipitated DNA. Amplification of the known AP1-binding region by PCR in the *CSF1* promoter served as a positive control. F. Luciferase assay of MCF7 cells co-transfected with the indicated luciferase reporter and the empty vector (Ctrl) or Twist1 expression plasmid. Experiments were repeated 3 times and the representative data are presented as Mean \pm SEM. * in Panels B–D, $P < 0.05$ by Student's *t* test.

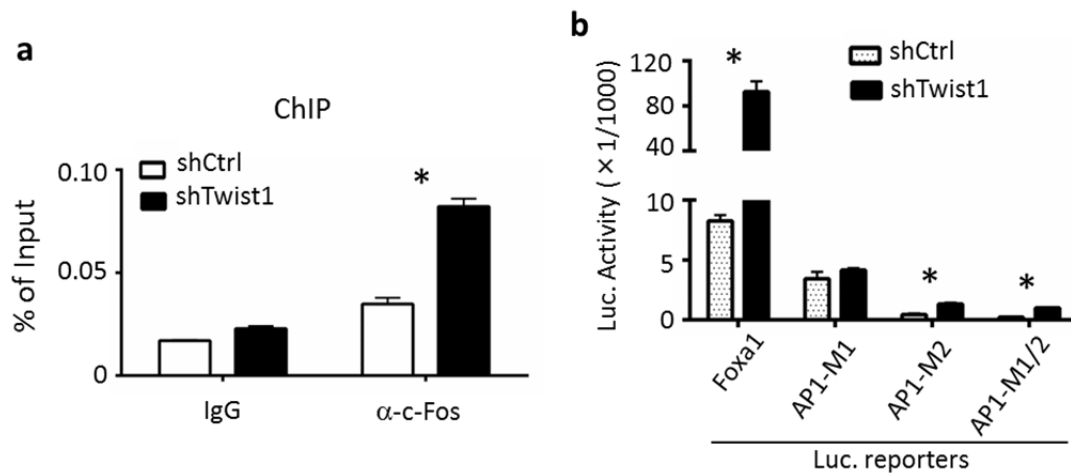


Figure 3.19. Twist1 inhibits AP1-activated *Foxa1* promoter activity in SUM1315 cells. **A.** Knockdown of *Twist1* mRNA by shTwist1 increased c-Fos recruitment to the *Foxa1* promoter. ChIP assays were performed with SUM1315 cells expressing non-targeting shRNA (shCtrl) or shTwist1 that targets *Twist1* mRNA and with control IgG or c-Fos antibody as indicated. **B.** Mutation of AP-binding sites in the *Foxa1* promoter decreased the promoter activity and knockdown of *Twist1* expression markedly increased wild type *Foxa1* promoter activity but only slightly increased the *Foxa1* promoter with mutated AP-1 sites. SUM1315 cells expressing shCtrl or shTwist1 were cultured in 24 well plates and transfected with the indicated *Foxa1* promoter-Luc reporters. Luciferase assay was carried out 24 hours later after the transfection. Experiments were repeated 3 times and the representative data with 3 technical replicates are presented as Mean \pm SEM. *, $P < 0.05$ by Student's *t* test.

3.11 Twist1-silenced *Foxa1* expression is not responsible for Twist1-induced cell morphological change but it mediates the expression of some Twist1-regulated genes

To examine whether Twist1-silenced *Foxa1* expression is responsible for Twist1-induced morphology and gene expression changes in breast cancer cells, we stably restored *Foxa1* expression in MCF7^{Twist1} cell lines (designated as MCF7^{Twist1+Foxa1} cell lines) with Twist1-silenced *Foxa1* expression (Fig. 3.20A). As expected, MCF7^{Ctrl} cells

showed epithelial tumor cell morphology identical to their parent MCF7 cells, while MCF7^{Twist1} cells had an elongated spindle shape consistent with their EMT phenotype. MCF7^{Twist1+Foxa1} cells with restored Foxa1 expression showed a cellular morphology very similar to MCF7^{Twist1} cells (Fig. 3.20B), suggesting that the silenced Foxa1 expression is not responsible for Twist1-induced morphological change of MCF7 cells. Furthermore, Twist1 expression effectively repressed E-cadherin, β -catenin, cytokeratin 8 (K8) and ER α expression in MCF7^{Twist1} cells as compared to MCF7^{Ctrl} cells, while restored Foxa1 expression only partially rescued K8 and ER α expression in MCF7^{Twist1+Foxa1} cells as compared to MCF7^{Twist1} cells (Fig. 3.20C). Moreover, Twist1 strongly induced vimentin, integrin β 1, integrin α 5, and MMP9 expression but did not change fibronectin expression in MCF7^{Twist1} cells as compared to MCF7^{Ctrl} cells. Restored Foxa1 expression had no effect on vimentin expression but inhibited Twist1-induced integrin β 1, integrin α 5 and MMP9 expression and slightly increased fibronectin in MCF7^{Twist1+Foxa1} cells as compared to MCF7^{Twist1} cells (Fig. 3.20 C-F). In addition, Slug (Snail2) expression was increased in MCF7^{Twist1} cells versus MCF7^{Ctrl} cells, but restored Foxa1 expression did not affect Twist1-induced Slug expression in MCF7^{Twist1+Foxa1} cells versus MCF7^{Twist1} cells. The expression levels of Snail1, Zeb1 and Zeb2 mRNAs were very low and remained unchanged in MCF7^{Ctrl}, MCF7^{Twist1} and MCF7^{Twist1+Foxa1} cells. These results suggest that silenced *Foxa1* is not responsible for Twist1-induced mesenchymal cell morphology and most EMT marker gene expression, but responsible for permitting the expression of ER α , K8 and other selective genes related to cell migration and invasion such as integrin β 1, integrin α 5 and MMP9.

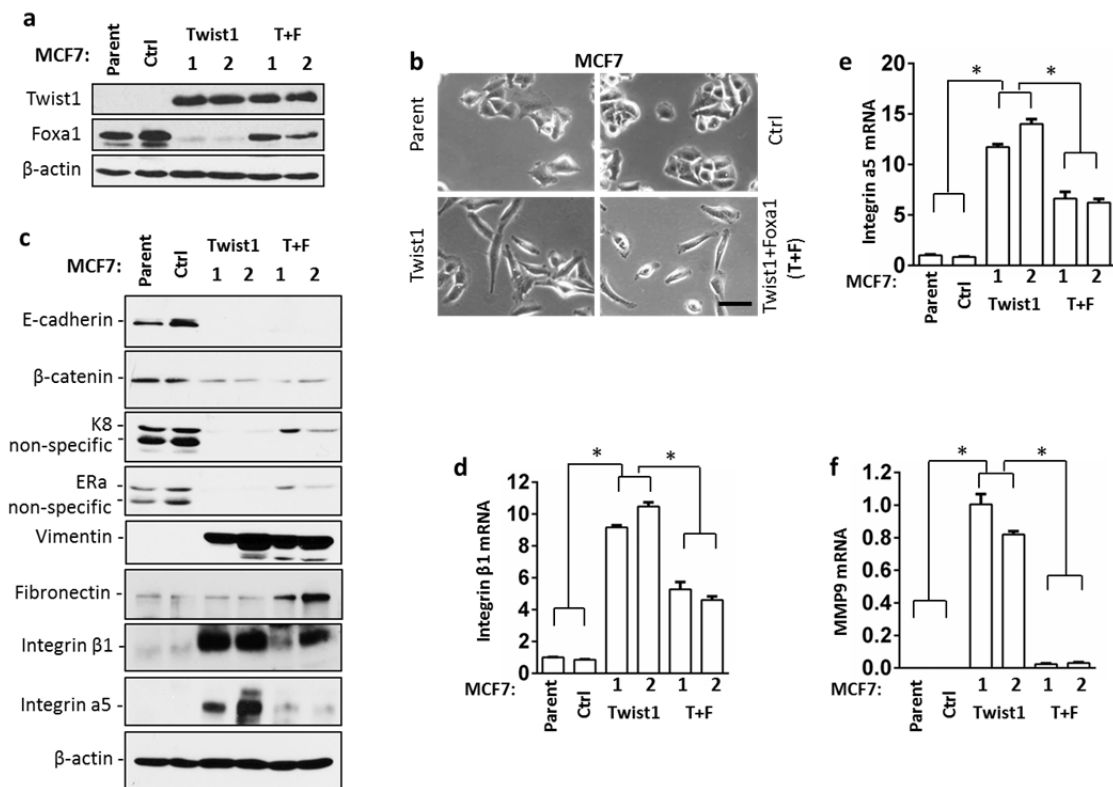


Figure 3.20. The effects of silenced *Foxa1* expression on Twist1-induced EMT cell morphogenesis and gene expression. A. Western blot analysis of the indicated proteins in MCF7 parent cells, MCF7^{Ctrl} cells, two lines (1 and 2) of MCF7^{Twist1} cells, and two lines (1 and 2) of MCF7^{Twist1+Foxa1} (T+F) cells. B. The images of MCF7 parent, MCF7^{Ctrl}, MCF7^{Twist1} and MCF7^{Twist1+Foxa1} (T+F) cells. Scale bar, 50 μm. C. Western blot analysis of the indicated proteins in the indicated cell lines. D-F. qPCR analysis of integrin β1, integrin α5 and *MMP9* mRNA levels in the indicated cell lines. *, P < 0.05 by Student's t test.

3.12 Silencing Foxa1 expression is required for Twist1 to promote migration, invasion and metastasis in breast cancer cells

Expression of Foxa1 alone showed no effects on MCF7 cell migration and invasion.

However, restored Foxa1 expression in MCF7^{Twist1+Foxa1} cells significantly suppressed

Twist1-induced cell migration on the culture plate and invasion through a Matrigel layer (Fig. 3.21 A and B). To examine whether Foxa1 could inhibit Twist1-promoted metastasis *in vivo*, we injected MCF7^{Ctrl}, MCF7^{Foxa1}, MCF7^{Twist1} and MCF7^{Twist1+Foxa1} cells into the tail veins of SCID mice. We examined the lung tissues 4 weeks after injection. We found metastatic tumor foci in 20% (1/5), 0% (0/5), 100% (5/5) and 20% (1/5) of lungs in mice received MCF7^{Ctrl}, MCF7^{Foxa1}, MCF7^{Twist1} and MCF7^{Twist1+Foxa1} cells, respectively (Fig. 3.21C). The average number of MCF7^{Twist1} cell metastasis foci developed in each lung was significantly increased versus the average numbers of MCF7^{Ctrl}, MCF7^{Foxa1}, and MCF7^{Twist1+Foxa1} cell metastasis foci per lung (Fig. 3.21D). Accordingly, the lung metastasis index reflecting the percentage of tumor area to lung tissue area was more than 25 fold higher in the recipient mice of MCF7^{Twist1} cells versus the recipient mice of MCF7^{Ctrl} or MCF7^{Twist1+Foxa1} cells (Fig. 3.18E). To examine if restored Foxa1 could partially reverse the Twist1-induced basal tumor phenotype *in vivo*, we injected MCF7^{Ctrl}, MCF7^{Foxa1}, MCF7^{Twist1} and MCF7^{Twist1+Foxa1} cells into the mammary gland fat pads of SCID mice to form xenograft tumors and profiled the expression levels of well-established luminal and basal breast cancer marker genes. Luminal markers including FOXA1, PGR, GRP160, BAG1, BLVRA, PDEF, XBP1 and MUC1 were repressed and basal markers including JAG1, EGFR, FOXC1, CK5, CDC20 and ITGB1 were induced in MCF7^{Twist1} tumors versus MCF7^{Ctrl} and most MCF7^{Foxa1} tumors. Restored Foxa1 expression increased the expression of many luminal markers including BLVRA, PDEF and XBP1 and decreased the expression of many basal markers including JAG1, CK5, CDC20 and ITGB1 in MCF7^{Twist1+Foxa1} tumors

versus MCF7^{Twist1} tumors (Fig. 3.22A). Again, Twist1 promoted MCF7^{Twist1} tumor metastasis, while restored Foxa1 inhibited MCF7^{Twist1+Foxa1} tumor metastasis in SCID mice (Fig. 3.22 B and C). Together, these results demonstrate that Twist1-repressed *Foxa1* expression may be important for BLBC progression and is required for Twist1-promoted migration, invasion and metastasis of breast cancer cells. These results demonstrate that Twist1-mediated downregulation of *Foxa1* expression is required for TWIST1-promoted breast cancer cell metastasis.

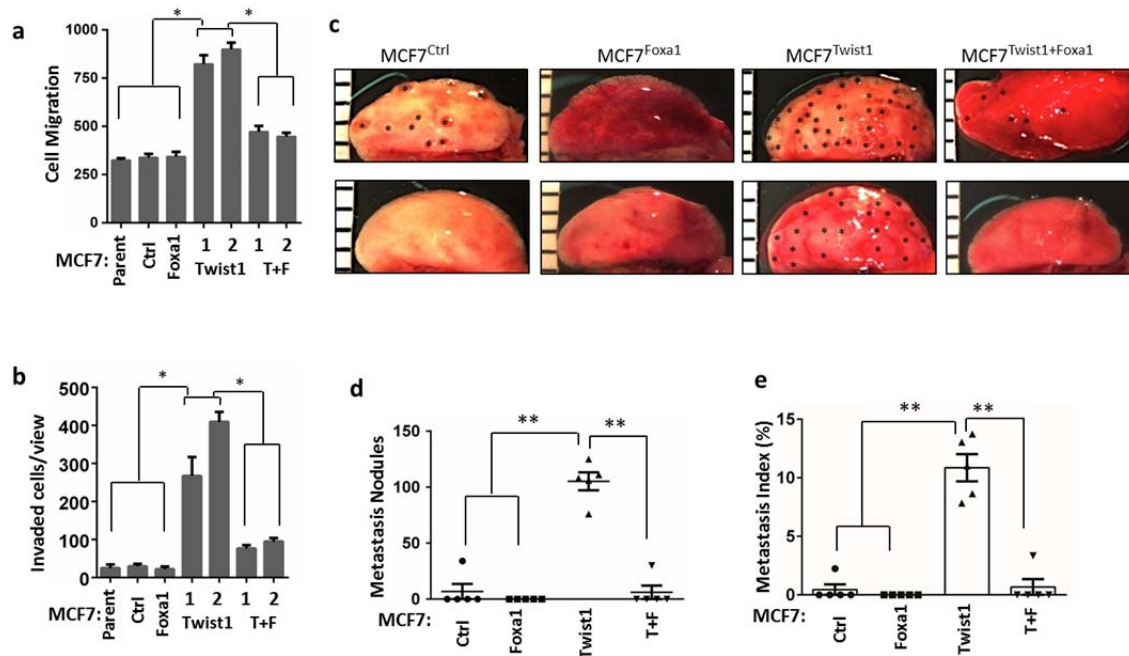


Figure 3.21. Restored *Foxa1* expression inhibited Twist1-promoted migration, invasion and metastasis of breast cancer cells. A & B. Cell migration and invasion assays for MCF7 parent, MCF7^{Ctrl}, MCF7^{Foxa1}, MCF7^{Twist1} and MCF7^{Twist1+Foxa1} cells. *, $P < 0.05$ by Student's t test. **C.** Lung photographs of SCID mice after receiving intravenous injection of MCF7^{Ctrl}, MCF7^{Foxa1}, MCF7^{Twist1} or MCF7^{Twist1+Foxa1} cells for 4 weeks. Asterisks indicate visible metastasis nodules. **D.** Metastasis nodules identified on the H&E-stained serial lung sections of SCID mice ($n=5$) injected with MCF7^{Ctrl}, MCF7^{Foxa1}, MCF7^{Twist1} or MCF7^{Twist1+Foxa1} cells for 4 weeks. **, $P < 0.01$ by Student's t test. **E.** Metastasis indexes were presented as the average ratios of tumor areas to lung areas measured on the images taken from H&E-stained serial lung sections. **, $P < 0.01$ by Student's t test.

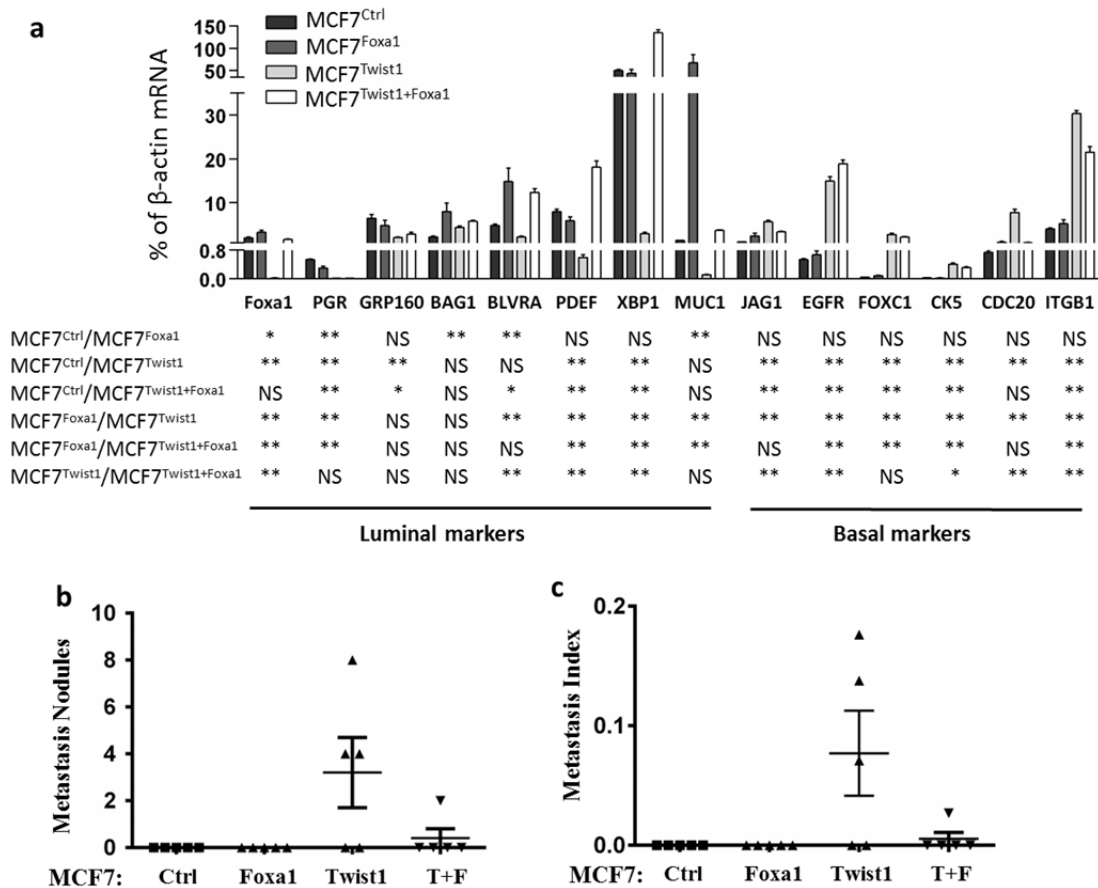


Figure 3.22. Restored Foxa1 expression increased the expression of most Twist1-suppressed luminal marker genes and decreased the expression of most Twist1-promoted basal marker genes in the xenograft tumors in mice. A. MCF7^{Ctrl}, MCF7^{Foxa1}, MCF7^{Twist1} or MCF7^{Twist1+Foxa1} cells were injected into the second pair mammary gland fat pads of each 8-week-old female SCID mouse (4×10^6 /fat pad). Five mice were used for each group. Injected mice were fed drinking water containing $1 \mu\text{g/ml}$ of 17β -estradiol. In 6 weeks after cell injection, 5, 4, 9 and 7 tumors were observed in mice receiving MCF7^{Ctrl}, MCF7^{Foxa1}, MCF7^{Twist1} or MCF7^{Twist1+Foxa1} cells, respectively. Mice were euthanized and the xenograft tumors were collected. Total RNA samples were prepared from 4 tumors in each group and qPCR analyses were performed to measure the mRNA levels of the indicated luminal and basal marker genes. Their relative expression levels were obtained by normalized to the level of b-actin mRNA in each sample. Four tumor RNA samples in each group were analyzed in duplicates and data are presented as Mean \pm SEM. One-Way ANOVA was performed to analyze the statistical differences among groups. * and **, $P < 0.05$ and 0.001 ; NS, not significant. B & C. The lungs were isolated from the above mice injected with MCF7^{Ctrl}, MCF7^{Foxa1}, MCF7^{Twist1} or MCF7^{Twist1+Foxa1} cells and examined for metastasis by counting the number of metastasis nodules and measuring the ratio of metastatic tumor area to total lung area (Metastasis Index) on the H&E-stained lung sections.

3.13 Breast tumor patients with high Twist1 and low Foxa1 expression exhibit poor distant metastasis-free survival

To assess the clinical relevance of the Twist1-Foxa1 regulatory axis in human breast cancer progression, we analyzed the association between the expression levels of *Twist1* and *Foxa1* and the clinical outcomes in a large breast cancer cohort with distant metastasis-free survival (DMFS) data¹²¹. The whole cohort of patients was divided into four groups according to the median *Twist1* and *Foxa1* expression. The Twist1^{High}/Foxa1^{Low} subgroup exhibited significantly worse DMFS than the Twist1^{Low}/Foxa1^{High} and the Twist1^{High}/Foxa1^{High} subgroups. DMFS of the Twist1^{Low}/Foxa1^{Low} subgroup is not significantly different from the DMFS curves of the other three groups (Fig. 3.23A). Further analyses revealed that the percentages of Twist1^{Low}Foxa1^{high} and Twist1^{High}Foxa1^{High} subgroup tumors in luminal A and luminal B subtypes are much higher than those in Basal-like and HER2-positive subtypes, while the percentages of Twist1^{Low}/Foxa1^{Low} and Twist1^{high}/Foxa1^{Low} tumors in luminal A and luminal B subtypes are much lower than those in the more aggressive basal-like and HER2-positive subtypes (Fig. 3.23B). Interestingly, when the cohort was further

subgrouped into luminal A, luminal B, HER2-positive and basal-like subtypes, only the $Twist1^{high}/Foxa1^{Low}$ patients with luminal A tumors exhibited significantly worse DMFS as compared to $Twist1^{Low}/Foxa1^{High}$ and $Twist1^{High}/Foxa1^{High}$ patients with luminal A tumors (Fig. 3.23 C-F). These results suggest that Twist1-mediated repression of *Foxa1* expression plays an important role in breast cancer metastasis and Foxa1 can effectively inhibit metastasis in tumors with high expression of both *Twist1* and *Foxa1*.

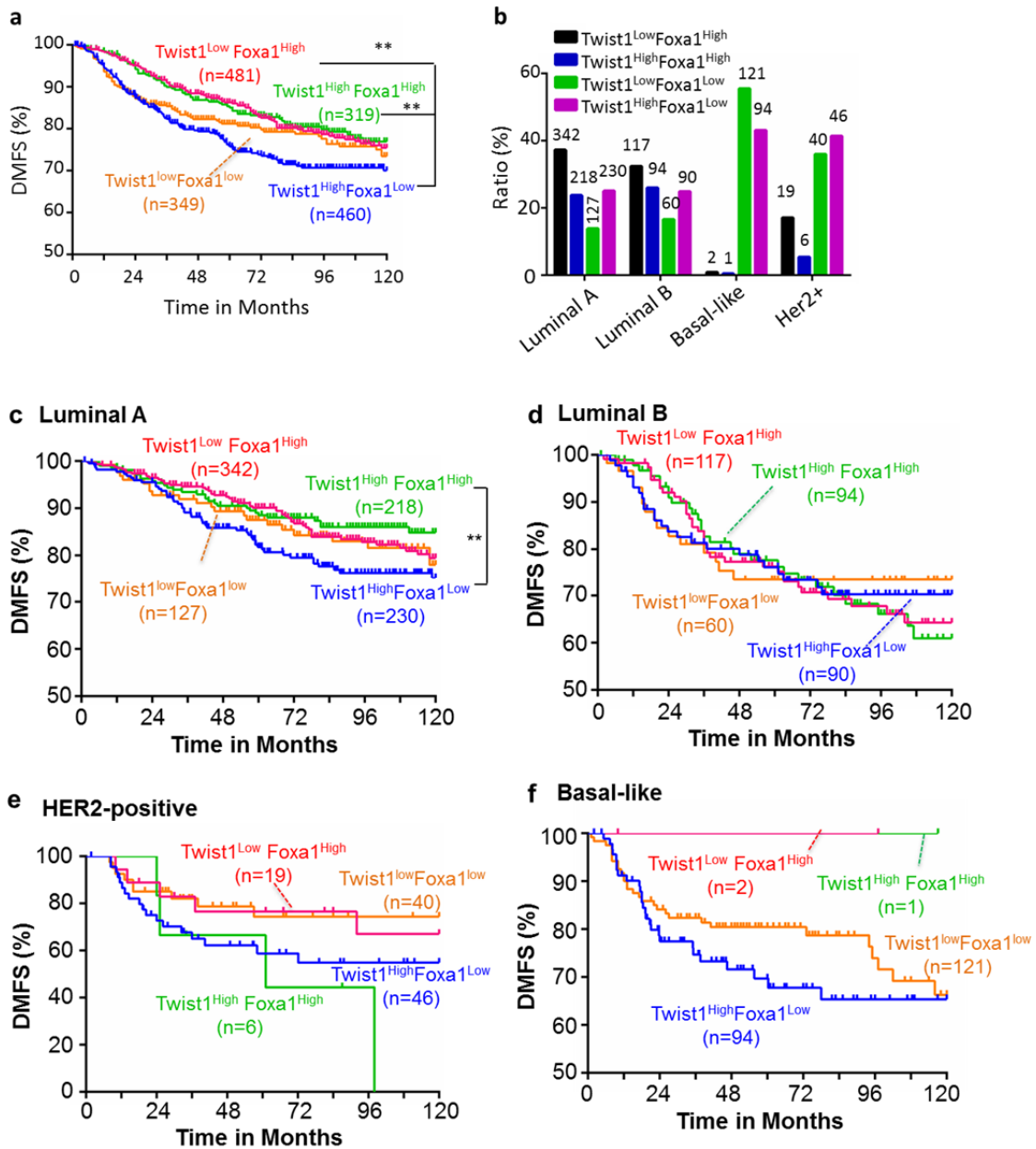


Figure 3.23. The association of *Twist1* and *Foxa1* expression levels with the clinical outcomes of the breast cancer patients. **A.** The distant metastasis-free survival (DMFS) curves of women with breast tumors expressing high or low levels of *Twist1* and *Foxa1* as indicated. The cohort (n=1609) was divided into high and low expression subgroups by the median. **B.** The distribution of patients with the indicated expression patterns of *Twist1* and *Foxa1* mRNAs in the 4 subtypes of breast cancer. The number of cases in each group is indicated above each bar. **C-F.** 10-year DMFS curves for luminal A (Panel C), luminal B (Panel D), HER2-positive (Panel E), and basal-like (Panel F) breast cancer patients with different expression levels of *Twist1* and *Foxa1* mRNAs. Sample number (n) is indicated for each subgroup. **, P < 0.01 by Log-rank test.

4. SUMMARY AND DISCUSSION

In this study, we developed the novel TVA/RCIP mouse model system in which deletion of a floxed gene such as *Twist1* and expression of an oncogene such as PyMT happen simultaneously in the RCIP virus-infected LECs expressing TVA. This model has several unique advantages. Firstly, TVA is only expressed in the mammary LECs in MMTV-TVA mouse line¹⁰⁵ and RCIP virus only infects the TVA-expressing cells, allowing specific delivery of Cre recombinase and PyMT (or any oncogene) to these mammary LECs. Secondly, the intraductally introduced RCIP virus only infects a small population of the mammary LECs expressing TVA and transform these cells into tumor cells. This closely simulates spontaneous tumorigenesis in humans with tumor initiation and growth in a normal surrounding cellular environment. Thirdly, the Cre-coding sequence is located before the short IRES and the PyMT sequences, which makes Cre expression much higher than PyMT expression and guarantees efficient knockout of the floxed genes in the tumor cells. Finally, the single virus construct-mediated co-expressions of Cre and PyMT also save time and resources for crossbreeding of multiple mouse lines. These unique features make this TVA/RCIP model system very useful for characterizing the role for any floxed genes during the process of mammary tumor initiation, progression and metastasis.

Using TVA/RCIP system, we selectively induced mammary tumorigenesis from *Twist1* null LECs in mice. We found that *Twist1* is not expressed in normal LECs and the RCIP

virus-induced initiation and growth of mammary tumors derived from LECs with or without *Twist1* knockout are the same, indicating that *Twist1* is not required for mammary tumor formation in LECs. Tumor cell proliferation, apoptosis and macrophage recruitment all showed no significant difference. These results of endogenous *Twist1* function further validates the previous studies showing knockdown of *Twist1* in breast cancer cell lines did not affect their proliferation in culture and xenograft tumor growth in mice^{26, 68}. Interestingly, a recent study reported an essential role of *Twist1* in developing skin tumors, suggesting the role of *Twist1* in carcinogenesis may depend on cell types¹²². Another study¹²³ using pancreatic tumor model showed that knock out of *Twist1* or *Snail* is dispensable for initiation and progression of primary pancreatic cancer. Our data is consistent with the pancreatic study that *Twist1* knockout does not influence breast tumor initiation, proliferation, apoptosis or macrophage recruitment.

Our results showed *Twist1* is expressed in a small population of tumor cells at advanced stages at levels similar to the stromal cells, indicating that only certain primary tumor cells gain *Twist1* expression during tumor progression. We did not find lung metastasis in mice with palpable mammary primary tumors that have been developed for 6 weeks, but did find extensive lung metastases in mice with palpable mammary primary tumors that have been developed for 10 weeks. These results suggest that *Twist1* expression is associated with metastasis in mammary tumors with functional *Twist1* gene. More importantly, *Twist1* null tumor cells yielded significantly fewer lung metastasis than

tumor cells with functional *Twist1*, indicating that the functional *Twist1* gene promotes tumor cell metastasis. Together, we conclude that Twist1 plays a tumor cell-autonomous function to promote metastasis and validate the results of previous studies showing that knockdown of *Twist1* in established breast cancer cell lines inhibits their metastasis in immune-defective host mice^{26, 64, 68}.

We then examined EMT markers by IF staining and found that Twist1 expressing tumor cells indeed showed EMT marker transition: decreased E-cadherin but increased vimentin, suggesting the association of EMT with lung metastasis. However, because we found metastatic tumor cells in the lung still maintain epithelial phenotype and do not express Twist1, it remains debatable whether the initial Twist1-expressing tumor cells in the mammary glands physically metastasize to the lung. A recent study using a squamous cell carcinoma mouse model with inducible Twist1 expression nicely demonstrated that although Twist1 expression strongly promotes tumor cell invasion and intravasation, turning off Twist1 expression is required for the disseminated tumor cells to establish metastasis in a distant organ⁴⁹. According to this model, it is possible that Twist1 expression in primary tumor cells induces partial EMT and drives local invasion and intravasation. Then, Twist expression is turned off in the tumor cells of lung metastases. However, it is also possible that the initial Twist1-expressing tumor cells did not metastasize to the lung, but these cells induce their surrounding Twist1-negative tumor cells to metastasize. Two recently published studies support this model^{123, 124}.

Since Twist1 is a transcription factor, it should promote breast cancer metastasis through either inhibiting or enhancing its target gene expression. In this study, we found that Twist1 expression negatively correlates with Foxa1 expression in both mouse and human breast tumors. Foxa1 expression is associated with LBC which has a good prognosis. Meanwhile Twist1 is associated with BLBC which has a poor prognosis due to its potential to drive cell invasiveness and metastasis. However, the regulatory and functional relationship between Twist1 and Foxa1 in breast cancer progression remains unknown. In this study, we found Twist1 expression negatively correlates with Foxa1 expression in human breast cancer cells and tumors. Mechanistically, Twist1 directly associates with *Foxa1* promoter to recruit NuRD complex and prevent AP-1 binding to *Foxa1* promoter, resulting in decreased H3K9 acetylation, reduced RNA polymerase II recruitment and silenced *Foxa1* expression. It is conceivable that constitutive AP-1 binding in LBC cells with no Twist1 plays a major role to maintain a high level of *Foxa1* expression and thus a luminal phenotype. Twist1 expression in partial or full EMT breast cancer cells may partially or fully inhibit AP-1 recruitment to *Foxa1* promoter through NuRD complex-mediated changes in histone codes and thus reduce or silence *Foxa1* expression, causing breast cancer progression toward BLBC. Therefore, our findings indicate that *Foxa1* is a direct target of Twist1 during breast cancer progression and provides a possible new mechanism for the loss of Foxa1 during breast cancer progression from a luminal ER α -positive subtype to an ER α -negative BLBC subtype.

In agreement with the established function of Twist1⁶⁴, ectopic expression of Twist1 in

MCF7 cells induced a mesenchymal morphology and gene expression signature but decreased epithelial signature. Using this cellular model, we addressed how much the Twist1-silenced *Foxa1* expression contributes to Twist1-induced mesenchymal morphogenesis and gene expression in breast cancer cells by restoring Foxa1 in Twist1-expressing MCF7 cells. Interestingly, though previous studies have shown Foxa1 represses EMT-linked mesenchymal morphogenesis in pancreatic cancer cells¹²⁵, we found that restored Foxa1 did not change the mesenchymal cell morphology induced by Twist1 in MCF7^{Twist1+Foxa1} cells. In agreement with this, restored Foxa1 did not rescue the expression level changes of either canonical epithelial genes such as E-cadherin and β -catenin or mesenchymal genes such as vimentin and Slug, which are inhibited or induced by Twist1 expression in MCF7 cells, respectively. We then also estimated the role of Foxa1 silencing in EMT by comparing the genes regulated by Foxa1 in the LBC cells to the previously published EMT signature genes^{101, 126}. Among the 1118 Foxa1-regulated genes¹⁰¹, we only found ARHGAP8, LMCD1, NMU, PPAP2B, PRKCH and SLPI in the 251 EMT signature gene lists¹²⁶. None of these 6 genes has been shown to regulate the mesenchymal morphogenesis of breast cancer cells. Together, these findings suggest that Twist1-silenced Foxa1 expression is not a major regulatory pathway for the mesenchymal morphogenesis and for the expression of most typical EMT signature genes in breast cancer cells.

Interestingly, restored Foxa1 does partially rescue ER α and K8 expression and strongly downregulate Twist1-induced integrin β 1, integrin α 5 and MMP9 expression. Since

ER α and K8 are markers of the LBC and integrins β 1 and α 5 are preferentially expressed in BLBC, it is conceivable that Twist1-silenced *Foxa1* expression plays a crucial role in promoting BLBC progression. Foxa1 could either directly or indirectly regulate these genes. It has been reported that Foxa1 upregulates but Twist1 directly represses ER α expression^{12, 91, 120}. The results of the present study suggest that both the loss of Foxa1-mediated activation due to Twist1-silenced Foxa1 expression and the Twist1-mediated active repression are required for shutting down ER α expression and developing endocrine resistance during breast cancer progression toward BLBC. These interpretations are consistent with the previous studies showing that Foxa1 expression is associated with good responses to endocrine therapy and the loss of Foxa1 is associated with BLBC progression^{93, 94, 97-102}. More importantly, restored Foxa1 robustly inhibited Twist1-promoted migration, invasion and metastasis. These could be partially attributed to the downregulation of Twist1-induced expression of MMP9 and integrins β 1 and 5α , since these proteins are known to promote cell invasiveness and metastasis^{110, 127-131}. In addition, we demonstrate that Twist1 expressed in MCF7 cells increased most BLBC markers but decreased most LBC markers in these cell-derived xenograft tumors, while restored Foxa1 in Twist1-expressing MCF7 cells decreased many BLBC markers but increased many LBC markers. These results further support the notion that Twist1-repressed Foxa1 expression may play an important role to promote BLBC progression.

In previous studies, the role of Twist1 in promoting metastasis was largely attributed to its capability to induce EMT and enhance cancer stem cell (CSC) features^{26, 51, 64, 71}.

Now, the consensus from present and previous studies suggests that Twist1 may serve as a master regulator in breast cancer progression by regulating multiple genes involved in multiple pathways. On one hand, Twist1 may regulate one subgroup of genes, such as downregulating E-cadherin and ER α ^{12, 68, 120} and upregulating Bmi1, AKT2, Wnt5a and vimentin ^{70, 85, 132} to promote EMT, CSC features, cell migration, invasion and metastasis. On the other hand, Twist1 may regulate another subgroup of genes, such as upregulating PDGFR α to induce invadopodia formation for cell invasion ⁷² and downregulating Foxa1 to decrease ER α , CK8 and other LBC markers and increase integrin α_5 , integrin β_1 , MMP9 and other BLBC markers for promoting BLBC progression and breast cancer cell migration, invasion and metastasis. Although these multiple Twist1-regulated genes and pathways may not be equally important, they may work cooperatively to drive breast cancer progression and metastasis. A single targeting event such as silencing *Foxa1* or upregulating *AKT2* can be required but may not be sufficient for Twist1-promoted migration, invasion and metastasis of breast cancer cells.

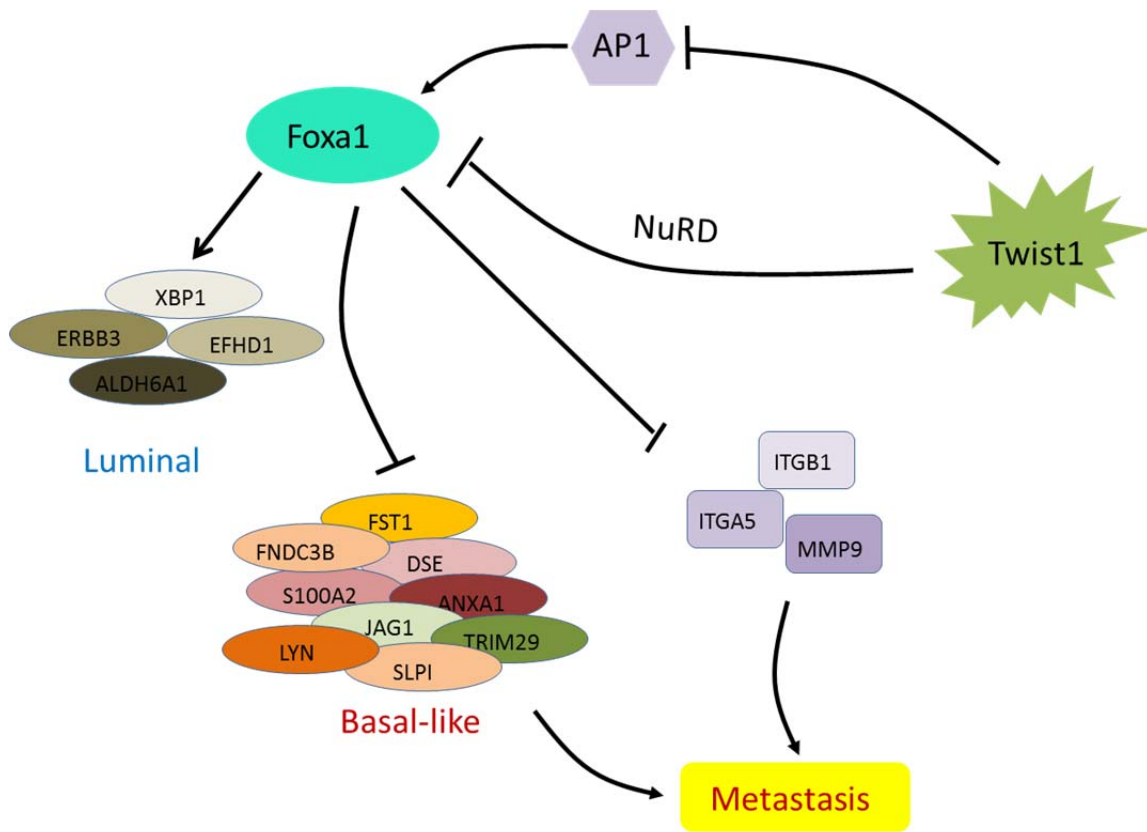


Figure 4.24. Summary of Twist1-Foxa1 regulatory axis in breast cancer cells

Analysis of a large cohort dataset showed that tumors with $\text{Twist1}^{\text{High}}\text{Foxa1}^{\text{Low}}$ expression are associated with worse DMFS versus $\text{Twist1}^{\text{Low}}\text{Foxa1}^{\text{High}}$ and $\text{Twist1}^{\text{High}}\text{Foxa1}^{\text{High}}$ tumors, which supports the notion that Twist1-silenced Foxa1 expression can promote breast cancer metastasis. Interestingly, this association is only observed in the mixed subtypes and luminal A subgroup, but not in the luminal B, HER2-positive or basal-like subgroups. We noticed that the tumor numbers with each expression profile are more evenly distributed in the luminal A and luminal B subgroups versus basal-like and HER2-positive subgroups. The latter two subtypes contain too few tumors with $\text{Twist1}^{\text{Low}}\text{Foxa1}^{\text{High}}$ and $\text{Twist1}^{\text{High}}\text{Foxa1}^{\text{High}}$ expressions and thus do not

support a valid statistical analysis to compare Twist1^{Low}Foxa1^{High} or Twist1^{High}Foxa1^{High} tumors with Twist1^{Low}Foxa1^{Low} or Twist1^{High}Foxa1^{Low} tumors. Nevertheless, the facts that *Twist1* is expressed at high levels in more than 40% of basal-like and HER2-positive tumors and Foxa1 is expressed at low levels in 96% of basal-like and 77% of HER2-positive tumors also support the notion that silenced Foxa1 expression is associated with more malignant breast cancer subtypes. For the luminal B subtype group, other factors in addition to Twist1 and Foxa1 may determine DMFS of these patients.

Analysis of tumor tissue microarrays by IHC also revealed an overall negative correlation between Twist1 and Foxa1 proteins. However, we did not find many Twist1-positive tumors from the examined breast tumor microarrays either because of too few BLBCs in the cohort or missed identification of some positive tumors due to the small area of tissue microarrays which are insufficient to cover heterogeneous regions for Twist1 expression in a tumor. IHC revealed that Twist1 is usually expressed only in a small subpopulation of tumor cells or a small region in a tumor. Most of these Twist1-positive tumors also contain many Foxa1-positive luminal tumor cells. These double positive tumors may contain Twist1-positive/Foxa1-positive, Twist1-positive/Foxa1-negative and/or Twist1-negative/Foxa1-positive cells. These observations support the notion that Twist1 is expressed in a subset of breast tumor cells and that Twist1 represses Foxa1 expression and drive EMT to promote BLBC progression from this subset of tumor cells.

In summary, we found that endogenous Twist1 mainly promotes breast cancer invasiveness and metastasis with no obvious function in affecting primary tumor development. Twist1 is expressed in a small population of tumor cells and its expression associates with EMT phenotype, invasiveness and metastasis. We further found that Twist1 directly represses the transcriptional activity of the *Foxa1* promoter in breast cancer cells. Twist1-silenced *Foxa1* expression is largely responsible for Twist1-mediated migration, invasion and metastasis but less responsible for Twist1-induced EMT morphology. On the other hand, silencing Foxa1 by Twist1 in breast cancer strongly promotes the transition from the luminal to basal gene signatures. These results not only uncover the mechanism of Foxa1 silencing in BLBC but also provide a new mechanism of Twist1's role in BLBC progression. Therefore, targeting Twist1 in BLBC treatment may be an effective approach to inhibit invasion and metastasis.

REFERENCES

1. Hanahan, D. & Weinberg, R.A. The hallmarks of cancer. *Cell* **100**, 57-70 (2000).
2. Hanahan, D. & Weinberg, R.A. Hallmarks of cancer: the next generation. *Cell* **144**, 646-674 (2011).
3. Fidler, I.J. The pathogenesis of cancer metastasis: the 'seed and soil' hypothesis revisited. *Nat Rev Cancer* **3**, 453-458 (2003).
4. Sorlie, T. *et al.* Gene expression patterns of breast carcinomas distinguish tumor subclasses with clinical implications. *Proc Natl Acad Sci U S A* **98**, 10869-10874 (2001).
5. Sorlie, T. *et al.* Repeated observation of breast tumor subtypes in independent gene expression data sets. *Proc Natl Acad Sci U S A* **100**, 8418-8423 (2003).
6. Perou, C.M. *et al.* Molecular portraits of human breast tumours. *Nature* **406**, 747-752 (2000).
7. Brenton, J.D., Carey, L.A., Ahmed, A.A. & Caldas, C. Molecular classification and molecular forecasting of breast cancer: ready for clinical application? *Journal of clinical oncology : official journal of the American Society of Clinical Oncology* **23**, 7350-7360 (2005).
8. Reis-Filho, J.S., Westbury, C. & Pierga, J.Y. The impact of expression profiling on prognostic and predictive testing in breast cancer. *Journal of clinical pathology* **59**, 225-231 (2006).

9. Rouzier, R. *et al.* Breast cancer molecular subtypes respond differently to preoperative chemotherapy. *Clinical cancer research : an official journal of the American Association for Cancer Research* **11**, 5678-5685 (2005).
10. Lin, E.Y. *et al.* Progression to malignancy in the polyoma middle T oncoprotein mouse breast cancer model provides a reliable model for human diseases. *Am J Pathol* **163**, 2113-2126 (2003).
11. McCune, K., Mehta, R., Thorat, M.A., Badve, S. & Nakshatri, H. Loss of ERalpha and FOXA1 expression in a progression model of luminal type breast cancer: insights from PyMT transgenic mouse model. *Oncology reports* **24**, 1233-1239 (2010).
12. Vesuna, F. *et al.* Twist contributes to hormone resistance in breast cancer by downregulating estrogen receptor-alpha. *Oncogene* **31**, 3223-3234 (2012).
13. Fan, C. *et al.* Concordance among gene-expression-based predictors for breast cancer. *N Engl J Med* **355**, 560-569 (2006).
14. Schock, F. & Perrimon, N. Molecular mechanisms of epithelial morphogenesis. *Annu Rev Cell Dev Biol* **18**, 463-493 (2002).
15. Thiery, J.P. & Sleeman, J.P. Complex networks orchestrate epithelial-mesenchymal transitions. *Nat Rev Mol Cell Biol* **7**, 131-142 (2006).
16. Greenburg, G. & Hay, E.D. Epithelia suspended in collagen gels can lose polarity and express characteristics of migrating mesenchymal cells. *J Cell Biol* **95**, 333-339 (1982).

17. Greenburg, G. & Hay, E.D. Cytodifferentiation and tissue phenotype change during transformation of embryonic lens epithelium to mesenchyme-like cells in vitro. *Dev Biol* **115**, 363-379 (1986).
18. Greenburg, G. & Hay, E.D. Cytoskeleton and thyroglobulin expression change during transformation of thyroid epithelium to mesenchyme-like cells. *Development* **102**, 605-622 (1988).
19. Boyer, B. & Thiery, J.P. Epithelium-mesenchyme interconversion as example of epithelial plasticity. *APMIS* **101**, 257-268 (1993).
20. Hay, E.D. An overview of epithelio-mesenchymal transformation. *Acta Anat (Basel)* **154**, 8-20 (1995).
21. Barrallo-Gimeno, A. & Nieto, M.A. The Snail genes as inducers of cell movement and survival: implications in development and cancer. *Development* **132**, 3151-3161 (2005).
22. Hajra, K.M., Chen, D.Y. & Fearon, E.R. The SLUG zinc-finger protein represses E-cadherin in breast cancer. *Cancer Res* **62**, 1613-1618 (2002).
23. Eger, A. *et al.* DeltaEF1 is a transcriptional repressor of E-cadherin and regulates epithelial plasticity in breast cancer cells. *Oncogene* **24**, 2375-2385 (2005).
24. Comijn, J. *et al.* The two-handed E box binding zinc finger protein SIP1 downregulates E-cadherin and induces invasion. *Molecular cell* **7**, 1267-1278 (2001).

25. Perez-Moreno, M.A. *et al.* A new role for E12/E47 in the repression of E-cadherin expression and epithelial-mesenchymal transitions. *J Biol Chem* **276**, 27424-27431 (2001).
26. Yang, J. *et al.* Twist, a master regulator of morphogenesis, plays an essential role in tumor metastasis. *Cell* **117**, 927-939 (2004).
27. Kimelman, D. Mesoderm induction: from caps to chips. *Nat Rev Genet* **7**, 360-372 (2006).
28. Viebahn, C. Epithelio-mesenchymal transformation during formation of the mesoderm in the mammalian embryo. *Acta Anat (Basel)* **154**, 79-97 (1995).
29. Tucker, G.C., Duband, J.L., Dufour, S. & Thiery, J.P. Cell-adhesion and substrate-adhesion molecules: their instructive roles in neural crest cell migration. *Development* **103 Suppl**, 81-94 (1988).
30. Duband, J.L. & Thiery, J.P. Distribution of laminin and collagens during avian neural crest development. *Development* **101**, 461-478 (1987).
31. Nichols, D.H. Neural crest formation in the head of the mouse embryo as observed using a new histological technique. *J Embryol Exp Morphol* **64**, 105-120 (1981).
32. Martins-Green, M. & Erickson, C.A. Basal lamina is not a barrier to neural crest cell emigration: documentation by TEM and by immunofluorescent and immunogold labelling. *Development* **101**, 517-533 (1987).
33. Markwald, R.R., Fitzharris, T.P. & Manasek, F.J. Structural development of endocardial cushions. *Am J Anat* **148**, 85-119 (1977).

34. Bolender, D.L. & Markwald, R.R. Epithelial-mesenchymal transformation in chick atrioventricular cushion morphogenesis. *Scan Electron Microsc*, 313-321 (1979).
35. Person, A.D., Klewer, S.E. & Runyan, R.B. Cell biology of cardiac cushion development. *Int Rev Cytol* **243**, 287-335 (2005).
36. Fitchett, J.E. & Hay, E.D. Medial edge epithelium transforms to mesenchyme after embryonic palatal shelves fuse. *Dev Biol* **131**, 455-474 (1989).
37. Liu, Y. Epithelial to mesenchymal transition in renal fibrogenesis: pathologic significance, molecular mechanism, and therapeutic intervention. *J Am Soc Nephrol* **15**, 1-12 (2004).
38. Yang, J. & Liu, Y. Dissection of key events in tubular epithelial to myofibroblast transition and its implications in renal interstitial fibrosis. *Am J Pathol* **159**, 1465-1475 (2001).
39. Jinde, K. *et al.* Tubular phenotypic change in progressive tubulointerstitial fibrosis in human glomerulonephritis. *Am J Kidney Dis* **38**, 761-769 (2001).
40. Kalluri, R. & Neilson, E.G. Epithelial-mesenchymal transition and its implications for fibrosis. *J Clin Invest* **112**, 1776-1784 (2003).
41. Yanez-Mo, M. *et al.* Peritoneal dialysis and epithelial-to-mesenchymal transition of mesothelial cells. *N Engl J Med* **348**, 403-413 (2003).
42. Oh, K.H. & Margetts, P.J. Cytokines and growth factors involved in peritoneal fibrosis of peritoneal dialysis patients. *Int J Artif Organs* **28**, 129-134 (2005).

43. Thiery, J.P. Epithelial-mesenchymal transitions in tumour progression. *Nat Rev Cancer* **2**, 442-454 (2002).
44. Kalluri, R. & Weinberg, R.A. The basics of epithelial-mesenchymal transition. *J Clin Invest* **119**, 1420-1428 (2009).
45. Zeisberg, M. & Neilson, E.G. Biomarkers for epithelial-mesenchymal transitions. *J Clin Invest* **119**, 1429-1437 (2009).
46. Trimboli, A.J. *et al.* Direct evidence for epithelial-mesenchymal transitions in breast cancer. *Cancer Res* **68**, 937-945 (2008).
47. Sarrio, D. *et al.* Epithelial-mesenchymal transition in breast cancer relates to the basal-like phenotype. *Cancer Res* **68**, 989-997 (2008).
48. Neve, R.M. *et al.* A collection of breast cancer cell lines for the study of functionally distinct cancer subtypes. *Cancer cell* **10**, 515-527 (2006).
49. Tsai, J.H., Donaher, J.L., Murphy, D.A., Chau, S. & Yang, J. Spatiotemporal regulation of epithelial-mesenchymal transition is essential for squamous cell carcinoma metastasis. *Cancer cell* **22**, 725-736 (2012).
50. Micalizzi, D.S., Farabaugh, S.M. & Ford, H.L. Epithelial-mesenchymal transition in cancer: parallels between normal development and tumor progression. *J Mammary Gland Biol Neoplasia* **15**, 117-134 (2010).
51. Mani, S.A. *et al.* The epithelial-mesenchymal transition generates cells with properties of stem cells. *Cell* **133**, 704-715 (2008).
52. Ye, X. *et al.* Distinct EMT programs control normal mammary stem cells and tumour-initiating cells. *Nature* **525**, 256-260 (2015).

53. McCoy, E.L. *et al.* Six1 expands the mouse mammary epithelial stem/progenitor cell pool and induces mammary tumors that undergo epithelial-mesenchymal transition. *J Clin Invest* **119**, 2663-2677 (2009).
54. Simpson, P. Maternal-Zygotic Gene Interactions during Formation of the Dorsoventral Pattern in *Drosophila* Embryos. *Genetics* **105**, 615-632 (1983).
55. Thisse, B., Stoetzel, C., Gorostiza-Thisse, C. & Perrin-Schmitt, F. Sequence of the twist gene and nuclear localization of its protein in endomesodermal cells of early *Drosophila* embryos. *EMBO J* **7**, 2175-2183 (1988).
56. Murre, C. *et al.* Interactions between heterologous helix-loop-helix proteins generate complexes that bind specifically to a common DNA sequence. *Cell* **58**, 537-544 (1989).
57. Jan, Y.N. & Jan, L.Y. HLH proteins, fly neurogenesis, and vertebrate myogenesis. *Cell* **75**, 827-830 (1993).
58. Chen, Z.F. & Behringer, R.R. twist is required in head mesenchyme for cranial neural tube morphogenesis. *Genes Dev* **9**, 686-699 (1995).
59. Pan, D.J., Huang, J.D. & Courey, A.J. Functional analysis of the *Drosophila* twist promoter reveals a dorsal-binding ventral activator region. *Genes Dev* **5**, 1892-1901 (1991).
60. Ip, Y.T., Park, R.E., Kosman, D., Bier, E. & Levine, M. The dorsal gradient morphogen regulates stripes of rhomboid expression in the presumptive neuroectoderm of the *Drosophila* embryo. *Genes Dev* **6**, 1728-1739 (1992).

61. Figeac, N., Daczewska, M., Marcelle, C. & Jagla, K. Muscle stem cells and model systems for their investigation. *Dev Dyn* **236**, 3332-3342 (2007).
62. O'Rourke, M.P. & Tam, P.P. Twist functions in mouse development. *Int J Dev Biol* **46**, 401-413 (2002).
63. Xu, Y. *et al.* Inducible knockout of Twist1 in young and adult mice prolongs hair growth cycle and has mild effects on general health, supporting Twist1 as a preferential cancer target. *Am J Pathol* **183**, 1281-1292 (2013).
64. Qin, Q., Xu, Y., He, T., Qin, C. & Xu, J. Normal and disease-related biological functions of Twist1 and underlying molecular mechanisms. *Cell Res* **22**, 90-106 (2012).
65. el Ghouzzi, V. *et al.* Mutations of the TWIST gene in the Saethre-Chotzen syndrome. *Nat Genet* **15**, 42-46 (1997).
66. Howard, T.D. *et al.* Mutations in TWIST, a basic helix-loop-helix transcription factor, in Saethre-Chotzen syndrome. *Nat Genet* **15**, 36-41 (1997).
67. Lee, T.K. *et al.* Twist overexpression correlates with hepatocellular carcinoma metastasis through induction of epithelial-mesenchymal transition. *Clinical cancer research : an official journal of the American Association for Cancer Research* **12**, 5369-5376 (2006).
68. Fu, J. *et al.* The TWIST/Mi2/NuRD protein complex and its essential role in cancer metastasis. *Cell Res* **21**, 275-289 (2010).
69. Pham, C.G. *et al.* Upregulation of Twist-1 by NF-kappaB blocks cytotoxicity induced by chemotherapeutic drugs. *Mol Cell Biol* **27**, 3920-3935 (2007).

70. Cheng, G.Z., Zhang, W. & Wang, L.H. Regulation of cancer cell survival, migration, and invasion by Twist: AKT2 comes to interplay. *Cancer Res* **68**, 957-960 (2008).
71. Yang, M.H. *et al.* Direct regulation of TWIST by HIF-1alpha promotes metastasis. *Nat Cell Biol* **10**, 295-305 (2008).
72. Eckert, M.A. *et al.* Twist1-induced invadopodia formation promotes tumor metastasis. *Cancer cell* **19**, 372-386 (2011).
73. Ling, X. & Arlinghaus, R.B. Knockdown of STAT3 expression by RNA interference inhibits the induction of breast tumors in immunocompetent mice. *Cancer Res* **65**, 2532-2536 (2005).
74. Cheng, G.Z. *et al.* Twist is transcriptionally induced by activation of STAT3 and mediates STAT3 oncogenic function. *J Biol Chem* **283**, 14665-14673 (2008).
75. Cheng, G.Z. *et al.* Twist transcriptionally up-regulates AKT2 in breast cancer cells leading to increased migration, invasion, and resistance to paclitaxel. *Cancer Res* **67**, 1979-1987 (2007).
76. Li, C.W. *et al.* AKT1 Inhibits Epithelial-to-Mesenchymal Transition in Breast Cancer through Phosphorylation-Dependent Twist1 Degradation. *Cancer Res* **76**, 1451-1462 (2016).
77. Wang, S. *et al.* Disruption of the SRC-1 gene in mice suppresses breast cancer metastasis without affecting primary tumor formation. *Proc Natl Acad Sci U S A* **106**, 151-156 (2009).

78. Qin, L., Liu, Z., Chen, H. & Xu, J. The steroid receptor coactivator-1 regulates twist expression and promotes breast cancer metastasis. *Cancer Res* **69**, 3819-3827 (2009).
79. Ai, L. *et al.* TRIM29 suppresses TWIST1 and invasive breast cancer behavior. *Cancer Res* **74**, 4875-4887 (2014).
80. Wei, S.C. *et al.* Matrix stiffness drives epithelial-mesenchymal transition and tumour metastasis through a TWIST1-G3BP2 mechanotransduction pathway. *Nat Cell Biol* **17**, 678-688 (2015).
81. Fang, J. *et al.* Purification and functional characterization of SET8, a nucleosomal histone H4-lysine 20-specific methyltransferase. *Current biology : CB* **12**, 1086-1099 (2002).
82. Nishioka, K. *et al.* PR-Set7 is a nucleosome-specific methyltransferase that modifies lysine 20 of histone H4 and is associated with silent chromatin. *Molecular cell* **9**, 1201-1213 (2002).
83. Talasz, H., Lindner, H.H., Sarg, B. & Helliger, W. Histone H4-lysine 20 monomethylation is increased in promoter and coding regions of active genes and correlates with hyperacetylation. *J Biol Chem* **280**, 38814-38822 (2005).
84. Yang, F. *et al.* SET8 promotes epithelial-mesenchymal transition and confers TWIST dual transcriptional activities. *EMBO J* **31**, 110-123 (2012).
85. Shi, J. *et al.* Disrupting the interaction of BRD4 with diacetylated Twist suppresses tumorigenesis in basal-like breast cancer. *Cancer cell* **25**, 210-225 (2014).

86. Weigel, D., Jurgens, G., Kuttner, F., Seifert, E. & Jackle, H. The homeotic gene fork head encodes a nuclear protein and is expressed in the terminal regions of the *Drosophila* embryo. *Cell* **57**, 645-658 (1989).
87. Weigel, D. & Jackle, H. The fork head domain: a novel DNA binding motif of eukaryotic transcription factors? *Cell* **63**, 455-456 (1990).
88. Lai, E., Prezioso, V.R., Tao, W.F., Chen, W.S. & Darnell, J.E., Jr. Hepatocyte nuclear factor 3 alpha belongs to a gene family in mammals that is homologous to the *Drosophila* homeotic gene fork head. *Genes Dev* **5**, 416-427 (1991).
89. Hannenhalli, S. & Kaestner, K.H. The evolution of Fox genes and their role in development and disease. *Nat Rev Genet* **10**, 233-240 (2009).
90. Kaestner, K.H., Knochel, W. & Martinez, D.E. Unified nomenclature for the winged helix/forkhead transcription factors. *Genes Dev* **14**, 142-146 (2000).
91. Bernardo, G.M. *et al.* FOXA1 is an essential determinant of ERalpha expression and mammary ductal morphogenesis. *Development* **137**, 2045-2054 (2010).
92. Augello, M.A., Hickey, T.E. & Knudsen, K.E. FOXA1: master of steroid receptor function in cancer. *EMBO J* **30**, 3885-3894 (2011).
93. Carroll, J.S. *et al.* Chromosome-wide mapping of estrogen receptor binding reveals long-range regulation requiring the forkhead protein FoxA1. *Cell* **122**, 33-43 (2005).
94. Laganiere, J. *et al.* From the Cover: Location analysis of estrogen receptor alpha target promoters reveals that FOXA1 defines a domain of the estrogen response. *Proc Natl Acad Sci U S A* **102**, 11651-11656 (2005).

95. Eeckhoute, J., Briche, I., Kurowska, M., Formstecher, P. & Laine, B. Hepatocyte nuclear factor 4 alpha ligand binding and F domains mediate interaction and transcriptional synergy with the pancreatic islet LIM HD transcription factor Isl1. *Journal of molecular biology* **364**, 567-581 (2006).
96. Eeckhoute, J. *et al.* Cell-type selective chromatin remodeling defines the active subset of FOXA1-bound enhancers. *Genome research* **19**, 372-380 (2009).
97. Carroll, J.S. & Brown, M. Estrogen receptor target gene: an evolving concept. *Molecular endocrinology* **20**, 1707-1714 (2006).
98. Badve, S. *et al.* FOXA1 expression in breast cancer--correlation with luminal subtype A and survival. *Clinical cancer research : an official journal of the American Association for Cancer Research* **13**, 4415-4421 (2007).
99. Hurtado, A., Holmes, K.A., Ross-Innes, C.S., Schmidt, D. & Carroll, J.S. FOXA1 is a key determinant of estrogen receptor function and endocrine response. *Nat Genet* **43**, 27-33 (2011).
100. Thorat, M.A. *et al.* Forkhead box A1 expression in breast cancer is associated with luminal subtype and good prognosis. *Journal of clinical pathology* **61**, 327-332 (2008).
101. Bernardo, G.M. *et al.* FOXA1 represses the molecular phenotype of basal breast cancer cells. *Oncogene* **32**, 554-563 (2013).
102. Naderi, A., Meyer, M. & Dowhan, D.H. Cross-regulation between FOXA1 and ErbB2 signaling in estrogen receptor-negative breast cancer. *Neoplasia* **14**, 283-296 (2012).

103. Chappell, S.A., Edelman, G.M. & Mauro, V.P. A 9-nt segment of a cellular mRNA can function as an internal ribosome entry site (IRES) and when present in linked multiple copies greatly enhances IRES activity. *Proc Natl Acad Sci U S A* **97**, 1536-1541 (2000).
104. Owens, G.C., Chappell, S.A., Mauro, V.P. & Edelman, G.M. Identification of two short internal ribosome entry sites selected from libraries of random oligonucleotides. *Proc Natl Acad Sci U S A* **98**, 1471-1476 (2001).
105. Du, Z. *et al.* Introduction of oncogenes into mammary glands in vivo with an avian retroviral vector initiates and promotes carcinogenesis in mouse models. *Proc Natl Acad Sci U S A* **103**, 17396-17401 (2006).
106. Qin, L. *et al.* NCOA1 Directly Targets M-CSF1 Expression to Promote Breast Cancer Metastasis. *Cancer Res* **74**, 3477-3488 (2014).
107. Soriano, P. Generalized lacZ expression with the ROSA26 Cre reporter strain. *Nat Genet* **21**, 70-71 (1999).
108. Mao, X., Fujiwara, Y. & Orkin, S.H. Improved reporter strain for monitoring Cre recombinase-mediated DNA excisions in mice. *Proc Natl Acad Sci U S A* **96**, 5037-5042 (1999).
109. Chen, Y.T., Akinwunmi, P.O., Deng, J.M., Tam, O.H. & Behringer, R.R. Generation of a Twist1 conditional null allele in the mouse. *Genesis* **45**, 588-592 (2007).

110. Qin, L. *et al.* The AIB1 oncogene promotes breast cancer metastasis by activation of PEA3-mediated matrix metalloproteinase 2 (MMP2) and MMP9 expression. *Mol Cell Biol* **28**, 5937-5950 (2008).
111. Tien, J.C. *et al.* The steroid receptor coactivator-3 is required for developing neuroendocrine tumor in the mouse prostate. *International journal of biological sciences* **10**, 1116-1127 (2014).
112. Xu, J. *et al.* The steroid receptor coactivator SRC-3 (p/CIP/RAC3/AIB1/ACTR/TRAM-1) is required for normal growth, puberty, female reproductive function, and mammary gland development. *Proc Natl Acad Sci U S A* **97**, 6379-6384 (2000).
113. Lee, D.K., Liu, Y., Liao, L., Wang, F. & Xu, J. The prostate basal cell (BC) heterogeneity and the p63-positive BC differentiation spectrum in mice. *Int J Biol Sci* **10**, 1007-1017 (2014).
114. Kuang, S.Q. *et al.* AIB1/SRC-3 deficiency affects insulin-like growth factor I signaling pathway and suppresses v-Ha-ras-induced breast cancer initiation and progression in mice. *Cancer research* **64**, 1875-1885 (2004).
115. Qin, L. *et al.* NCOA1 promotes angiogenesis in breast tumors by simultaneously enhancing both HIF1alpha- and AP-1-mediated VEGFa transcription. *Oncotarget* **6**, 23890-23904 (2015).
116. Longo, P.A., Kavran, J.M., Kim, M.S. & Leahy, D.J. Transient mammalian cell transfection with polyethylenimine (PEI). *Methods in enzymology* **529**, 227-240 (2013).

117. Allred, D.C., Harvey, J.M., Berardo, M. & Clark, G.M. Prognostic and predictive factors in breast cancer by immunohistochemical analysis. *Mod Pathol* **11**, 155-168 (1998).
118. Wang, Y. *et al.* Gene-expression profiles to predict distant metastasis of lymph-node-negative primary breast cancer. *Lancet* **365**, 671-679 (2005).
119. Kao, J. *et al.* Molecular profiling of breast cancer cell lines defines relevant tumor models and provides a resource for cancer gene discovery. *PLoS One* **4**, e6146 (2009).
120. Fu, J. *et al.* TWIST represses estrogen receptor-alpha expression by recruiting the NuRD protein complex in breast cancer cells. *International journal of biological sciences* **8**, 522-532 (2012).
121. Gyorffy, B. *et al.* An online survival analysis tool to rapidly assess the effect of 22,277 genes on breast cancer prognosis using microarray data of 1,809 patients. *Breast Cancer Res Treat* **123**, 725-731 (2010).
122. Beck, B. *et al.* Different levels of Twist1 regulate skin tumor initiation, stemness, and progression. *Cell stem cell* **16**, 67-79 (2015).
123. Fischer, K.R. *et al.* Epithelial-to-mesenchymal transition is not required for lung metastasis but contributes to chemoresistance. *Nature* **527**, 472-476 (2015).
124. Zheng, X. *et al.* Epithelial-to-mesenchymal transition is dispensable for metastasis but induces chemoresistance in pancreatic cancer. *Nature* **527**, 525-530 (2015).

125. Song, Y., Washington, M.K. & Crawford, H.C. Loss of FOXA1/2 is essential for the epithelial-to-mesenchymal transition in pancreatic cancer. *Cancer research* **70**, 2115-2125 (2010).
126. Taube, J.H. *et al.* Core epithelial-to-mesenchymal transition interactome gene-expression signature is associated with claudin-low and metaplastic breast cancer subtypes. *Proc Natl Acad Sci U S A* **107**, 15449-15454 (2010).
127. Sawada, K. *et al.* Loss of E-cadherin promotes ovarian cancer metastasis via alpha 5-integrin, which is a therapeutic target. *Cancer research* **68**, 2329-2339 (2008).
128. Sottnik, J.L. *et al.* Integrin alpha2beta 1 (alpha2beta1) promotes prostate cancer skeletal metastasis. *Clin Exp Metastasis* **30**, 569-578 (2013).
129. Gupta, S.K., Oommen, S., Aubry, M.C., Williams, B.P. & Vlahakis, N.E. Integrin alpha9beta1 promotes malignant tumor growth and metastasis by potentiating epithelial-mesenchymal transition. *Oncogene* **32**, 141-150 (2013).
130. Mitra, A.K. *et al.* Ligand-independent activation of c-Met by fibronectin and alpha(5)beta(1)-integrin regulates ovarian cancer invasion and metastasis. *Oncogene* **30**, 1566-1576 (2011).
131. Hsu, R.Y. *et al.* LPS-induced TLR4 signaling in human colorectal cancer cells increases beta1 integrin-mediated cell adhesion and liver metastasis. *Cancer research* **71**, 1989-1998 (2011).
132. Yang, M.H. *et al.* Bmi1 is essential in Twist1-induced epithelial-mesenchymal transition. *Nat Cell Biol* **12**, 982-992 (2010).